A DISSERTATION FOR THE DEGREE OF DOCTOR OF PHILOSOPHY

Searching for Early Fruit Abscission-Related Genes in Self-Abscising Apple (*Malus* × *domestica*)

자가적과성 사과 품종의 유과기 탈리 연관 유전자 탐색

BY

SEONG HEO

FEBRUARY, 2016

DEPARTMENT OF HORTICULTURAL SCIENCE AND BIOTECHNOLOGY

THE GRADUATE SCHOOL OF SEOUL NATIONAL UNIVERSITY

A DISSERTATION FOR THE DEGREE OF DOCTOR OF PHILOSOPHY

Searching for Early Fruit Abscission-Related Genes in Self-Abscising Apple (*Malus* × *domestica*)

자가적과성 사과 품종의 유과기 탈리 연관 유전자 탐색

BY

SEONG HEO

FEBRUARY, 2016

DEPARTMENT OF HORTICULTURAL SCIENCE AND BIOTECHNOLOGY

THE GRADUATE SCHOOL OF SEOUL NATIONAL UNIVERSITY

Searching for Early Fruit Abscission-Related Genes in Self-Abscising Apple (*Malus* × *domestica*)

UNDER THE DIRECTION OF DR. HEE JAE LEE SUBMITTED TO THE FACULTY OF THE GRADUATE SCHOOL OF SEOUL NATIONAL UNIVERSITY

BY

SEONG HEO

DEPARTMENT OF HORTICULTURAL SCIENCE AND BIOTECHNOLOGY

NOVEMBER, 2015

APPROVED AS A QUALIFIED DISSERTATION OF SEONG HEO

FOR THE DEGREE OF DOCTOR OF PHILOSOPHY

BY THE COMMITTEE MEMBERS

DECEMBER, 2015

CHAIRMAN _____
Ki Sun Kim, Ph.D.

VICE-CHAIRMAN _____
Hee Jae Lee, Ph.D.

MEMBER _____
Daeil Kim, Ph.D.

MEMBER _____
Ji Hae Jun, Ph.D.

MEMBER _____
Jin Hoe Huh, Ph.D.

Searching for Early Fruit Abscission-Related Genes in Self-Abscising Apple (*Malus × domestica*)

Seong Heo

Department of Horticultural Science and Biotechnology

The Graduate School of Seoul National University

ABSTRACT

Based on the fruit abscission pattern from full bloom to 30 days after full bloom, 48 apple genetic resources were classified into three groups: 1) a non-abscising group, in which no fruit is abscised; 2) a June drop group, in which the abscission process occurs non-selectively in clusters; and 3) a self-abscising group, in which only central or last fruit in a cluster remains to grow, and the others are abscised. Most cultivars in the self-abscising group showed a fruit abscission pattern in which central fruit dominated over lateral fruits in a cluster, inducing their growth inhibition and final abscission. Exceptionally, in *Malus coronaria* 'Charlottae', central fruit could not dominate lateral fruits, but was abscised first in a cluster. The date of full bloom and fruit weight were significantly related to fruit abscission. The earlier the date of full bloom and the smaller the fruit in the abscission

groups were, the less early fruit abscission occurred.

To search the MADS-box gene which regulates abscission zone development in pedicels, like *JOINTLESS* in tomato, lateral pedicels (LP) were investigated in self-abscising apple 'Saika' during early abscission. A novel MADS-box gene, *MdJOINTLESS*, was identified in young pedicels through the amplification using degenerate primers annealing to a highly conserved domain. Through DNA sequence comparison with the MADS-box gene family, *MdJOINTLESS* was classified into the *SHORT VEGETATIVE PHASE* (*SVP*) clade composed of *SVP* (*Arabidopsis thaliana*), *IbMADS3* (*Ipomoea batatas*), *StMADS16* (*Solanum tuberosum*), *PsSVP* (*Pisum sativum*), and *JOINTLESS* (*Solanum lycopersicum*) which share high sequence similarity. However, *MdJOINTLESS* did not function as *JOINTLESS* in transgenic tomato, although these MADS-box homologues have high homology. The other MADS-box genes analogous to *SEPALLATA* and *MACROCALYX* might be involved in the formation of AZ in apple as *SLMBP21* and *MACROCALYX* genes in tomato.

A comparative analysis was conducted between central pedicels (CP) and LP in the self-abscising apple 'Saika' to identify the genes that trigger the abscission mechanism, as the destinies of the pedicels in a cluster are obvious. Transcriptome analysis was performed using RNA-Seq to compare expression profiles between surviving CP and abscised LP. A total of 797,647 expressed sequence tags were assembled into 65,876 contigs, which were annotated and analyzed through gene ontology analysis. A total of 1,585 differentially expressed genes (DEGs) were identified in CP and LP. Analyses on DEGs and qRT-PCR suggested that *IAA3*/*SHY2* was up-

regulated in CP and *IAA14*/*SLR* was differentially expressed in LP. *IAA3*/*SHY2* may participate in meristem development which is mediated through auxin signal transduction and *IAA14*/*SLR* is at least partly involved in the abscission mechanism of LP. The *AUX*/*IAA* genes may be related to the roles of determining the fate of pedicels in early abscission.

Key words: Abscission zone, *AUX/IAA*, Auxin signaling, Fruit thinning, MADS-box, RNA-Seq, Self-abscission

Student Number: 2009-30970

CONTENTS

CHAPTER 2. Isolation of a Novel MADS-Box Gene, *MdJOINTLESS*, from Pedicels during Early Fruit Abscission in the Self-Abscising Apple (*Malus* × *domestica*)

LIST OF TABLES

LIST OF FIGURES

LIST OF ABBREVIATIONS

ABA	abscisic acid
AFLP	amplified fragment length polymorphism
AHS	auxin hydrogen symporter
ARF	auxin response factor
AUX/IAA	auxin/indole-3-acetic acid
AZ	abscission zone
CP	central pedicel
CTAB	cetyltrimethyl ammonium bromide
DAFB	days after full bloom
DEG	differentially expressed gene
EST	expressed sequence tag
FB	full bloom
GO	gene ontology
LP	lateral pedicel
MADS	*MCM1, AGAMOUS, DEFICIENS, SRF*
NGS	next generation sequencing
PCR	polymerase chain reaction
qRT-PCR	quantitative real-time reverse-transcription polymerase chain reaction
RACE	rapid amplification of cDNA end
RPKM	reads per kilobase per million
SHY2	*SHORT HYPOCOTYL2*
SLR	*SOLITARY-ROOT*
SVP	*SHORT VEGETATIVE PHASE*

GENERAL INTRODUCTION

Apple (*Malus* × *domestica* Borkh.) which belong to the genus *Malus* and the subfamily of Maloideae in the family of Rosaceae, is the most agronomically important fruit tree in temperature regions. It is the pome fruit, a false fruit developed from enlarged floral tube and fleshy receptacle, which is the region below the whorl of sepals in apple flower. Vavilov (1930) suggested that the wild apple of Turkestan (Kazakstan, Krygystan, Uzbekistan, Turkmenistan, and Tajikistan) and its close relatives were the progenitors of the domesticated apple. Janick et al. (1996) reported that apple tree originated from Tian Shan region in Kazakstan, Central Asia (formerly Alma-Ata). The various species including the wild ancestor of domesticated apple, *M. sieversii*, have been still found in this region (Mabberley et al., 2001). The genus *Malus* consists of approximately 55 species, including *M.* × *domestica* (Phipps et al., 1990). The *Malus* species are highly diverse, because they have a tendency to hybridize each other easily in *Malus* genus. Additionally, many species are composed of small fruited crabapples with polyploidization and apomixis characteristic.

During domestication of plants, species with lower abscission characteristic have been selected (Doebley et al., 2006; Li et al., 2006; Lin et al., 2012; Nakano and Ito, 2013). However, the abscission characteristic is especially worthy of attention in modern agriculture. Tomato (*Solanum lycopersicum*) mutants that do not have abscission zone (AZ) at pedicel

have replaced into abscission-competent tomato cultivars for industrial processing of puree or juice (Nakano and Ito, 2013). Similarly, saving labor and time is always needed in fruit crop cultivation.

The self-abscising characteristic of apple fruit is a prominent labor-saving trait during cultivation. The ‘Saika’ cultivar was selected as a self-fruit-thinning cultivar at the Aomori Apple Experiment Station, Japan (Kon et al., 2000). ‘Saika’ was originated from a cross between ‘Akane’ and ‘Orin’, and has widely been distributed as ‘Aori No. 9’. Its self-abscising characteristic resulted from ‘Akane’, which has been extensively used in breeding program for self-abscission and ‘Orin’ is a donor with commercial fruit quality. ‘Saika’ fruits form a hierarchy within a cluster, and the hierarchy is the order in which the flowers are pollinated and developed into fruit.

The first self-abscising hybrid which is originated through planned breeding program might be released from Institut National de la Recherche Agronomique (INRA), France. Up to now, INRA published two papers regarding the self-abscising selections. Based on microarray experiments using the hybrid ‘X3177’, Celton et al. (2014a) reported that additional amphivasal vascular bundles transport sugars toward central fruit, and they allow central fruit to develop dominance over lateral fruits. In addition, the candidate genes which control self-abscising trait were revealed by quantitative trait loci analyses using the hybrid ‘X3263’ and they were involved in fruit nutrition, xylem differentiation, responses to starvation, and organ abscission (Celton et al., 2014b).

To investigate abscission-related genes during early fruit abscission and ultimately introduce this characteristic into apple breeding programs, screening of apple genetic resources was conducted according to the abscission patterns within 30 days after full bloom (Chapter I). Like *JOINTLESS* gene in tomato, the homologue which develops the AZ was investigated in the pedicel of apple (Chapter II). Transcriptome analysis was performed to reveal the differentially expressed genes (DEGs) between surviving central pedicel (CP) and abscised lateral pedicel (LP) from self-abscising apple ‘Saika’ (Chapter III).

LITERATURE REVIEW

Abscission Mechanism

Abscission includes four steps: (1) differentiation of AZ, (2) acquisition of competence to respond to abscission-promoting signals during the pre-abscission stage, (3) activation of abscission, and (4) sealing of breaks in the proximal region (Nakano et al., 2013; Patterson, 2001). The generally accepted model is that a basipetal transport of indole-3-acetic acid (IAA) through the AZ prevents abscission process by changing the AZ insensitive to ethylene (Bangerth, 2000; Meir et al., 2010). If the IAA source is removed, the AZ becomes sensitive to ethylene and abscission process begins (Addicott, 1982; Meir et al., 2006). Accordingly, cell wall-degrading enzymes, such as cellulase, polygalacturonase, expansin, and xyloglucan endohydrolase, and endotransglycosylase, increased to break down cell adhesion (Cai and Lashbrook, 2008; Lashbrook and Cai, 2008; Roberts and Gonzalez-Carranza, 2009).

IAA deficiency led to up-regulate or down-regulate IAA-responsive genes in early phase of abscission (Meir et al., 2010). These genes induced the expression of transcription factors or post-translation regulators and AZ-specific genes. Then, the AZ became ethylene-sensitive, and acquired the abscission competence. In late phase of abscission, the abscission process was executed by genes which were specifically up-regulated in the AZ, such as cell wall-degrading enzymes (Meir et al., 2010).

Differentiation of AZ

AZ differentiation may be regulated by several genes and transcription factors. In tomato, *LATERAL SUPRRESSOR* (*Ls*) which encodes a member of VHIID protein family (Schumacher et al., 1999) is required for the AZ development of pedicels (Cai and Lashbrook, 2008). From the analyses of AZ mutant tomatoes, moreover, *JOINTLESS* is known to play a crucial role in the AZ development of pedicels (Mao et al., 2000). *JOINTLESS* was reported to interact with other MADS-box genes, *MACROCALYX* and *SEPALLATA* (*SLMBP21*), forming protein complexes to specify formation of the AZ (Liu et al., 2014; Nakano et al., 2012). *SLMBP21* may act as a glue in order to attach *JOINTLESS* and *MACROCALYX*, like *SEPALLATA* gene in quartet model describing floral organ formation (Liu et al., 2014).

In *Arabidopsis*, the double mutant in transcription factors *BLADE-ON-PETIOLE 1* (*BOP1*) and *BOP2* showed that the floral organs were not abscised even after senescence and wilting (McKim et al., 2008). *BOP1* and *BOP2*, which encode BTB/POZ domain and ankyrin repeat-containing proteins, regulate redundantly the differentiation of AZ in floral organs (McKim et al., 2008).

In rice, the differentiation of AZ in pedicels was found to be regulated by *SHATTERING 4* (*SH4*) (Li et al., 2006), *qSH1* (Konishi et al., 2006), and *SHATTERING ABORTION 1* (*SHAT1*) (Zhou et al., 2012). *SH4* and *qSH1* were identified as positive regulators to activate the AZ at the pedicel. *qSH1* is a BELL homeobox gene like *REPLUMLESS* (or *VAAMANA*), while *SH4* encodes a protein having Myb3 DNA binding domain. *SHAT1* which belongs

to AP2 transcription factor family is also reported to be involved in shattering rice grain.

Abscission-Related Genes

Tomato ethylene receptor (*tETR*) mRNA which is the same as *never ripe* (*nr*) gene was increased in the AZ and seemed to mediate ethylene sensitivity by modulating its levels during AZ development (Payton et al., 1996). The *green ripe* (*gr*) and *nr2* mutants of tomato showed delayed abscission and senescence by reduced expression of ethylene receptor *LeETR1* (Barry et al., 2005; Whitelaw et al., 2002; Yen et al., 1995). Although ethylene was revealed to be not essential to proceed abscission process, it can accelerate abscission under ethylene-dependent pathway (Patterson and Bleecker, 2004). Furthermore, abscission process is unrelated to expression level of ethylene receptors (Meir et al., 2006).

Overexpression of MADS-box gene, *AGAMOUS-like 15* (*AGL15*) resulted in retardation of abscission and transition to reproductive phase (Fernandez et al., 2000). Leucine-rich repeat receptor kinase genes, *HAESA* (*HAE*, *Arabidopsis*) and *GmSARK* (soybean), are involved in regulation of floral abscission and leaf senescence in ethylene-independent manner (Jinn et al., 2000; Li et al., 2006). The expression of *HAE* is not altered in *etr1-1* (ethylene-insensitive) mutant and in response to treatment with an ethylene precursor, 1-aminocyclopropane-1-carboxylic acid (Jinn et al., 2000). Comparing five *dab* (delayed floral organ abscission) mutants (*dab1-1*, *dab2-1*, *dab3-1*, *dab3-2*, and *dab3-3*) with ethylene-insensitive mutants *etr1-1* and *ein2-1*, ethylene was confirmed to be not an initiator for

activation of floral organ abscission (Patterson and Bleecker, 2004).

The ethylene sensitive mutant of *inflorescence deficient in abscission* (*ida*) which encodes a ligand with an N-terminal signal peptide remained floral organs attached to plant body after shedding of mature seeds and development of AZs (Butenko et al., 2003). The *IDA* gene is suggested to be involved in ethylene-independent pathway that controls floral abscission (Butenko et al., 2003). Constitutively overexpressing *35S*:*IDA* line exhibited earlier abscission of floral organs and differentiation of AZs initiated after bloom stage. *HAE* and *HEASA-like 2* (*HLS2*) were identified as receptor-like kinases for a ligand *IDA* (Jinn et al., 2000; Stenvik et al., 2008) and mitogen-activated-protein kinase signaling cascade plays an important roles in plant response to pathogens, hormone responses, and regulation of abscission (Cho et al., 2008). The signaling pathway for floral abscission was established from putative ligand (*IDA*) and receptors (*HAE* and *HSL2*) to cytoplasmic effectors (*MKK4*, *MKK5*, *MPK3*, and *MPK6*) (Cho et al., 2008).

Other genes influencing abscission abnormality were discovered by genetic modification researches. Two *NONEXPRESSOR OF PR GENES1* (*NPR1*)-like gene mutants lost floral organ abscission which are members of a gene family containing ankyrin repeats (Hepworth et al., 2005). *Hawaiian skirt* (*hws*) mutant that partially deleted in the F-box gene failed to abscise flowers where individual sepals are fused along the lower part of their margins in *Arabidopsis* (González-Carranza et al., 2007). Showing similar aspect like *hws*, abscission of *ZINC FINGER PROTEIN 2* (*AtZFP2*) mutant was also delayed in floral organs with altered floral morphology (Cai

and Lashbrook, 2008).

A loss-of-function mutation in *AUXIN RESPONSE FACTOR 2* (*ARF2*) exhibited delays in flowering, leaf senescence, and floral organ abscission (Ellis et al., 2005). The transcriptions of *ACS2*, *ACS6*, and *ACS8* that are possible to engage with floral senescence and abscission were down-regulated in *arf2-6* mutant. *ARF2* may participate not only in auxin signaling, but also in ethylene response (Okushima et al., 2005).

Meir et al. (2006) examined to identify DEGs in *Mirabilis jalapa* AZs with the removal of IAA source and the application of exogenous hormone. The expressions of *Mj-AUXIN/INDOLE-3-ACETIC ACID 1 (AUX/IAA1)* and *Mj-AUX/IAA2* were repressed by leaf deblading and stem decapitation with polygalacturonase inhibitor protein, β-expansin, and β-tubulin. On the contrary, several genes associated with ethylene or stress response and unknown sequences were up-regulated in the AZ following deblading/decapiatation or the application of naphthylphthalamic acid, an inhibitor of ethylene. In addition, sucrose accelerated abscission process and induced some of the up-regulated genes in the stem stump (Meir et al., 2006).

In cestrum (*Cestrum elegans*), synthetic auxins, such as 1-naphthaleneacetic acid and 2,4-dichlorophenoxyacetic acid, were applied to reduce floret abscission, confirming that the application of auxins on floret abscission induces the expression of *AUX/IAA* genes in the AZs. *Ce-IAA5* of six *AUX/IAA* homologous genes was specifically up-regulated in floret bud AZ and regulation of the abscission process might require expression of specific *AUX/IAA* gene (Abebie et al., 2008).

The gene expression profiling was performed by microarray analysis with tomato flowers that acquired abscission competence following auxin depletion (Meir et al., 2010). According to the postulated abscission model, tomato pedicel abscission is progressed in two steps, early (regulatory responses) and late (abscission execution) phases. In early phases, the down-regulated genes were directly affected by IAA depletion, such as *AUX/IAA* genes and transcription factors (*knotted*, *HAT*, and *bHLH*). The up-regulated genes after IAA depletion are *PK7*, *ERF1c*, *WRKY IId-1*, and protein phosphatase. Other transcription factors which were regulated by the modified IAA-related genes, were also expressed. In late phases, the AZ specific genes were expressed as if ethylene production increased in the AZ: Set I, genes related to ethylene signal transduction or abscission regulators, *ETR4*, *CTR1*, *EFT1c*, and others; Set II, genes encoding cell wall-modifying proteins; Set III, genes involved in pathogenesis-related defense and others.

MADS-Box Genes

MADS-box transcription factors are the family of DNA-binding proteins conserved in plants, fungi, and animals. MADS-box gene is composed of the N-terminal M(MADS) domain, followed by the I (intervening), K (keratin like), and C (carboxyl-terminal) domains. Generally, MADS-box genes contribute to the reproductive development, including the control of flowering time, floral organ identity, and floral meristem identity in plants. However, some MADS-box genes play multiple roles in flower development,

and in vegetative development. In tomato, *JOINTLESS* controls the AZ development in pedicels (Mao et al., 2000). *MdMADS4* from the apple 'Fuji' was highly expressed in the vascular bundles in the floral tube and the carpellary vascular bundles in the fruit at early developmental stages (Sung et al., 2000). *SHATTERPROOF1* (*SHP1*) and *SHP2* were involved in AZ differentiation (Liljegren et al., 2000).

MADS-Box Genes in Apple

A total of 147 MADS-box genes were included in the apple genome (Velasco et al., 2010). Among MADS-box genes in apple, three apple genes belonged to *StMADS11* (or *SHORT VEGETATIVE PHASE* (*SVP*)) subclade, closed to *Arabidopsis SVP* and *AGAMOUS-LIKE 24* (*AGL24*) (Velasco et al., 2010). *SVP* and *AGL24* are known to regulate floral transition and floral meristem identity (Gregis et al., 2008). Moreover, ectopic overexpression of *SVP* and several other *StMADS11* members causes the development of leaf-like sepals, suggesting that *SVP* plays a role in the regulation of sepal development (He et al., 2004; Masiero et al., 2004).

Apple Genomics

Apple 'Golden Delicious' has 742.3 Mb per haploid genome through BAC library sequencing and 454 pyrosequencing by Velasco et al. (2010). Only 103,076 contigs were assembled into 1,629 metacontigs which cover about 81.3% of the apple genome. Metacontigs were anchored to 17

linkage groups based on 1,643 markers. The total number of genes was estimated to be 57,386. However, pear (*Pyrus bretschneideri*) has only about 42,000 genes (Wu et al., 2013). Wu et al. (2013) suggested the number of apple genes might drop down to 45,293. Similarly, in other close relatives, peach (*Prunus persica*) and strawberry (*Fragaria vesca*) have 27,852 and 34,809 genes, respectively (Shulaev et al., 2011; The International Peach Genome Initiative, 2013). Therefore, the number of apple genes suggested by Wu et al. (2013) would be more consistent with gene numbers of other Rosaceae family, considering genome sizes of each genus in Rosaceae family.

Apple has a haploid chromosome set of x = 17, whereas other members of Rosaceae are x = 8 (Amygdaleoideae) or x = 9 (Spiraeoideae) (Velasco et al., 2010). Thus, apple has long been considered to be originated from allopolyploidization between species related to Amygdaleoideae and Spiraeoideae (Chevreau et al., 1985) or from autopolyploidization of a Spiraeoideae ancestor and the subsequent loss of one chromosome (Campbell et al., 1995). Apple genome research supported the autopolyploidization hypothesis and revealed that apple genome derives from a gillenia-like progenitor (Velasco et al., 2010). Genome-wide duplication has resulted from nine ancestral chromosomes to 17 chromosomes between 60 and 65 million years ago.

Apple Transcriptomics

Microarray has been used to show the gene expression profile in apple buds and fruits (Costa et al., 2010; Janssen et al., 2008; Vimolmangkang et al., 2014) and to find DEGs related to fruit abscission (Botton et al., 2011; Celton et al., 2014a; Giulia et al., 2013; Zhu et al., 2011). Zhu et al. (2011) compared the gene expression patterns between fruit abscission induced by shading and a synthetic auxin treatment. Botton et al. (2011) and Giulia et al. (2013) showed that sugar starvation was a more important trigger of fruit abscission. Sugar starvation mediated reactive oxygen species accumulation, and abscisic acid (ABA) and ethylene signaling, resulting in activation of the abscission process (Botton et al., 2011). Furthermore, the abscission process accompanied an increase in ABA content (Giulia et al., 2013). Celton et al. (2014a) performed microarray experiments with CP and LP from self-abscising apple hybrid 'X3177'.

First apple expressed sequence tag (EST) analysis was conducted by Newcomb et al. (2006), and they identified about 43,000 non-redundant ESTs. Sanzol (2010) assembled 116,879 EST sequences from 'Royal Gala' cDNA libraries and identified 33,211 unigenes. A cDNA-amplified fragment length polymorphism (AFLP) analysis was used to identify DEGs between abscising and non-abscising fruitlets using benzylaminopurine spray (Dal Cin et al., 2009). Additionally, cDNA-AFLP analysis was also used for investigating rootstock effects (Jensen et al., 2003) and interaction between apple and fire blight (*Erwinia amylovora*) (Baldo et al., 2010). Suppression

subtractive hybridization method was performed to identify DEGs after infection with apple scab (*Venturia inaequalis*) (Degenhardt et al., 2005).

Recently, transcriptome analysis has been progressed with the application of next generation sequencing equipments. Transcriptome sequencing (RNA-Seq) generates digital read counts by mapping mRNA sequences to reference transcriptome (Korf, 2013; Wang et al., 2009). RNA-Seq has been applied to identify candidate genes for apple scab resistance (Gusberti et al., 2013), and to investigate gene expression patterns in columnar apple primary roots (Petersen et al., 2015).

LITERATURE CITED

Abebie, B., A. Lers, S. Philosoph-Hadas, R. Goren, J. Riov, and S. Meir. 2008. Differential effects of NAA and 2,4-D in reducing floret abscission in cestrum (*Cestrum elegans*) cut flowers are associated with their differential activation of *Aux/IAA* homologous genes. Ann. Bot. 101:249-259.

Addicott, F.T. 1982. Abscission. Univ. of California Press, Berkeley, CA, USA, p. 113-140.

Baldo, A., J.L. Norelli, R.E. Farrell, Jr., C.L. Bassett, H.S. Aldwinckle, and M. Malnoy. 2010. Identification of genes differentially expressed during interaction of resistant and susceptible apple cultivars (*Malus* x *domestica*) with *Erwinia amylovora*. BMC Plant Biol. 10:1.

Bangerth, F. 2000. Abscission and thinning of young fruit and their regulation by plant hormones and bioregulators. Plant Growth Regul. 31:43-59.

Barry, C.S., R.P. McQuinn, A.J. Thompson, G.B. Seymour, D. Grierson, and J.J. Giovannoni. 2005. Ethylene insensitivity conferred by the Green-ripe and Never-ripe 2 ripening mutants of tomato. Plant Physiol. 138:267-275.

Botton, A., G. Eccher, C. Forcato, A. Ferrarini, M. Begheldo, M. Zermiani, S. Moscatello, A. Battistelli, R. Velasco, B. Ruperti, and A. Ramina. 2011. Signaling pathways mediating the induction of apple fruitlet abscission. Plant Physiol. 155:185-208.

Butenko, M.A., S.E. Patterson, P.E. Grini, G.E. Stenvik, S.S. Amundsen, A. Mandal, and R.B. Aalen. 2003. *INFLORESCENCE DEFICIENT IN ABSCISSION* controls floral organ abscission in *Arabidopsis* and

identifies a novel family of putative ligands in plants. Plant Cell 15:2296-2307.

Cai, S. and C.C. Lashbrook. 2008. Stamen abscission zone transcriptome profiling reveals new candidates for abscission control: enhanced retention of floral organs in transgenic plants overexpressing *Arabidopsis ZINC FINGER PROTEIN2*. Plant Physiol. 146:1305-1321.

Campbell, C.S., M.J. Donoghue, B.G. Baldwin, and M.F. Wojciechowski. 1995. Phylogenetic relationships in Maloideae (Rosaceae): evidence from sequences of the internal transcribed spacers of nuclear ribosomal DNA and its congruence with morphology. Amer. J. Bot. 27:903-918.

Celton, J.M., E. Dheilly, M.C. Guillou, F. Simonneau, M. Juchaux, E. Costes, F. Laurens, and J.P. Renou. 2014a. Additional amphivasal bundles in pedicel pith exacerbate central fruit dominance and induce self-thinning of lateral fruitlets in apple. Plant Physiol. 164:1930-1951.

Celton, J.M., J.J. Kelner, S. Martinez, A. Bechti, A. Khelifi Touhami, M.J. James, C.E. Durel, F. Laurens, and E. Costes. 2014b. Fruit self-thinning: a trait to consider for genetic improvement of apple tree. Plos One 9:e91016.

Chevreau, E., Y. Lespinasse, and M. Gallet. 1985. Inheritance of pollen enzymes and polyploid origin of apple (*Malus* x *domestica* Borkh.). Theor. Appl. Genet. 71:268-277.

Cho, S.K., C.T. Larue, D. Chevalier, H. Wang, T.L. Jinn, S. Zhang, and J.C. Walker. 2008. Regulation of floral organ abscission in *Arabidopsis thaliana*. Proc. Natl. Acad. Sci. USA 105:15629-15634.

Costa, F., R. Alba, H. Schouten, V. Soglio, L. Gianfranceschi, S. Serra, S.

Musacchi, S. Sansavini, G. Costa, Z. Fei, and J. Giovannoni. 2010. Use of homologous and heterologous gene expression profiling tools to characterize transcription dynamics during apple fruit maturation and ripening. BMC Plant Biol. 10:229.

Dal Cin, V., E. Barbaro, M. Danesin, H. Murayama, R. Velasco, and A. Ramina. 2009. Fruitlet abscission: a cDNA-AFLP approach to study genes differentially expressed during shedding of immature fruits reveals the involvement of a putative auxin hydrogen symporter in apple (*Malus × domestica* L. Borkh.). Gene 442:26-36.

Degenhardt, J., A.N. Al-Masri, S. Kurkcuoglu, I. Szankowski, and A.E. Gau. 2005. Characterization by suppression subtractive hybridization of transcripts that are differentially expressed in leaves of apple scab-resistant and susceptible cultivars of *Malus domestica*. Mol. Genet. Genom. 273:326-335.

Doebley, J.F., B.S. Gaut, and B.D. Smith. 2006. The molecular genetics of crop domestication. Cell 127:1309-1321.

Ellis, C.M., P. Nagpal, J.C. Young, G. Hagen, T.J. Guilfoyle, and J.W. Reed. 2005. *AUXIN RESPONSE FACTOR1* and *AUXIN RESPONSE FACTOR2* regulate senescence and floral organ abscission in *Arabidopsis thaliana*. Development 132:4563-4574.

Fernandez, D.E., G.R. Heck, S.E. Perry, S.E. Patterson, A.B. Bleecker, and S.C. Fang. 2000. The embryo MADS domain factor *AGL15* acts postembryonically inhibition of perianth senescence and abscission via constitutive expression. Plant Cell 12:183-198.

Giulia, E., B. Alessandro, D. Mariano, B. Andrea, R. Benedetto, and R.

Angelo. 2013. Early induction of apple fruitlet abscission is characterized by an increase of both isoprene emission and abscisic acid content. Plant Physiol. 161:1952-1969.

Gonzalez-Carranza, Z.H., U. Rompa, J.L. Peters, A.M. Bhatt, C. Wagstaff, A.D. Stead, and J.A. Roberts. 2007. *Hawaiian skirt*: an F-box gene that regulates organ fusion and growth in *Arabidopsis*. Plant Physiol. 144:1370-1382.

Gregis, V., A. Sessa, L. Colombo, and M.M. Kater. 2008. *AGAMOUS-LIKE24* and *SHORT VEGETATIVE PHASE* determine floral meristem identity in *Arabidopsis*. Plant J. 56:891-902.

Gusberti, M., C. Gessler, and G.A. Broggini. 2013. RNA-Seq analysis reveals candidate genes for ontogenic resistance in *Malus-Venturia* pathosystem. Plos One 8:e78457.

He, C., T. Munster, and H. Saedler. 2004. On the origin of floral morphological novelties. FEBS Lett. 567:147-151.

Hepworth, S.R., Y. Zhang, S. McKim, X. Li, and G.W. Haughn. 2005. *BLADE-ON-PETIOLE*-dependent signaling controls leaf and floral patterning in *Arabidopsis*. Plant Cell 17:1434-1448.

International Peach Genome Initiative, I. Verde, A.G. Abbott, S. Scalabrin, S. Jung, S. Shu, F. Marroni, T. Zhebentyayeva, M.T. Dettori, J. Grimwood, F. Cattonaro, A. Zuccolo, L. Rossini, J. Jenkins, E. Vendramin, L.A. Meisel, V. Decroocq, B. Sosinski, S. Prochnik, T. Mitros, A. Policriti, G. Cipriani, L. Dondini, S. Ficklin, D.M. Goodstein, P. Xuan, C. Del Fabbro, V. Aramini, D. Copetti, S. Gonzalez, D.S. Horner, R. Falchi, S. Lucas, E. Mica, J. Maldonado, B. Lazzari, D. Bielenberg, R.

Pirona, M. Miculan, A. Barakat, R. Testolin, A. Stella, S. Tartarini, P. Tonutti, P. Arus, A. Orellana, C. Wells, D. Main, G. Vizzotto, H. Silva, F. Salamini, J. Schmutz, M. Morgante, and D.S. Rokhsar. 2013. The high-quality draft genome of peach (*Prunus persica*) identifies unique patterns of genetic diversity, domestication, and genome evolution. Nat. Genet. 45:487-494.

Janick, J., J.N. Cummins, S.K. Brown, and M. Hemmat. 1996. Apples, p. 1-77. In: J. Janick and J.N. Moore (eds.). Fruit breeding: tree and tropical fruits. John Wiley & Sons, New York, NY, USA.

Janssen, B.J., K. Thodey, R.J. Schaffer, R. Alba, L. Balakrishnan, R. Bishop, J.H. Bowen, R.N. Crowhurst, A.P. Gleave, S. Ledger, S. McArtney, F.B. Pichler, K.C. Snowden, and S. Ward. 2008. Global gene expression analysis of apple fruit development from the floral bud to ripe fruit. BMC Plant Biol. 8:16.

Jensen, P.J., J. Rytter, E.A. Detwiler, J.W. Travis, and T.W. McNellis. 2003. Rootstock effects on gene expression patterns in apple tree scions. Plant Mol. Biol. 53:493-511.

Jinn, T.L., J.M. Stone, and J.C. Walker. 2000. *HAESA*, an *Arabidopsis* leucine-rich repeat receptor kinase, controls floral organ abscission. Gene Dev. 14:108-117.

Kon, T., S. Sato, T. Kudo, K. Fujita, and T. Fukasawa-Akawa. 2000. Apple breeding at Aomori Apple Experiment Station, Japan. Acta Hort. 538:215-218.

Konishi, S., T. Izawa, S.Y. Lin, K. Ebana, Y. Fujuta, T. Sasaki, and M. Yano. 2006. An SNP caused loss of seed shattering during rice domestication. Science 312:1392-1396.

Korf, I. 2013. Genomics: the state of the art in RNA-Seq analysis. Nat. Methods 10:1165-1166.

Lashbrook, C.C. and S. Cai. 2008. Cell wall remodeling in *Arabidopsis* stamen abscission zones: temporal aspects of control inferred from transcriptional profiling. Plant Signal. Behav. 3:733-736.

Li, C., A. Zhou, and T. Sang. 2006. Rice domestication by reducing shattering. Science 311:1936-1939.

Liljegren, S.J., G.S. Ditta, Y. Eshed, B. Savidge, J.L. Bowman, and M.F. Yanofsky. 2000. *SHATTERPROOF* MADS-box genes control seed dispersal in *Arabidopsis*. Nature 404:766-770.

Lin, Z., X. Li, L.M. Shannon, C.T. Yeh, M.L. Wang, G. Bai, Z. Peng, J. Li, H.N. Trick, T.E. Clemente, J. Doebley, P.S. Schnable, M.R. Tuinstra, T.T. Tesso, F. White, and J. Yu. 2012. Parallel domestication of the *Shattering1* genes in cereals. Nat. Genet. 44:720-724.

Liu, D., D. Wang, Z. Qin, D. Zhang, L. Yin, L. Wu, J. Colasanti, A. Li, and L. Mao. 2014. The *SEPALLATA* MADS-box protein *SLMBP21* forms protein complexes with *JOINTLESS* and *MACROCALYX* as a transcription activator for development of the tomato flower abscission zone. Plant J. 77:284-296.

Mabberley, D.J., C.E. Jarvis, and B.E. Juniper. 2001. The name of the apple. Telopea 9:421-430.

Mao, L., D. Begum, H.W. Chuang, M.A. Budiman, E.J. Szymkowiak, E.E.

Irish, and R.A. Wing. 2000. *JOINTLESS* is a MADS-box gene controlling tomato flower abscission zone development. Nature 406:910-913.

Masiero, S., M.A. Li, I. Will, U. Hartmann, H. Saedler, P. Huijser, Z. Schwarz-Sommer, and H. Sommer. 2004. *INCOMPOSITA*: a MADS-box gene controlling prophyll development and floral meristem identity in *Antirrhinum*. Development 131:5981-5990.

McKim, S., G.E. Stenvik, M.A. Butenko, W. Dristiansen, S.K. Cho, S.R. Hepworth, R.B. Aalen, and G.W. Haughn. 2008. The *BLADE-IN-PETIOLE* genes are essential for abscission zone formation in *Arabidopsis*. Development 135:1537-1546.

Meir, S., D.A. Hunter, J.C. Chen, V. Halaly, and M.S. Reid. 2006. Molecular changes occurring during acquisition of abscission competence following auxin depletion in *Mirabilis jalapa*. Plant Physiol. 141:1604-1616.

Meir, S., S. Philosoph-Hadas, S. Sundaresan, K.S. Selvaraj, S. Burd, R. Ophir, B. Kochanek, M.S. Reid, C.Z. Jiang, and A. Lers. 2010. Microarray analysis of the abscission-related transcriptome in the tomato flower abscission zone in response to auxin depletion. Plant Physiol. 154:1929-1956.

Nakano, T. and Y. Ito. 2013. Molecular mechanisms controlling plant organ abscission. Plant Biotechnol. 30:209-216.

Nakano, T., J. Kimbara, M. Fujisawa, M. Kitagawa, N. Ihashi, H. Maeda, T. Kasumi, and Y. Ito. 2012. *MACROCALYX* and *JOINTLESS* interact in the transcriptional regulation of tomato fruit abscission zone development. Plant Physiol. 158:439-450.

Nakano, T., M. Fujisawa, Y. Shima, and Y. Ito. 2013. Expression profiling of tomato pre-abscission pedicels provides insights into abscission zone properties including competence to respond to abscission signals. BMC Plant Biol. 9:13-40.

Newcomb, R.D., R.N. Crowhurst, A.P. Gleave, E.H. Rikkerink, A.C. Allan, L.L. Beuning, J.H. Bowen, E. Gera, K.R. Jamieson, B.J. Janssen, W.A. Laing, S. McArtney, B. Nain, G.S. Ross, K.C. Snowden, E.J. Souleyre, E.F. Walton, and Y.K. Yauk. 2006. Analyses of expressed sequence tags from apple. Plant Physiol. 141:147-166.

Okushima, Y., I. Mitina, H.L. Quach, and A. Theologis. 2005. *AUXIN RESPONSE FACTOR 2* (*ARF2*): a pleiotropic developmental regulator. Plant J. 43:29-46.

Patterson, S.E. 2001. Cutting loose: abscission and dehiscence in *Arabidopsis*. Plant Physiol. 126:494-500.

Patterson, S.E. and A.B. Bleecker. 2004. Ethylene-dependent and -in dependent processes associated with floral organ abscission in *Arabidopsis*. Plant Physiol. 134:194-203.

Payton, S., R.G. Fray, S. Brown, and D. Grierson. 1996. Ethylene receptor expression is regulated during fruit ripening, flower senescence, and abscission. Plant Mol. Biol. 31:1227-1231.

Petersen, R., H. Djozgic, B. Rieger, S. Rapp, and E. Schmidt. 2015. Columnar apple primary roots share some features of the columnar-specific gene expression profile of aerial plant parts as evidenced by RNA-Seq analysis. BMC Plant Biol. 15:34.

Phipps, J.B., K.R. Robertson, P.G. Smith, and J.R. Rohrer. 1990. A checklist

of the subfamily Maloideae (Rosaceae). Can. J. Bot. 68:2209-2269.

Roberts, J.A. and Z.H. Gonzalez-Carranza. 2009. Pectinase functions in abscission. Stewart Postharvest Rev. 1:1-4.

Sanzol, J. 2010. Dating and functional characterization of duplicated genes in the apple (*Malus* × *domestica* Borkh.) by analyzing EST data. BMC Plant Biol. 10:87.

Schumacher, K., T. Schmitt, M. Rossberg, G. Schmitz, and K. Theres. 1999. The *Lateral suppressor* (*Ls*) gene of tomato encodes a new member of the VHIID protein family. Proc. Natl. Acad. Sci. USA 96:290-295.

Shulaev, V., D.J. Sargent, R.N. Crowhurst, T.C. Mockler, O. Folkerts, A.L. Delcher, P. Jaiswal, K. Mockaitis, A. Liston, S.P. Mane, P. Burns, T.M. Davis, J.P. Slovin, N. Bassil, R.P. Hellens, C. Evans, T. Harkins, C. Kodira, B. Desany, O.R. Crasta, R.V. Jensen, A.C. Allan, T.P. Michael, J.C. Setubal, J.M. Celton, D.J. Rees, K.P. Williams, S.H. Holt, J.J. Ruiz Rojas, M. Chatterjee, B. Liu, H. Silva, L. Meisel, A. Adato, S.A. Filichkin, M. Troggio, R. Viola, T.L. Ashman, H. Wang, P. Dharmawardhana, J. Elser, R. Raja, H.D. Priest, D.W. Bryant, Jr., S.E. Fox, S.A. Givan, L.J. Wilhelm, S. Naithani, A. Christoffels, D.Y. Salama, J. Carter, E. Lopez Girona, A. Zdepski, W. Wang, R.A. Kerstetter, W. Schwab, S.S. Korban, J. Davik, A. Monfort, B. Denoyes-Rothan, P. Arus, R. Mittler, B. Flinn, A. Aharoni, J.L. Bennetzen, S.L. Salzberg, A.W. Dickerman, R. Velasco, M. Borodovsky, R.E. Veilleux, and K.M. Folta. 2011. The genome of woodland strawberry (*Fragaria vesca*). Nat. Genet. 43:109-116.

Stenvik, G.E., N.M. Tandstad, Y. Guo, C.L. Shi, W. Kristiansen, A. Holmgren, S.E. Clark, R.B. Aalen, and M.A. Butenko. 2008. The EPIP peptide of

INFLORESCENCE DEFICIENT IN ABSCISSION is sufficient to induce abscission in *Arabidopsis* through the receptor-like kinases *HAESA* and *HAESA-LIKE2*. Plant Cell 20:1805-1817.

Sung, S.K., G.H. Yu, J. Nam, D.H. Jeong, and G. An. 2000. Developmentally regulated expression of two MADS-box genes, *MdMADS3* and *MdMADS4*, in the morphogenesis of flower buds and fruits in apple. Planta 210:519-528.

Vavilov, N.I. 1930. Wild progenitors of the fruit trees of Turkistan and the Caucasus and the problem of the origin of fruit trees. Intl. Hort. Congr. Group B 271-286.

Velasco, R., A. Zharkikh, J. Affourtit, A. Dhingra, A. Cestaro, A. Kalyanaraman, P. Fontana, S.K. Bhatnagar, M. Troggio, D. Pruss, S. Salvi, M. Pindo, P. Baldi, S. Castelletti, M. Cavaiuolo, G. Coppola, F. Costa, V. Cova, A. Dal Ri, V. Goremykin, M. Komjanc, S. Longhi, P. Magnago, G. Malacarne, M. Malnoy, D. Micheletti, M. Moretto, M. Perazzolli, A. Si-Ammour, S. Vezzulli, E. Zini, G. Eldredge, L.M. Fitzgerald, N. Gutin, J. Lanchbury, T. Macalma, J.T. Mitchell, J. Reid, B. Wardell, C. Kodira, Z. Chen, B. Desany, F. Niazi, M. Palmer, T. Koepke, D. Jiwan, S. Schaeffer, V. Krishnan, C. Wu, V.T. Chu, S.T. King, J. Vick, Q. Tao, A. Mraz, A. Stormo, K. Stormo, R. Bogden, D. Ederle, A. Stella, A. Vecchietti, M.M. Kater, S. Masiero, P. Lasserre, Y. Lespinasse, A.C. Allan, V. Bus, D. Chagne, R.N. Crowhurst, A.P. Gleave, E. Lavezzo, J.A. Fawcett, S. Proost, P. Rouze, L. Sterck, S. Toppo, B. Lazzari, R.P. Hellens, C.E. Durel, A. Gutin, R.E. Bumgarner, S.E. Gardiner, M. Skolnick, M. Egholm, Y. Van de Peer, F. Salamini, and R. Viola. 2010.

The genome of the domesticated apple (*Malus* × *domestica* Borkh.). Nat. Genet. 42:833-839.

Vimolmangkang, S., D. Zheng, Y. Han, M.A. Khan, R.E. Soria-Guerra, and S.S. Korban. 2014. Transcriptome analysis of the exocarp of apple fruit identifies light-induced genes involved in red color pigmentation. Gene 534:78-87.

Wang, Z., M. Gerstein, and M. Snyder. 2009. RNA-Seq: a revolutionary tool for transcriptomics. Nat. Rev. Genet. 10:57-63.

Whitelaw, C.A., N.N. Lyssenko, L. Chen, D. Zhou, A.K. Mattoo, and M.L. Tucker. 2002. Delayed abscission and shorter internodes correlate with a reduction in the ethylene receptor *LeETR1* transcript in transgenic tomato. Plant Physiol. 128:978-987.

Wu, J., Z. Wang, Z. Shi, S. Zhang, R. Ming, S. Zhu, M.A. Khan, S. Tao, S.S. Korban, H. Wang, N.J. Chen, T. Nishio, X. Xu, L. Cong, K. Qi, X. Huang, Y. Wang, X. Zhao, J. Wu, C. Deng, C. Gou, W. Zhou, H. Yin, G. Qin, Y. Sha, Y. Tao, H. Chen, Y. Yang, Y. Song, D. Zhan, J. Wang, L. Li, M. Dai, C. Gu, Y. Wang, D. Shi, X. Wang, H. Zhang, L. Zeng, D. Zheng, C. Wang, M. Chen, G. Wang, L. Xie, V. Sovero, S. Sha, W. Huang, S. Zhang, M. Zhang, J. Sun, L. Xu, Y. Li, X. Liu, Q. Li, J. Shen, J. Wang, R.E. Paull, J.L. Bennetzen, J. Wang, and S. Zhang. 2013. The genome of the pear (*Pyrus bretschneideri* Rehd.). Genome Res. 23:396-408.

Yen, H.C., S. Lee, S.D. Tanksley, M.B. Lanahan, H.J. Klee, and J.J. Giovannoni. 1995. The tomato *Never-ripe* locus regulates ethylene-inducible gene expression and is linked to a homolog of the *Arabidopsis ETR1* gene. Plant Physiol. 107:1343-1353.

Zhou, Y., D. Lu, C. Li, J. Luo, B.F. Zhu, J. Zhu, Y. Shangguan, Z. Wang, T. Sang, B. Zhou, and B. Han. 2012. Genetic control of seed shattering in rice by the *APETALA2* transcription factor *SHATTERING ABORTION1*. Plant Cell 24:1034-1048.

Zhu, H., C.D. Dardick, E.P. Beers, A.M. Callanhan, R. Xia, and R. Yuan. 2011. Transcriptomics of shading-induced and NAA-induced abscission in apple (*Malus* × *domestica*) reveals a shared pathway involving reduced photosynthesis, alterations in carbohydrate transport and signaling and hormone crosstalk. BMC Plant Biol. 11:138.

CHAPTER 1

Classification of Apple Genetic Resources According to Early Fruit Abscission Patterns

ABSTRACT

Based on the fruit abscission pattern from full bloom (FB) to 30 days after full bloom, 48 apple genetic resources were classified into three groups: 1) a non-abscising group, in which no fruits are abscised; 2) a June drop group, in which the abscission process occurs non-selectively in clusters; and 3) a self-abscising group, in which only central or last fruit in a cluster remains to grow, and the others are abscised. Most cultivars in the self-abscising group showed a fruit abscission pattern, in which central fruit dominated over lateral fruits in a cluster, inducing their growth inhibition and final abscission. Exceptionally, in *Malus coronaria* 'Charlottae', central fruit could not dominate lateral fruits, but was abscised first in a cluster. The date of FB and fruit weight were significantly related to fruit abscission. The earlier the date of FB and the smaller the fruit in the abscission groups were, the less early fruit abscission occurred.

INTRODUCTION

Apple trees generally produce excess fruitlets to the extent, so that the trees are not able to maintain the fruit load. Fruit thinning is an essential practice for producing apples of commercial size and quality (Dennis, Jr., 2000). However, chemical thinning results in considerable variability in efficacy depending on environmental conditions (Wertheim, 2000). Furthermore, thinning chemicals sometimes have harmful side effects including tree vigor and yield reduction (Black et al., 1995; Marini, 1996), fruit malformation and russetting (Bound et al., 1993), and reduction of pollinating insect population (Dennis, Jr., 2000). In small-scale cultivation, hand thinning is often practiced to obtain bigger, higher-quality fruit, but it is labor- and time-intensive. Because self-abscising cultivars can be an effective alternative and suit modern apple production, the development of cultivars with this characteristic has recently been implemented in breeding programs.

Early fruit abscission is characterized by the survival of only one fruit in a cluster, while the other fruits are abscised within 30 days after full bloom (DAFB). Early fruit abscission is induced by competition occurring among fruitlets in a cluster (intra-fruitlet), among fruitlets throughout the entire tree (inter-fruitlet), and between fruitlets and bourse shoots (Bangerth, 2000). Although many factors are associated with the induction of fruit abscission, the interplay between auxin and ethylene has long been thought to trigger fruit abscission (Abebie et al., 2008; Abeles and Rubinstein, 1964; Sexton, 1997; Taylor and Whitelaw, 2001). Ethylene production is reported to

activate abscission by increasing the expression of hydrolytic enzymes and by decreasing auxin transport according to the model of senescence-triggered abscission based on leaf explants (Bonghi et al., 1993; Suttle and Hultstrand, 1991). However, this model cannot be applied to the abscission of young apple fruit, because no increase in ethylene production is observed at the early stages of abscission (Bangerth, 2000; Sun et al., 2009). Bangerth (2000) proposed a correlative inhibition model, suggesting that central fruit, which blooms first in a cluster, dominates auxin export by repressing transport from adjacent lateral fruits. The growth of dominated fruits is inhibited and their abscission is initiated, resulting in programmed organ shedding.

Inter-fruitlets or intra-fruitlets carbohydrate competition could lead to sugar starvation in abscising fruitlets, because fruitlets having lower sink strength abscised more readily (Botton et al., 2011; Iwanami et al., 2012; Lakso et al., 2006). Apple microarray experiments have suggested that sugar starvation, rather than auxin transport, is a more important trigger of fruit abscission. Sugar starvation mediates reactive oxygen species accumulation, and abscisic acid (ABA) and ethylene signaling, resulting in activation of the abscission process (Botton et al., 2011). Furthermore, the abscission process accompanies an increase in ABA content (Giulia et al., 2013).

To investigate abscission-related characteristics during early fruit development and ultimately introduce these characteristics into breeding programs, the abscission patterns of 48 representative apple cultivars (*Malus* × *domestica* Borkh.) and *Malus* species were evaluated. The apple

genetic resources were classified according to their fruit abscission pattern based on the numbers of fruits persisting from full bloom (FB) to 30 DAFB, and they were examined in terms of the date of FB and fruit weight.

MATERIALS AND METHODS

Forty eight apple genotypes were grown at the orchard of the National Institute of Horticultural and Herbal Science, Suwon, Korea. Their early fruit abscission patterns were evaluated from FB until 30 DAFB by counting persisting fruits. The number of remaining fruits were counted from 100 fruitlets of different cultivars or species. Five to ten trees of each cultivar or species were used to evaluate the early fruit abscission patterns. The dates of FB were recorded following the examination references of fruit trees in the Rural Development Administration, Korea. The date was defined as the observation date when at least 90% of the flowers throughout the tree bloomed. Fruits were weighed at 30 DAFB. All flowers were hand-pollinated with mixed pollens collected from various cultivars to avoid self-incompatibility resulting from the same S-genotypes.

RESULTS AND DISCUSSION

According to the patterns of fruit abscission within 30 DAFB, the 48 apple genetic resources could be categorized into three groups (Table 1-1): 1) a non-abscising group, in which no fruit is abscised; 2) a June drop group, in which the abscission process occurs non-selectively in clusters; and 3) a self-abscising group, in which only central or last fruit in a cluster remains to grow and the others are abscised. Most crabapples belonged to the non-abscising group, and non-abscised fruits even adhered to the peduncles in their dried form until the following year. No abscission occurred in this group, suggesting that the abscission mechanism is abolished or disrupted in the course of abscission. For example, few fruits abscised in the non-abscising cultivar *M. baccata* 'Manchurian' (Fig. 1-1). The majority of commercial cultivars were included in the June drop group. Their abscission process occurred non-selectively throughout the entire tree; as a result, either all of the fruits in a cluster were abscised, or all of the fruits survived. 'Fuji' in the June drop group maintained almost five fruits per cluster until 30 DAFB, while entire clusters were sometimes detached beginning at 10 DAFB (Fig. 1-1).

The self-abscising group showed a selective abscission pattern. Only central fruit persisted in a cluster and four lateral fruits were shed within 30 DAFB. In the self-abscising group, 'Saika', for example, lateral fruits were dropped, and only one fruit persisted in a cluster when abscission

Table 1-1. Classification of apple genetic resources using the early fruit abscission pattern from FB to 30 DAFB. The parentage information was from Kitahara et al. (2005) and http://www.orangepippin.com.

Abscission pattern	Cultivar
Non-abscising	Flower of Kent, M.9, M.26, M.27, *M. baccata* Manchurian, *M. floribunda* 821, *M. asiatica*, *M. sieboldii*, *M. gloriosa*, *M. arnoldiana*, *M. macromalus*, *M. sargentii*, *M. prunifolia*, MM.106, Ottawa 322, P.14
June drop	Chukwang, Discovery, Earliblaze, Fuji, Gala, Gamhong, Golden Delicious, Hongro, Jonagold, Ralls Janet, Red Delicious, Saenara, Sekaiichi, Shinano Sweet, Tsugaru
Self-abscising	Akane, Arlet, Belle de Boskoop, Caravel, Carroll, Hokuto, Hwahong, Kizashi, Kougetsu, *M. coronaria* Charlottae, Mutsu, Saika, Sansa, Suntan, Virginia Gold, X3191, Yoko

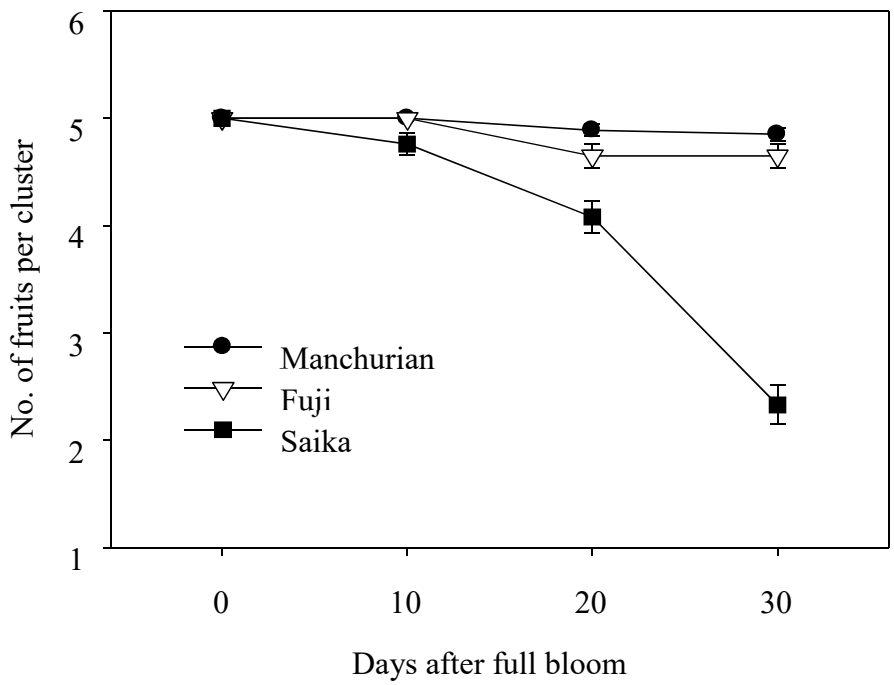

Fig. 1-1. Early fruit abscission from FB to 30 DAFB in *Malus baccata* ‘Manchurian’, ‘Fuji’, and ‘Saika’, each representing the non-abscising, June drop, and self-abscising groups, respectively. Fruit abscission was evaluated in 100 flower clusters from at least five trees. Vertical bars are the standard errors of the means.

occurred. However, the number of remaining fruits was 2.3 on the basis of the entire tree, because no abscission occurred in some clusters (Fig. 1-1). Consequently, less additional fruit thinning is required for the cultivars in the self-abscising group.

Based on the date of FB, most *Malus* species that belonged to the non-abscising group (88.2%) bloomed at early dates (Fig. 1-2A). The majority of commercial cultivars that belonged to the June drop or self-abscising group had a later date of FB than the non-abscising group (Fig. 1-2). The earlier the date of FB was, the less early fruit abscission occurred.

Fruit weight of the non-abscised was significantly related to fruit abscission, with smaller fruit among the abscission groups associated with less early abscission (Fig. 1-3). *Malus* species in the non-abscising group weighed less than 30 g, a distinctive feature of crabapples, whereas the rest weighed more than 50 g. Crabapples may evade intra-fruitlet competition in a cluster or inter-fruitlet competition throughout the entire tree due to their small fruit size. For most commercial cultivars, however, competition may be a main factor because their fruits are big enough to trigger early abscission. Considering the inter-fruitlets or intra-fruitlets carbohydrate competition, limited allocation of photosynthates causing sugar starvation would occur in abscising fruitlets. Sink strength is reported to be an important force driving early abscission (Botton et al., 2011; Celton et al., 2014; Giulia et al., 2013; Iwanami et al., 2012; Lakso et al., 2006).

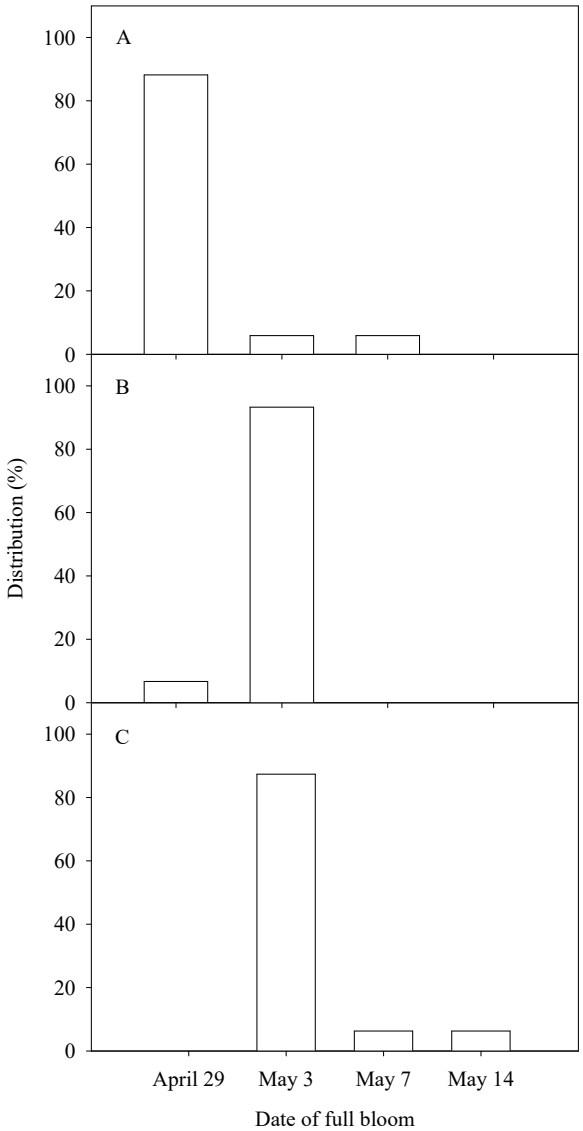

Fig. 1-2. Distribution of apple genetic resources with regard to the date of FB in the different fruit abscission groups. A, non-abscising group; B, June drop group; C, self-abscising group.

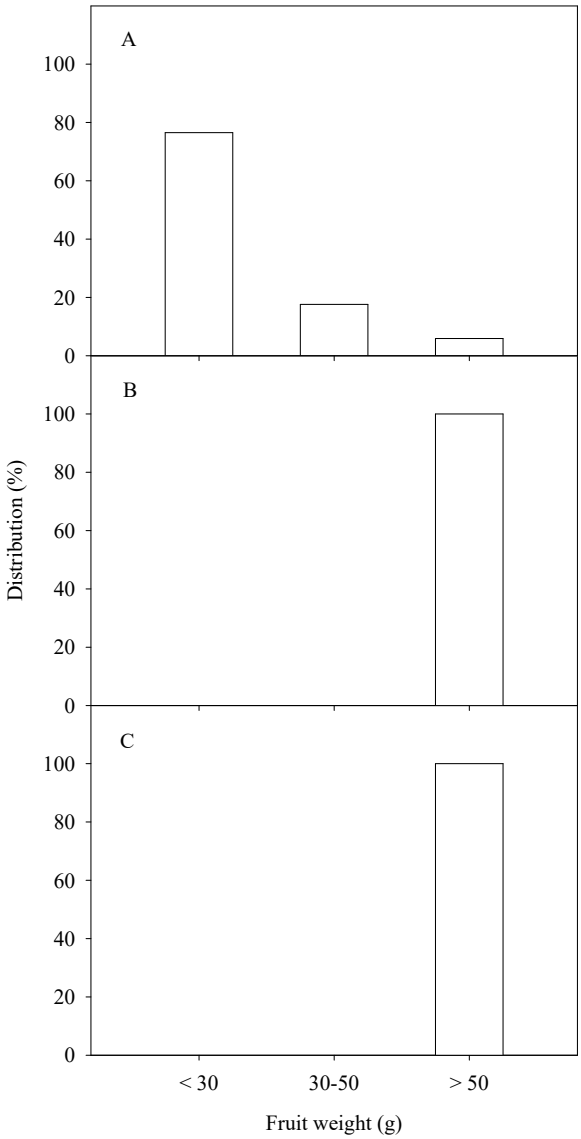

Fig. 1-3. Distribution of apple genetic resources with regard to fruit weight in the different fruit abscission groups. A, non-abscising group; B, June drop group; C, self-abscising group.

Most cultivars in the self-abscising group, like ‘Saika’, showed a fruit abscission pattern in which central fruit dominated over lateral fruits in a cluster, inducing their growth inhibition and final abscission (Fig. 1-4A). There was one exception; in *M. coronaria* ‘Charlottae’, central fruit did not dominate lateral fruits, but was abscised first in a cluster (Fig. 1-4B). The fruit nearest the peduncle survived, although bloomed last. Therefore, its pollination and fertilization were likely the most delayed. Although the apical flower bloomed earlier, it dropped first from a cluster. Fruits were shed sequentially from the distal fruit toward the peduncle. Finally, only the proximal fruit in a cluster survived. The apical fruit might be prevented from exporting auxin by lateral fruits and eventually be abscised. Then, the second flower is threatened by the third flower, the third by the fourth, and so on sequentially due to the lack of pedicel clustering.

In *M. coronaria* ‘Charlottae’, pedicels are not clustered at a peduncle (Fig. 1-5B); rather, they separate independently, rotating along the apical pedicel from the central axis, so they look like lateral shoots emerging from a primary shoot, forming a counter-clockwise whorl. Accordingly, the first flower (apical fruit) is most hampered, and the fifth flower (proximal fruit) has a high possibility of surviving, because it is disturbed the least. These observations show that the factors inducing abscission in ‘Saika’ may be transported basipetally through fruit pedicels, prioritizing interconnection with the main canal of the stem (Fig. 1-5A), whereas in *M. coronaria* ‘Charlottae’, other factors may be transported acropetally the toward apical

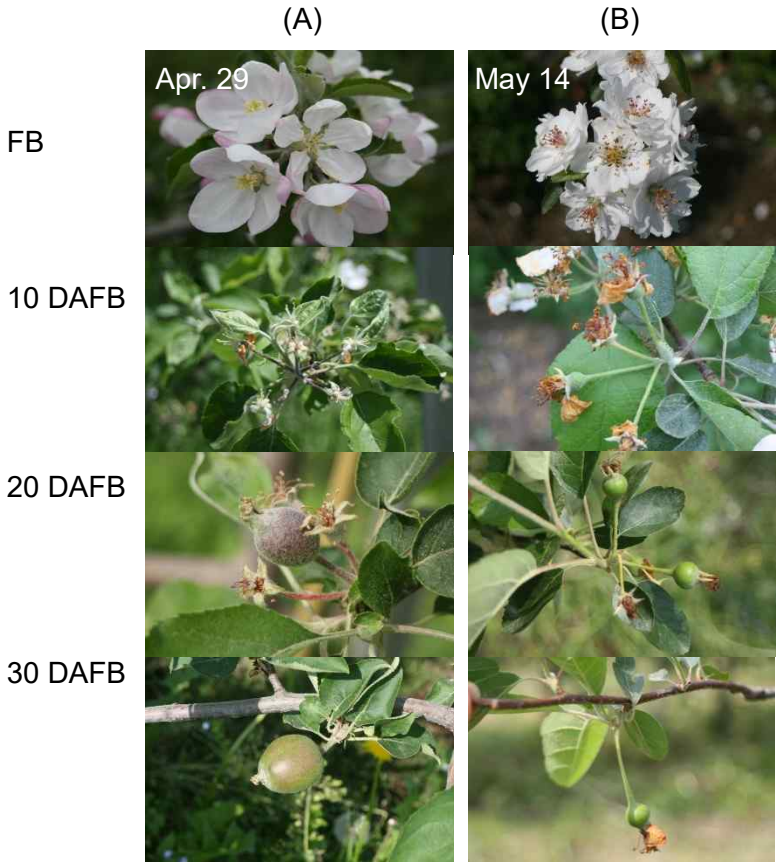

Fig. 1-4. Abscission patterns of young fruits within a cluster in self-abscising apple cultivars. A, ‘Saika’; B, *Malus coronaria* ‘Charlottae’.

(A)

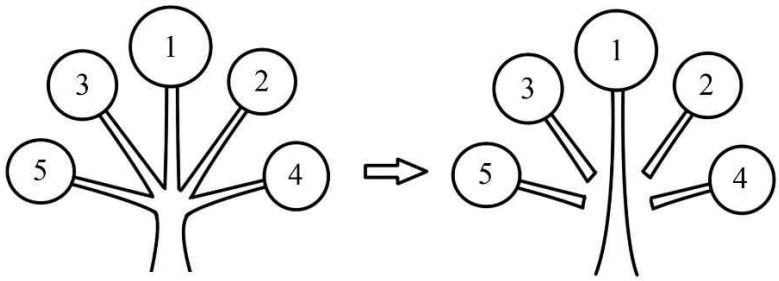

(B)

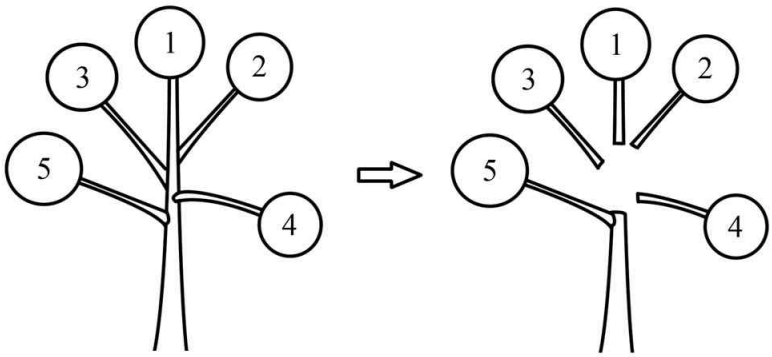

Fig. 1-5. Self-abscission patterns in apple genetic resources. (A) ‘Saika’. Central fruit dominated lateral fruits and caused most of lateral fruits to be abscised; (B) *Malus coronaria* ‘Charlottae’. Fruits abscised successively from central one in a cluster and the last one survives to grow and ripen. Numbers represent the flowering order.

fruit (Fig. 1-5B). The fruit abscission in ‘Saika’ could be explained by a correlative inhibition model, in which inhibition of auxin transport is considered the main signal inducing the early fruit abscission (Bangerth, 2000). Central fruit, which is connected to the main canal of the auxin stream in a stem, predominates in auxin transport, strengthening its comparative advantage over lateral fruits, whereas lateral fruits cannot join this canalization and easily abscise.

In this study, apple genetic resources were classified using the early fruit abscission pattern. The main factor inducing fruit abscission may be sugar starvation associated with a source-sink relationship (Botton et al., 2011; Celton et al., 2014; Guilia et al., 2013; Iwanami et al., 2012; Lakso et al., 2006) or genes related to auxin signaling (Dal Cin et al., 2009). The mechanisms of early fruit abscission should be explained more clearly in the near future.

LITERATURE CITED

Abebie, B., A. Lers, S. Philosoph-Hadas, R. Goren, J. Riov, and S. Meir. 2008. Differential effects of NAA and 2,4-D in reducing floret abscission in cestrum (*Cestrum elegans*) cut flowers are associated with their differential activation of *Aux/IAA* homologous genes. Ann. Bot. 101:249-259.

Abeles, F.B. and B. Rubinstein. 1964. Regulation of ethylene evolution and leaf abscission by auxin. Plant Physiol. 39:963-969.

Bangerth, F. 2000. Abscission and thinning of young fruit and their regulation by plant hormones and bioregulators. Plant Growth Regul. 31:43-59.

Black, B.L., M.J. Bukovac, and J. Hull, Jr. 1995. Effect of spray volume and time of NAA application on fruit size and cropping of Redchief 'Delicious' apple. Sci. Hort. 64:253-264.

Bonghi, Z.C., G.Casadoro, A. Ramina, and N. Rascio. 1993. Abscission in leaf and fruit explants of *Prunus persica* (L.) Batsch. New Phytol. 123:555-565.

Botton, A., G. Eccher, C. Forcato, A. Ferrarini, M. Begheldo, M. Zermiani, S. Moscatello, A. Battistelli, R. Velasco, B. Ruperti, and A. Ramina. 2011. Signaling pathways mediating the induction of apple fruitlet abscission. Plant Physiol. 155:185-208.

Bound, S.A., K.M. Jones, B. Graham, M.J. Oakford, and M. Tichon. 1993. Modelling the effects of timing and rates of application of benzyladenine as a secondary thinner of 'Fuji' apple after ethephon. J. Hort. Sci. 68:967-973.

Celton, J.M., E. Dheilly, M.C. Guillou, F. Simonneau, M. Juchaux, E. Costes, F. Laurens, and J.P. Renou. 2014. Additional amphivasal bundles in pedicel pith exacerbate central fruit dominance and induce self-thinning of lateral fruitlets in apple. Plant Physiol. 164:1930-1951.

Dal Cin, V., R. Velasco, and A. Ramina. 2009. Dominance induction of fruitlet shedding in *Malus* × *domestica* (L. Borkh): molecular changes associated with polar auxin transport. BMC Plant Biol. 9:139.

Dennis, Jr., F.G. 2000. The history of fruit thinning. Plant Growth Regul. 31:1-16.

Giulia, E., B. Alessandro, D. Mariano, B. Andrea, R. Benedetto, and R. Angelo. 2013. Early induction of apple fruitlet abscission is characterized by an increase of both isoprene emission and abscisic acid content. Plant Physiol. 161:1952-1969.

Iwanami, H., Y. Moriya-Tanaka, C. Honda, M. Wada, S. Moriya, K. Okada, T. Haji, and K. Abe. 2012. Relationships among apple fruit abscission, source strength, and cultivar. Sci. Hort. 146:39-44.

Kitahara, K., S. Matsumoto, T. Yamamoto, J. Soejima, T. Kimura, H. Komatsu, and K. Abe. 2005. Parent identification of eight apple cultivars by S-RNase analysis and simple sequence repeat markers. HortScience 40:314-317.

Lakso, A.N., T.L. Robinson, and D.W. Greene. 2006. Integration of environment, physiology, and fruit abscission via carbon balance modeling: implications for understanding growth regulator responses. Acta Hort. 727:321-326.

Marini, R.P. 1996. Chemically thinning spur ‘Delicious’ apples with carbaryl, NAA, and ethephon at various stages of fruit development. HortTechnology 6:241-246.

Sexton, R. 1997. The role of ethylene and auxin in abscission. Acta Hort. 463:435-444.

Sun, L., M.J. Bukovac, P.L. Forsline, and S. van Nocker. 2009. Natural variation in fruit abscission-related traits in apple (*Malus*). Euphytica 165:55-67.

Suttle, J.C. and J.F. Hultstrand. 1991. Ethylene-induced leaf abscission in cotton seedlings: the physiological bases for age-dependent differences in sensitivity. Plant Physiol. 95:29-33.

Taylor, J.E. and C.A. Whitelaw. 2001. Signals in abscission. New Phytol. 151:323-340.

Wertheim, S.J. 2000. Developments in the chemical thinning of apple and pear. Plant Growth Regul. 31:85-100.

CHAPTER 2

Isolation of a Novel MADS-Box Gene, *MdJOINTLESS*, from Pedicels during Early Fruit Abscission in the Self-Abscising Apple (*Malus* × *domestica*)

ABSTRACT

To search the MADS-box gene which regulates abscission zone (AZ) development in pedicels, like *JOINTLESS* in tomato, lateral pedicels in self-abscising apple 'Saika' were investigated during early abscission. A novel MADS-box gene, *MdJOINTLESS*, was identified in young pedicels through the amplification using degenerate primers annealing to a highly conserved domain. Using DNA sequence analyses with the MADS-box gene family, *MdJOINTLESS* was classified into the *SHORT VEGETATIVE PHASE* (*SVP*) clade that included *SVP* (*Arabidopsis thaliana*), *IbMADS3* (*Ipomoea batatas*), *StMADS16* (*Solanum tuberosum*), *PsSVP* (*Pisum sativum*), and *JOINTLESS* (*Solanum lycopersicum*). However, *MdJOINTLESS* did not function as *JOINTLESS* in transgenic tomato, although these MADS-box homologues have high homology. Additionally, the MADS-box genes, *SEPALLATA* and *MACROCALYX*, were discovered in pedicel cDNA libraries and might be involved in the formation of AZ in the apple, which is similar to the roles of *SLMBP21* and *MACROCALYX* genes in tomato.

INTRODUCTION

Fruit abscission typically occurs in a developmentally separated region called the abscission zone (AZ). The AZ, which is formed at the junction between the fruit and the branch of the plant, is composed of six to eight layers of small, square, and densely packed cells (Sexton and Roberts, 1982; Sun et al., 2009). The cells in the AZ are arrested during growth and development and are arranged in transverse sections relative to the adjacent vascular cells (Sun et al., 2009). Moreover, the tracheary elements in the AZ are less developed and their lignins are less abundant (Patterson, 2001). Below the AZ, the protective layers are formed in the proximal region of the peduncle. Abscission is processed by the expanded cells of the AZ and the immature vascular system that does not support the pedicels and fruits.

AZ differentiation is regulated by several genes and transcription factors. In tomato, the *LATERAL SUPRRESSOR* gene, which encodes a member of VHIID protein family, is required for AZ development in the pedicel (Schumacher et al., 1999). Another gene *JOINTLESS* also plays a crucial role in the development of the AZ in tomato (Mao et al., 2000) and interacts with the other MADS-box proteins, MACROCALYX and SEPALLATA (SLMBP21), forming protein complexes that regulate AZ formation (Liu et al., 2014; Nakano et al., 2012). SLMBP21 is thought to attach *JOINTLESS* to *MACROCALYX*, as is the case with the *SEPALLATA* gene in the quartet model describing floral organ formation (Liu et al., 2014).

In *Arabidopsis*, the double mutant lacking the transcription factors *BLADE-ON-PETIOLE 1* (*BOP1*) and *BOP2* failed to abscise the floral organs, even after senescence and wilting (McKim et al., 2008). *BOP1* and *BOP2* encode BTB/POZ domain and ankyrin repeat-containing proteins, which redundantly regulate AZ differentiation in floral organs (Mckim et al., 2008).

In rice, differentiation of the pedicel AZ is regulated by *SHATTERING 4* (*SH4*) (Li et al., 2006), *qSH1* (Konishi et al., 2006), and *SHATTERING ABORTION 1* (*SHAT1*) (Zhou et al., 2012). *SH4* and *qSH1* both activate AZ formation at the pedicel. *SH4* encodes a Myb3 DNA-binding domain-containing protein (Li et al., 2006), whereas *qSH1* is a BELL homeobox gene such as *REPLUMLESS* (or *VAAMANA*) (Konishi et al., 2006). *SHAT1* belongs to the AP2 transcription factor family and is involved in rice grain shattering (Zhou et al., 2012).

Here, the *MdJOINTLESS* gene, which is expressed in pedicels during early fruit abscission, was characterized in the self-abscising apple ‘Saika’. The *MdJOINTLESS* represents a novel MADS-box gene that belongs to the *SHORT VEGETATIVE PHASE* (*SVP*) clade along with *JOINTLESS* from tomato. Additional MADS-box genes were also identified from cDNA libraries constructed from pedicels during early abscission.

MATERIALS AND METHODS

Plant Material

Ten-year-old ‘Saika’ apple (*Malus* × *domestica* Borkh.) trees, grafted on M.9 rootstocks were grown at the National Institute of Horticultural and Herbal Science, Suwon, Korea. All flowers were artificially pollinated with mixed pollens collected from various cultivars to avoid the self-incompatibility resulting from the same S-genotypes. The pedicels from lateral fruitlet in a cluster were collected 20 days after full bloom (DAFB). They were immediately frozen in liquid nitrogen and stored at −80°C until use.

RNA Extraction

Frozen tissue samples were pulverized with a mortar and pestle using liquid nitrogen. Approximately 100 mg of powdered tissues was used to extract total RNA by the cetyltrimethyl ammonium bromide (CTAB) method (Chang et al., 1993). The extracted RNA was precipitated, and the resulting pellet was resuspended in diethylpyrocarbonate-treated water. RNA quality was assessed by electrophoresis on an 1% agarose gel and quantified using a NanoDrop ND-1000 spectrophotometer (Thermo Scientific, Waltham, MA, USA).

Isolation of Genomic DNA and DNA Gel Blot Analysis

One gram of frozen pedicel tissues was suspended in 2.5 mL of extraction buffer consisting of 2% (w/v) CTAB, 100 mM Tris-HCl (pH 8.0), 20 mM EDTA, 1.42 M NaCl, 5 mM ascorbic acid, and 2% (w/v) polyvinylpyrrolidone. Genomic DNA was isolated according to the method of Heo et al. (2006), with minor modifications. Approximately 10 μg of genomic DNA was digested using the restriction enzymes, *Eco*RI, *Eco*RV, *Hin*dIII, or *Bam*HI. The digested DNA was separated on a 0.7% agarose gel and transferred onto a Hybond-N^+ membrane (Amersham Pharmacia Biotech, Pittsburgh, PA, USA). The blot was hybridized to ^{32}P-radiolabelled pMdJOINTLESS cDNA probes at 65°C with stringent washing conditions. A final high-stringency wash was conducted in 0.1% saline-sodium phosphate EDTA and 0.1% sodium dodecyl sulfate at 65°C for 20 min.

Identification of the *JOINTLESS* Homologue, *MdJOINTLESS*

For isolation of the *JOINTLESS* homologue, *MdJOINTLESS*, 1 μg of total RNA was subjected to first-strand cDNA synthesis using T(18) primers and PowerScript reverse transcriptase (Clontech, Mountain View, CA, USA). For second-strand cDNA synthesis, two degenerate primers were designed using the CODEHOP program targeting the conserved amino acid sequences MAREKIQIK from the MADS-box domain and RQMRGEDLQG from the K-box region. The sequences of the primers were 5'-ATGGCKAGAGARAARATTMAGATMAAGAA-3' and 5'-CCTTGRAGHTCY

TCHCCYCTCATYTGCCT-3'. Second-strand cDNA synthesis was performed according to the following procedure: initial denaturation at 94°C for 4 min, 35 cycles of 94°C for 1 min, 60°C for 1 min, 72°C for 3 min, and a final extension for 5 min at 72°C. A single DNA band was detected by agarose gel electrophoresis and was extracted using QIAquick gel extraction kit (Qiagen, Valencia, CA, USA) according to the manufacturer's instructions. The extracted DNA was cloned into the pGEM-T easy vector (Promega, Madison, WI, USA) according to the manufacturer's instructions, and sequenced. Rapid amplification of cDNA end (RACE) was performed using the SMART^{TM} RACE cDNA amplification kit (Clontech) with adaptors and specific primers that were based on a partial cDNA sequence. The polymerase chain reaction (PCR) products were cloned and sequenced as described above.

Quantitative Real-Time Reverse-Transcription PCR (qRT-PCR)

The cDNA was synthesized from 1 μg of total RNA using Superscript III reverse-transcriptase (Invitrogen, Carlsbad, CA, USA) according to the manufacturer's instructions. Real-time PCR reactions were performed with Applied Biosystems 7500 Fast Real-Time PCR System and SYBR Premix EX Taq kit (Takara, Tokyo, Japan). The mixture was composed of a 50 μL reaction solution containing 18 μL double distilled H_2O, 25 μL 2× premix, 1 μL forward primer (10 mM), 1 μL reverse primer (10 mM), 4 μL of template, and 1 μL ROX reference dye II. Transcript values were normalized and

calibrated relative to *Malus* × *domestica* actin (CN935584) protein as a housekeeping internal standard gene according to the $2^{-\Delta\Delta C_T}$ method (Livak and Schmittgen, 2001). Three biological and technical replicates were used in this experiments.

Vector Construction and Tomato Transformation

A full-length open reading frame of *MdJOINTLESS* was amplified. The amplified product was cloned in the sense orientation between CaMV 35S promoter and the nopaline synthase terminator. The resulting recombinant plasmid pBI121-*MdJOINTLESS* was mobilized into *Agrobacterium tumefaciens* strain LBA4404 and it was introduced into *jointless* mutant tomato plants. For the suppression experiment, an antisense construct was generated by insert that contain a 675 bp region from the C-terminus and 3'-UTR of *MdJOINTLESS* fused with 35S promoter, and it was introduced into wild-type tomato plants. Tomato cotyledon discs were co-cultivated with *A. tumefaciens* LBA4404 containing vectors. The discs were cultivated on a basal medium for 2 days and transferred to shoot induction medium and subcultured every 4 weeks into new medium for 4 months. Regenerating shoots were transferred to rooting medium and transgenic plants (T_0) and control were transplanted to soil.

Construction of cDNA Libraries and Expressed Sequence Tag (EST)

Sequencing

Poly(A)$^+$ RNA was obtained from total RNA by oligo(dT) cellulose chromatography using a poly(A) Quick mRNA isolation kit (Stratagene, La Jolla, CA, USA). cDNA libraries were constructed as described by Han et al. (2007). The library was amplified once on agar plates and stored in a 7% dimethyl sulfoxide solution at −80°C. Randomly selected cDNAs were then sequenced. In total, 12,454 ESTs were analyzed using BlastN program, and all MADS-box genes were assorted for phylogenetic analyses with whole-apple MADS-box genes reported by Velasco et al. (2010).

RESULTS AND DISCUSSION

AZ of Self-Abscising Apple 'Saika'

Apple cultivars having self-abscising fruit retained their central fruit, and abscise lateral fruits within 30 DAFB. During early fruit abscission, the AZ was developed, and abscission occurred in lateral pedicel (LP) of the self-abscising apple cultivar 'Saika' (Fig. 2-1). At 20 DAFB in LP, the AZ was developed at the junction between the pedicel and the peduncle, with the protective layers formed immediately below the AZ (Fig. 2-2A). The AZ was composed of six to eight layers of small, square, and densely packed cells (Fig. 2-2A). The cells of the AZ were transversely arranged relative to vascular system and adjacent cells (Fig. 2-2B).

Isolation and Sequence Analysis of a New MADS-Box Gene from Pedicels

The RT-PCR produced a single cDNA band at the expected size of 350 bp, from which full length cDNA was reconstructed using 3'-RACE. This final product, named *MdJOINTLESS* (Genbank accession No. DQ402055) was a novel MADS-box gene isolated from the pedicel tissues of young fruit. *MdJOINTLESS* showed the highest sequence similarity to members of the *SVP* group of MADS-box genes (Fig. 2-3A). The *MdJOINTLESS* gene encoded a putative 224 amino acids protein that was 77 and 78% identical to *JOINTLESS* (tomato) and

Fig. 2-1. Early fruit abscission of the self-abscising apple ‘Saika’ from FB to 30 DAFB. All lateral fruit were abscised within 30 DAFB. (A) FB, (B) 15 DAFB, (C) 25 DAFB, and (D) 30 DAFB. The AZ is seen at the base of the fruit cluster.

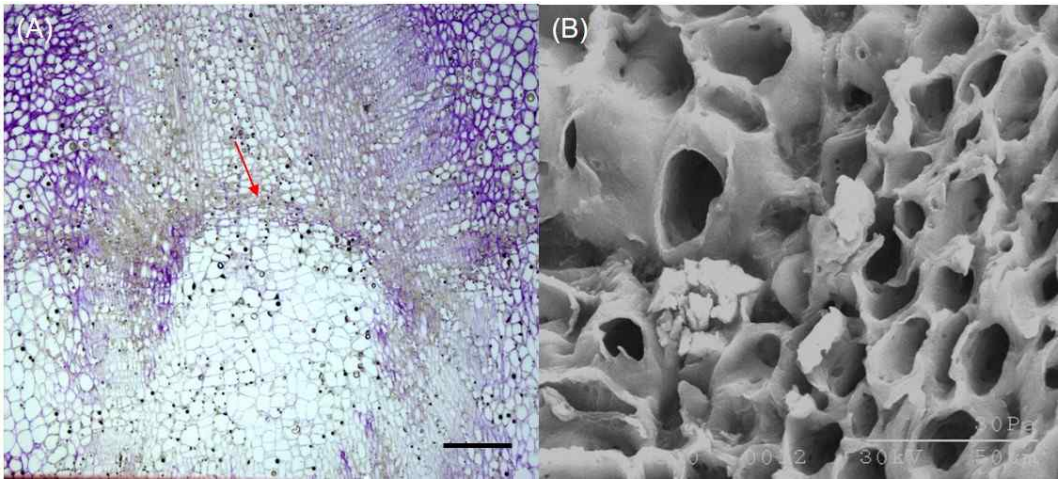

Fig. 2-2. The AZ developed at pedicel of lateral fruits in the self-abscising apple ‘Saika’. (A) The AZs located between the pedicel and the peduncle were manually dissected from longitudinal sections for the observation under a light microscope. (B) Scanning electron micrograph of the pedicel AZ. The square cell layers are seen at the lower right corner. These cells were transversely arranged relative to the adjacent cells. Scale bars are 100 μm (A) and 50 μm (B).

(A)

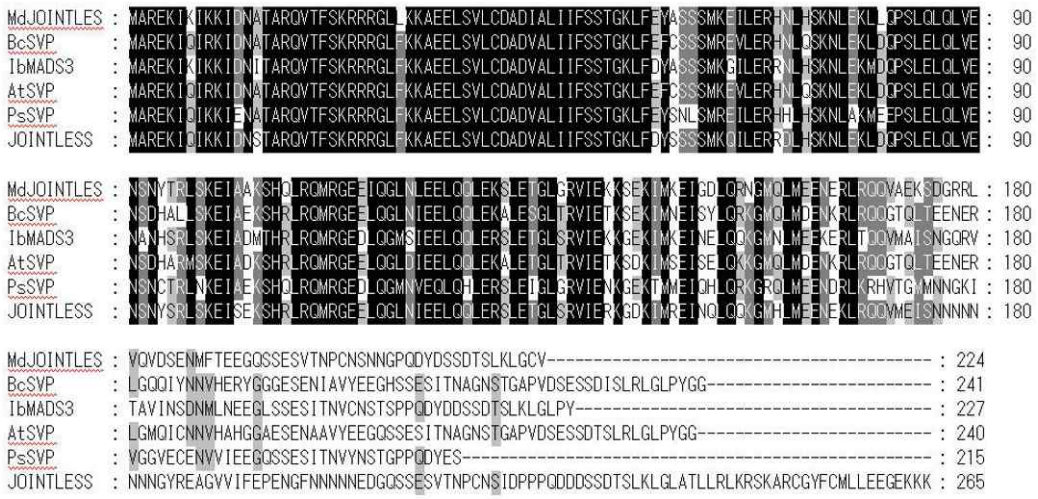
MdJOINTLES
BcSVP
IbMADS3
AtSVP
PsSVP
JOINTLESS

(B)

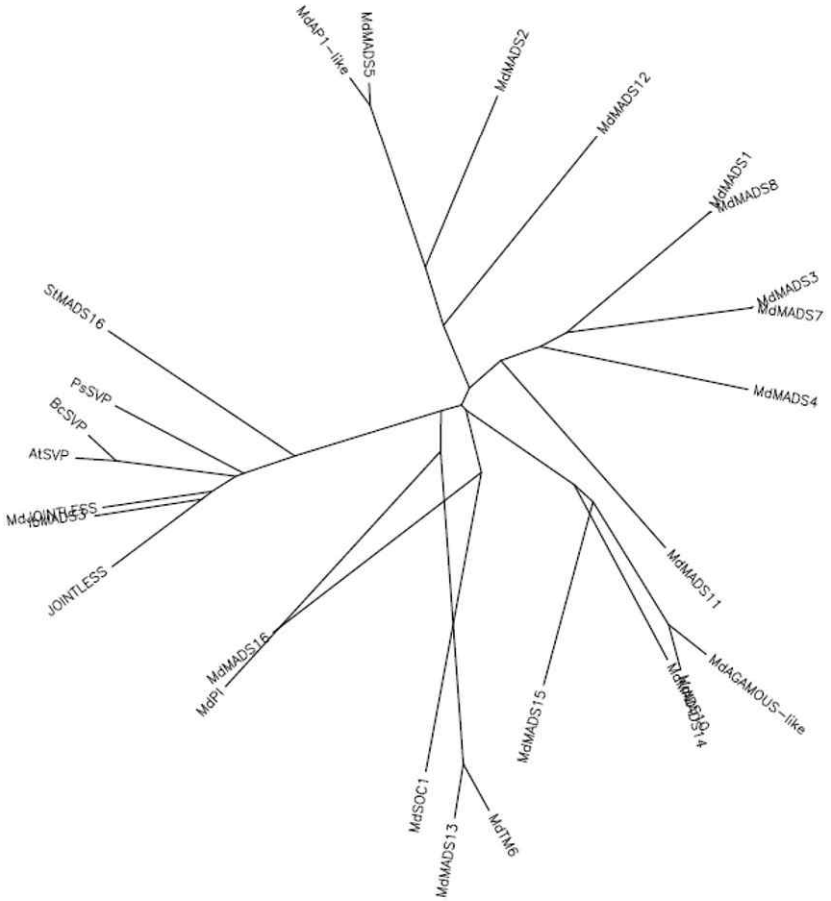
MdAP1-like
MdMADS5
MdMADS2
MdMADS12
MdMADS1
MdMADS8
MdMADS3
MdMADS7
MdMADS4
MdMADS11
MdAGAMOUS-like
MdMADS15
MdTM6
MdMADS13
MdSOC1
MdMADS16
MdPI
JOINTLESS
AtSVP
BcSVP
PsSVP
StMADS16

Fig. 2-3. Multiple alignment (A) and phylogenetic analysis (B) of the deduced amino acid sequence of *MdJOINTLESS* with other MADS-box protein homologues. (A) Comparison of *MdJOINTLESS* with *SVP* from *Brassica campestris* (DQ922944), *IbMADS3* from *Ipomoea batatas* (AB054255), *SVP* from *Arabidopsis thaliana* (NP_179840), *SVP* from *Pisum sativum* (AY830919), and *JOINTLESS* from *Solanum lycopersicum* (AF275345). Dark boxes indicate amino acid identity or similarity between all six sequences, whereas grey boxes indicate amino acid identity or similarity among any four sequences. (B) An unrooted tree showing the phylogenetic relationships between *MdJOINTLESS* and MADS-box proteins from apple (*Malus* × *domestica* Borkh.) and other plants, including: *StMADS16* (AF008651) from *Solanum tuberosum*; *MdMADS1* (AAC25922), *MdMADS2* (AAC83170), *MdMADS3* (AAD51422), *MdMADS4* (AAC25922), *MdMADS5* (CAA04321), *MdMADS7* (CAA04323), *MdMADS8* (CAA04919), *MdMADS10* (CAA04324), *MdMADS11* (CAA04325), *MdMADS12* (CAC86183), *MdMADS13* (CAC80856), *MdMADS14* (CAC80857), *MdMADS15* (CAC80858), *MdMADS16* (AB370212), *MdTM6* (AB081093), *MdPI* (CAC28021), *MdAGAMOUS* (AAQ03090), *MdAP1* (AAL61543), and *MdSOC1* (DQ887181). The phylogenetic tree was generated in MEGA Version 5 using the neighbor-joining method with the *P*-distance amino acid substitution model and 100 bootstrap replicates.

IbMADS3 (sweet potato), respectively (Fig. 2-3B). These MADS-box genes were repressors of floral transition during the vegetative phase (Hartmann et al., 2000), and after the floral transition, they were expressed in the floral meristem (Gregis et al., 2013).

Genomic Analysis and Expression Pattern of *MdJOINTLESS*

The DNA gel blot revealed a single hybridization band when digested with *Eco*RV, and it revealed two bands after digestion with *Hin*dIII (Fig. 2-4). These data suggest that *MdJOINTLESS* is a single or low-copy-number gene in 'Saika'. Although 'Saika' is a triploid apple, it is common to have single or low-copy-number of *MdJOINTLESS* in diploid apple cultivars.

Quantification of expression levels of *MdJOINTLESS* gene was performed through qRT-PCR analysis in central pedicel (CP) and LP of self-abscising apple (Fig. 2-5). Based on normalization of gene expression to that of *MdActin*, *MdJOINTLESS* was expressed higher in CP than in LP at FB. *MdJOINTLESS* was detectable in both pedicels at 10 DAFB and its expression levels were lower than those at FB. However, the relative expression of *MdJOINTLESS* was higher in CP than in LP (Fig. 2-5). In LP, the expression of *MdJOINTLESS* showed similar level from FB to 10 DAFB, while, in CP, the expression level at 10 DAFB was the half of that at FB. According to the qRT-PCR result, *MdJOINTLESS* might not be involved in

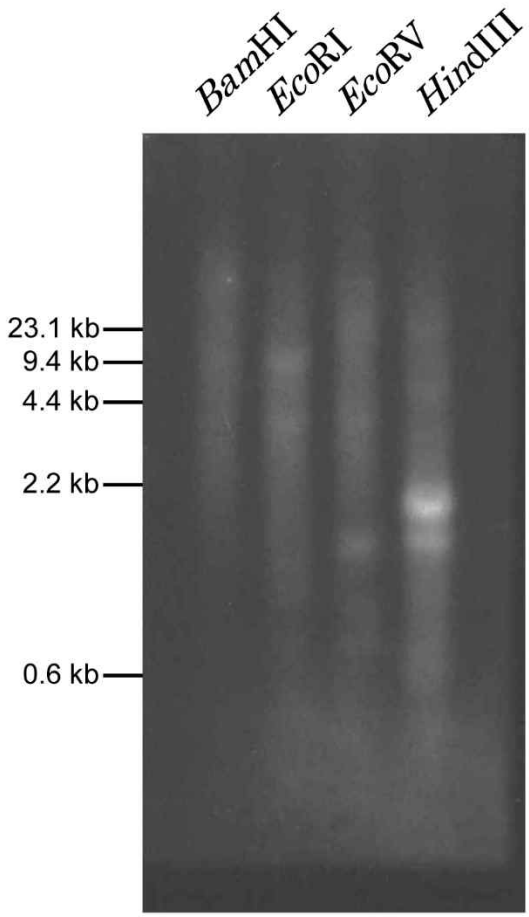

Fig. 2-4. Genomic DNA gel blot analysis of the *MdJOINTLESS* gene. 'Saika' apple genomic DNA (10 μg per lane) was isolated from pedicel tissues; digested with *Bam*HI, *Eco*RI, *Eco*RV, or *Hin*dIII; and separated on a 0.7% agarose gel. DNA was transferred to a nylon membrane and hybridized with ^{32}P-labeled pMdJOINTLESS probes under stringent conditions.

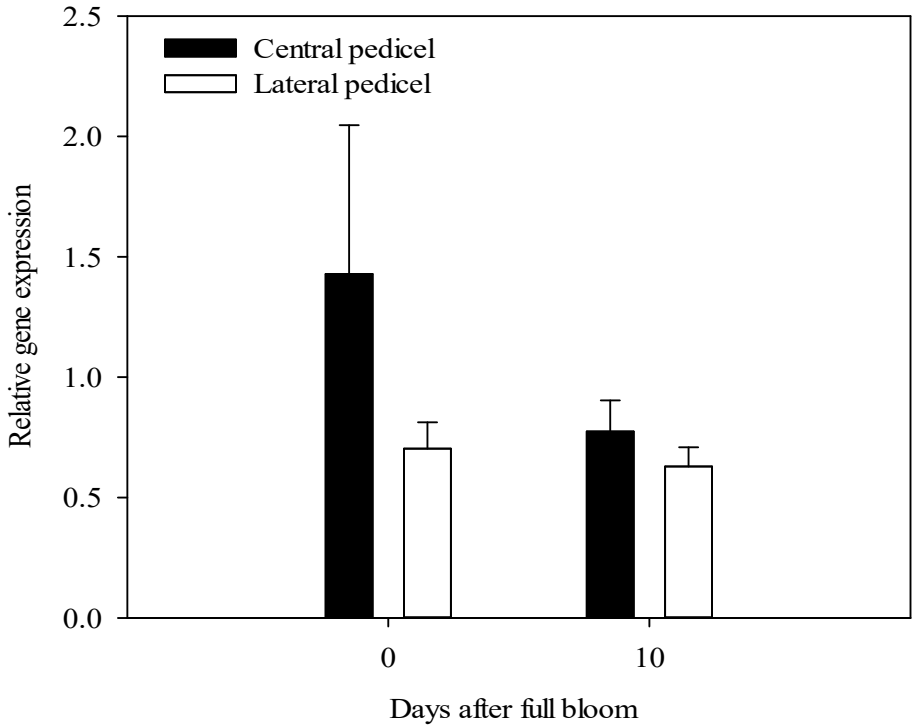

Fig. 2-5. Relative expression levels of *MdJOINTLESS* gene between CP and LP of self-abscising apple 'Saika' from FB to 10 DAFB. Data were normalized using housekeeping *MdActin* gene. Vertical bars are the standard errors of the means.

formation of AZ in apple. The highest expression level of *MdJOINTLESS* was found actually in CP, although its expression was also up-regulated in LP.

Phenotypes of Transgenic Tomato Plants

MdJOINTLESS sense and antisense constructs were prepared for complementation and suppression of *MdJOINTLESS* in pedicel of tomato (Fig. 2-6). The recombinant *MdJOINTLESS* gene was introduced into tomato plants through *Agrobacterium*-mediated transformation. After inoculation, each three T_2 homo lines were obtained during the progressing of two generations through self-fertilization. The control plants showed AZ formation on pedicels (Fig. 2-6A). In suppression experiment with antisense construct, the AZ still existed at pedicels (Fig. 2-6B). In complementation, the AZ did not develop (Fig. 2-6C), indicating that *MdJOINTLESS* did not induce AZ development in tomato transgenic plants.

Phylogenetic Analysis with MADS-Box Genes from Pedicel cDNA Libraries

MADS-box genes contribute to reproductive development by regulating flowering timing and floral organogenesis (Theissen and Saedler, 2001; Weigel, 1995). However, some genes are also involved in vegetative development, including the regulation of the AZ (Liu et al.,

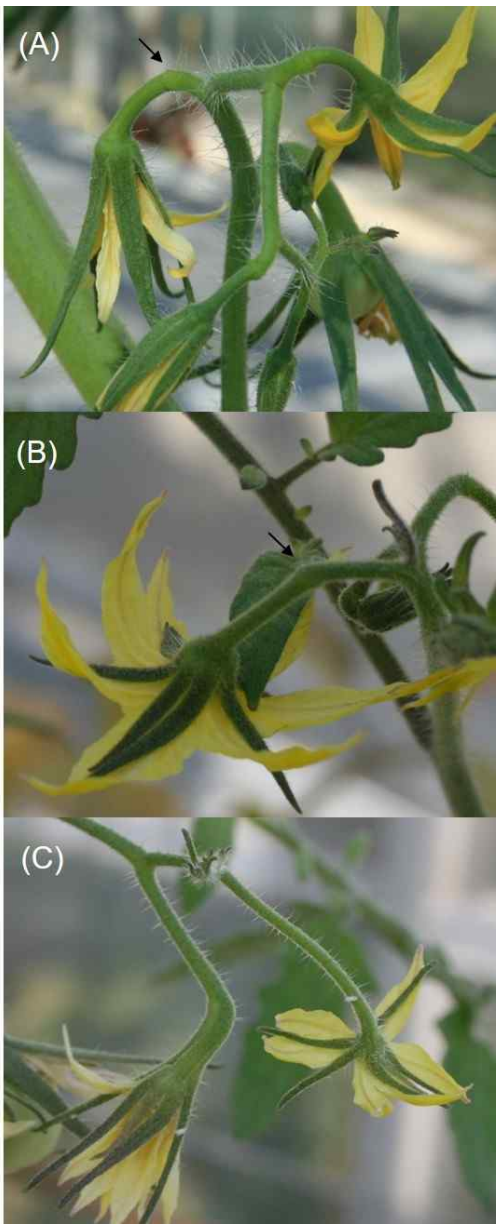

Fig. 2-6. Antisense suppression and sense complementation of *MdJOINTLESS* to wild-type and *jointless* tomato plants. (A) The AZ in wild-type control. (B) A pedicel with AZ development which was not suppressed by the antisense transgene. (C) The AZ was not formed on its pedicel, although the sense construct was transformed to *jointless* mutants. Arrows show the position of the AZ.

2014; Mao et al., 2000; Nakano et al., 2012). The MADS-box genes in pedicel cDNA libraries from ‘Saika’ were compared with the MADS-box genes reported from apple genome sequencing project (Velasco et al., 2010) (Fig. 2-7). The following *SEPALLATA*-like genes were significantly up-regulated in pedicel cDNA libraries: MDP0000326906, MDP0000370413, MDP0000326390, MDP0000574222, MDP0000605482, and MDP0000366022. The following *MACROCALYX* homologues were also discovered: MDP0000 289836, MDP0000013331 and MDP0000269921. These data suggest that other MADS-box genes are also involved in pedicel AZ formation, as are the *SEPALLATA*-like gene and *MACROCALYX* in tomato.

In tomato, the AZ is in the pedicel and *JOINTLESS* is important for development. This gene belongs to the MADS-box gene family and is similar to *SVP* genes, which are generally expressed in vegetative organs and are involved in floral transition. *SVP* genes differ in function compared to other MADS-box genes and are involved in floral organ determination. To identify the *JOINTLESS* homologue that plays a similar role in the apple, pedicels were used from self-abscising apple during early abscission.

Based on phylogenetic analyses in tomato, *MdJOINTLESS* was identified as the *JOINTLESS* homologue; thus, RT-PCR and RACE approaches were used in this study to isolate the transcripts of MADS-box gene family members. However, qRT-PCR and transformation results show

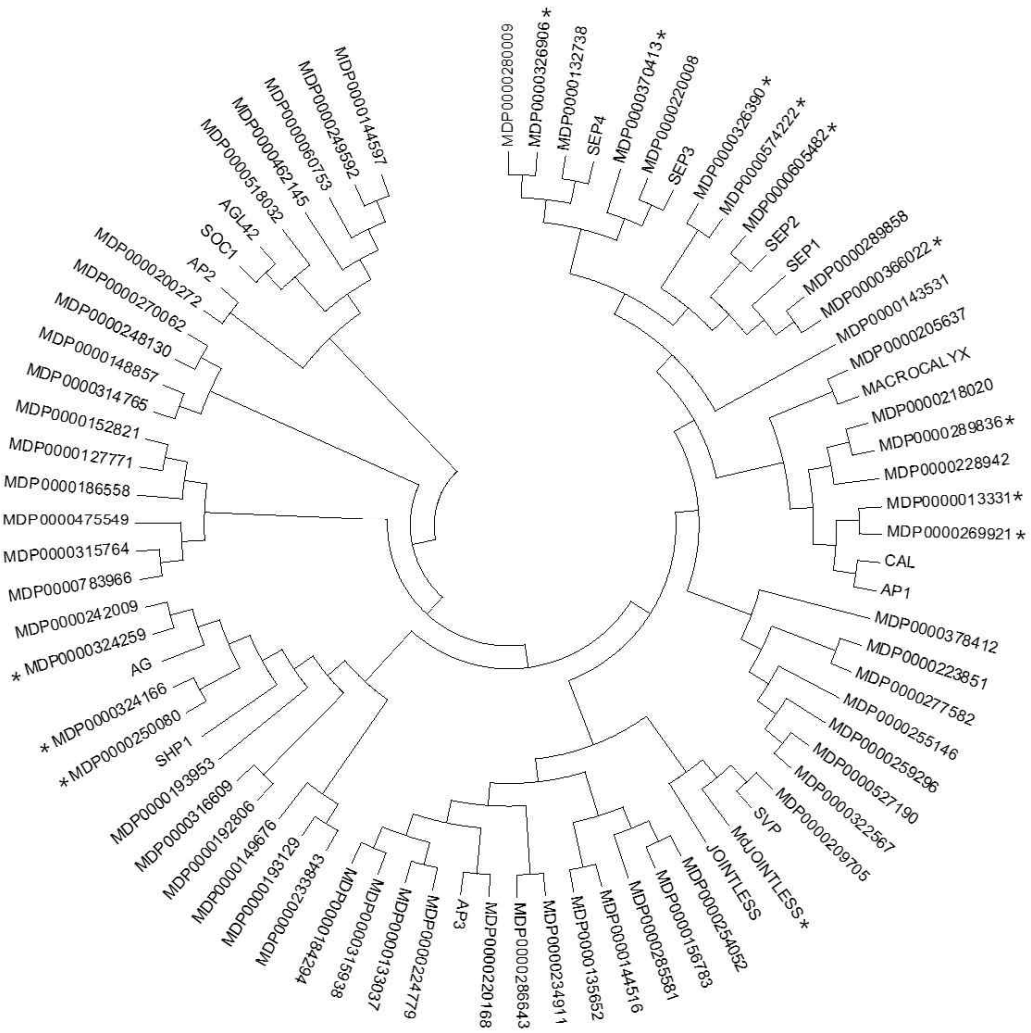

Fig. 2-7. Phylogenetic tree of apple MADS-box genes, using the neighbor-joining method. The MADS-box genes or transcripts marked with asterisks were from pedicel cDNA libraries of self-abscising apple ‘Saika’.

that *MdJOINTLESS* might not be responsible for the development of AZ. *MdJOINTLESS* was more highly expressed in CP than in LP. This might result from the sequence difference between *MdJOINTLESS* and *JOINTLESS*.

According to the DNA blot analyses in this study, 'Saika' had one or two *JOINTLESS* homologues in its genome. In addition, three homologues to *SVP* gene existed in 'Golden Delicious' genome (Velasco et al., 2010), thus other homologues, not *MdJOINTLESS*, may be related to the AZ development in the apple. Based on phylogenetic analyses with MADS-box genes derived from pedicel cDNA libraries, other MADS-box genes were also expressed in pedicels and did not belong to the *SVP* clade. Thus, these genes may also be involved in the formation of the AZ in the apple, as are *SLMBP21* and *MACROCALYX* gene in tomato.

To confirm the function of *MdJOINTLESS* in apple, cisgenic apples with an *MdJOINTLESS* construct are necessary. The characteristics of cisgenic apples have currently being investigated at the National Institute of Horticultural and Herbal Science. *MdJOINTLESS* antisense insertion might lead to lethal phenotypes, but overexpression of *MdJOINTLESS* induced columnar phenotype which is characterized by thick stems, the decreased lateral branching, and spur type trees. The leaves generated at main stems were not abscised, while the leaves at lateral branches were easily detached. In addition, these cisgenic apples have not formed flowers yet.

The columnar characteristics can be led to the highly enhanced

basipetal transport of auxin and result in high level of apical dominance (Krost et al., 2012). The columnar growth is controlled by a dominant allele of *Columnar* (*Co*) gene (Krost et al., 2012). The *Co* gene might not influence flowering or floral transition, but exert a direct effect on vegetative growth by regulating hormones and inducing apical dominance. Since *MdJOINTLESS*, which belongs to *SVP* clade, inhibited floral transition and floral meristem identity, it might induce vegetative growth compulsorily in cisgenic lines of *MdJOINTLESS*, resulting in the appearance of columnar phenotype.

LITERATURE CITED

Chang, S., J. Puryear, and J. Cairney. 1993. A simple and efficient method for isolating RNA from pine trees. Plant Mol. Biol. Rep. 11:113-116.

Gregis, V., F. Andrés, A. Sessa, R.F. Guerra, S. Simonini, J.L. Mateos, S. Torti, F. Zambelli, G.M. Prazzoli, K.N. Bjerkan, P.E. Grini, G. Pavesi, L. Colombo, G. Coupland, and M.M. Kater. 2013. Identification of pathways directly regulated by *SHORT VEGETATIVE PHASE* during vegetative and reproductive development in *Arabidopsis*. Genome Biol. 14:R56.

Han, S.E., Y.S. Seo, D. Kim, S.K. Sung, and W.T. Kim. 2007. Expression of *MdCAS1* and *MdCAS2*, encoding apple β-cyanoalanine synthase homologs, is concomitantly induced during ripening and implicates MdCASs in the possible role of the cyanide detoxification in Fuji apple (*Malus* × *domestica* Borkh.) fruits. Plant Cell Rep. 26:1321-1331.

Hartmann, U., S. Hohmann, K. Nettesheim, E. Wisman, H. Saedler, and P. Huijser. 2000. Molecular cloning of *SVP*: a negative regulator of the floral transition in *Arabidopsis*. Plant J. 21:351-360.

Heo, S., D. Kim, H.K. Yun, J.H. Hwang, H.J. Lee, and Y.U. Shin. 2006. Development of AFLP markers linked to the resistance against *Alternaria* blotch in apple (*Malus* × *domestica*). Hort. Environ. Biotechnol. 47:324-328.

Konishi, S., T. Izawa, S.Y. Lin, K. Ebana, Y. Fujuta, T. Sasaki, and M. Yano. 2006. An SNP caused loss of seed shattering during rice domestication. Science 312:1392-1396.

Krost, C., R. Petersen, and E.R. Schmidt. 2012. The transcriptomes of columnar and standard type apple trees (*Malus* × *domestica*): a comparative study. Gene 498:223-230.

Li, C., A. Zhou, and T. Sang. 2006. Rice domestication by reducing shattering. Science 311:1936-1939.

Liu, D., D. Wang, Z. Qin, D. Zhang, L. Yin, L. Wu, J. Colasanti, A. Li, and L. Mao. 2014. The *SEPALLATA* MADS-box protein *SLMBP21* forms protein complexes with *JOINTLESS* and *MACROCALYX* as a transcription activator for development of the tomato flower abscission zone. Plant J. 77:284-296.

Livak, K.J. and T.D. Schmittgen. 2001. Analysis of relative gene expression data using real-time quantitative PCR and the $2^{-\Delta\Delta C_T}$ method. Methods 25:402-408.

Mao, L., D. Begum, H.W. Chuang, M.A. Budiman, E.J. Szymkowiak, E.E. Irish, and R.A. Wing. 2000. *JOINTLESS* is a MADS-box gene controlling tomato flower abscission zone development. Nature 406:910-913.

McKim, S.M., G.E. Stenvik, M.A. Butenko, W. Kristiansen, S.K. Cho, S.R. Hepworth, R.B. Aalen, and G.W. Haughn. 2008. The *BLADE-ON-PETIOLE* genes are essential for abscission zone formation in *Arabidopsis*. Development 135:1537-1546.

Nakano, T., J. Kimbara, M. Fujisawa, M. Kitagawa, N. Ihashi, H. Maeda, T. Kasumi, and Y. Ito. 2012. *MACROCALYX* and *JOINTLESS* interact in the transcriptional regulation of tomato fruit abscission zone development. Plant Physiol. 158:439-450.

Patterson, S.E. 2001. Cutting loose: abscission and dehiscence in *Arabidopsis*. Plant Physiol. 126:494-500.

Schumacher, K., T. Schmitt, M. Rossberg, G. Schmitz, and K. Theres. 1999. The *Lateral suppressor* (*Ls*) gene of tomato encodes a new member of the VHIID protein family. Proc. Natl. Acad. Sci. USA 96:290-295.

Sexton, R. and J.A. Roberts. 1982. Cell biology of abscission. Annu. Rev. Plant Physiol. 33:133-162.

Sun, L., M.J. Bukovac, P.L. Forsline, and S. van Nocker. 2009. Natural variation in fruit abscission-related traits in apple (*Malus*). Euphytica 165:55-67.

Theissen, G. and H. Saedler. 2001. Floral quartets. Nature 409:469-471.

Velasco, R., A. Zharkikh, J. Affourtit, A. Dhingra, A. Cestaro, A. Kalyanaraman, P. Fontana, S.K. Bhatnagar, M. Troggio, D. Pruss, S. Salvi, M. Pindo, P. Baldi, S. Castelletti, M. Cavaiuolo, G. Coppola, F. Costa, V. Cova, A. Dal Ri, V. Goremykin, M. Komjanc, S. Longhi, P. Magnago, G. Malacarne, M. Malnoy, D. Micheletti, M. Moretto, M. Perazzolli, A. Si-Ammour, S. Vezzulli, E. Zini, G. Eldredge, L.M. Fitzgerald, N. Gutin, J. Lanchbury, T. Macalma, J.T. Mitchell, J. Reid, B. Wardell, C. Kodira, Z. Chen, B. Desany, F. Niazi, M. Palmer, T. Koepke, D. Jiwan, S. Schaeffer, V. Krishnan, C. Wu, V.T. Chu, S.T. King, J. Vick, Q. Tao, A. Mraz, A. Stormo, K. Stormo, R. Bogden, D. Ederle, A. Stella, A. Vecchietti, M.M. Kater, S. Masiero, P. Lasserre, Y. Lespinasse, A.C. Allan, V. Bus, D. Chagne, R.N. Crowhurst, A.P. Gleave, E. Lavezzo, J.A. Fawcett, S. Proost, P. Rouze, L. Sterck, S. Toppo, B. Lazzari, R.P. Hellens, C.E. Durel, A. Gutin, R.E. Bumgarner, S.E. Gardiner, M.

Skolnick, M. Egholm, Y. Van de Peer, F. Salamini, and R. Viola. 2010. The genome of the domesticated apple (*Malus* × *domestica* Borkh.). Nat. Genet. 42:833-839.

Weigel, D. 1995. The genetics of flower development: from floral induction to ovule morphogenesis. Annu. Rev. Genet. 29:19-39.

Zhou, Y., D. Lu, C. Li, J. Luo, B.F. Zhu, J. Zhu, Y. Shangguan, Z. Wang, T. Sang, B. Zhou, and B. Han. 2012. Genetic control of seed shattering in rice by the *APETALA2* transcription factor *SHATTERING ABORTION1*. Plant Cell 24:1034-1048.

CHAPTER 3

Abscission-Related Genes Revealed by RNA-Seq Analysis Using Self-Abscising Apple (*Malus* × *domestica*)

ABSTRACT

A comparative analysis was conducted between central pedicel (CP) and lateral pedicel (LP) in the self-abscising apple cultivar 'Saika' to identify the genes that trigger the abscission mechanism, as the destinies of the pedicels in a cluster are obvious. Transcriptome analysis was performed using RNA-Seq to compare expression profiles between surviving CP and abscised LP. A total of 797,647 expressed sequence tags were assembled into 65,876 contigs, which were annotated and analyzed through gene ontology analysis. A total of 1,585 differentially expressed genes (DEGs) were identified in CP and LP. Analyses on DEGs and quantitative real-time reverse-transcription polymerase chain reaction showed that *IAA3*/*SHY2* was up-regulated in CP and *IAA14*/*SLR* was differentially expressed in LP. *IAA3*/*SHY2* may participate in meristem development which is mediated through auxin signal transduction and *IAA14*/*SLR* is at least partly involved in the mechanism of abscission in LP. The *AUX*/*IAA* genes may be related to the roles of determining the fate of pedicels in early abscission.

INTRODUCTION

Fruit abscission has evolved to ensure tree survival and is useful for labor-saving tree cultivation. As apple trees, including most *Malus* spp., bloom during anthesis, they cannot maintain all the fruit that set due to the high fruit load. Some apple trees have developed various self-regulatory mechanisms to control fruit load by reducing the number of fruits after pollination, but do not control the number of flowers at anthesis. These mechanisms progress through various phases: June drop, when growing fruits abscised; pre-harvest drop, when ripe fruits abscised close to harvest; and ripening abscission, when the fruit mature. However, lateral fruits, excluding central fruit in the same cluster, abscise early in the abscission phase within 30 days after full bloom (DAFB). This 'self-thinning' characteristic, which differs from other abscission mechanisms, occurs in some cultivars.

Abscission includes four steps: (1) differentiation of the abscission zone (AZ), (2) acquisition of competence to respond to abscission-promoting signals during the pre-abscission stage, (3) activation of abscission, and (4) sealing of breaks in the proximal region (Nakano et al., 2013; Patterson, 2001). Differentiation of the AZ is initiated by transcription factors and other regulators. In tomato, *JOINTLESS* (Mao et al., 2000) forms protein complexes to develop the AZ by interacting with other MADS-box genes, such as *MACROCALYX* (Nakano et al., 2012) and *SEPALLATA* (*SLMBP21*) (Liu et al., 2014). Abscission of the *Arabidopsis* floral organ is regulated by the BTB/POZ domain and ankyrin repeat-containing *NPR1*-like proteins

including *BLADE-ON-PETIOLE 1* (*BOP1*) and *BOP2* (McKim et al., 2008). During activation of the abscission step, the *INFLORESCENCE DEFICIENT IN ABSCISSION* (*IDA*) peptide ligand, triggers abscission signals through the receptor-like kinases *HAESA* (*HAE*) and *HAESA-LIKE 2* (*HSL2*) (Butenko et al., 2003; Jinn et al., 2000; Stenvik et al., 2008), and the signal is transduced into the nucleus by mitogen activating protein kinase cascade (Cho et al., 2008). Finally, *KNOTTED*-like homeobox genes regulate transcription of genes associated with cell separation (Shi et al., 2011).

The major components inducing abscission are sugar starvation and plant hormones, particularly auxin. Sugar starvation activates trehalose-6-phophate and plays important roles triggering abscission by mediating the accumulation of reactive oxygen species as well as abscisic acid (ABA) and ethylene signaling (Botton et al., 2011). Furthermore, isoprene emissions and ABA content increase during early fruit abscission (Giulia et al., 2013). In another self-abscising apple, 'X3177', additional amphivasal vascular bundles transport sugars toward central fruit, allowing it to develop dominance over lateral fruits (Celton et al., 2014).

Fruit abscission may result from interactions between auxin and ethylene in response to developmental processes or a changing environment (Abebie et al., 2008). According to the 'senescence-triggered abscission model' in leaves and mature fruit, ethylene is the primary signal that regulates the initial abscission step (van Doorn and Stead, 1997). However, this model does not account for the abscission of young apple fruit, as increased ethylene evolution is not observed at the early abscission stage (Sun et al., 2009). Instead, basipetal polar auxin transport is the initial

driving force for the abscission of young fruit, based on the ‘correlatively driven model’ (Bangerth, 2000). Central fruit from the first blossom in the same cluster develops earlier than the other fruits by dominating lateral fruit development. The dominant central fruit produces most of the auxin and accumulates the starch transported from other sources for development, whereas lateral fruit show reduced growth rates and less auxin transport to peduncle (Bangerth, 2000). The AZ is sensitized to ethylene and is destined to abscise when auxin reaches the shedding threshold concentration because of low auxin transport from young fruit.

According to Dal Cin et al. (2009a, b), genes related to polar auxin transport may be involved in abscission during the shedding of immature fruit. Similarly, transcript levels of the *MdPIN1* and *MdIAA3* genes decreased in seed from abscising fruit, and the accumulation of *Malus × domestica LIKE AUX1 (MdLAX1)*, *MdLAX2*, *MdPIN1*, and *MdPIN10* gene transcripts, which may be responsible for seed development and the induction of abscission, is repressed by ethylene (Dal Cin et al., 2009b). A cDNA-amplified fragment length polymorphism analysis to identify differentially expressed genes (DEGs) between abscising and non-abscising fruitlets using benzylaminopurine spray treatment revealed that *auxin hydrogen symporter* (*AHS*) transcript levels were lower in the cortex of abscising fruit (Dal Cin et al., 2009a). In contrast, auxin influx carrier genes, including *AUXIN RESISTANT 1* (*AUX1*), *LAX1*, and *LAX3*, were strongly expressed at the site of floral organ abscission (Basu et al., 2013), suggesting the involvement of auxin signaling in abscission.

The *AXR3* gene, which is a member of the *AUXIN/INDOLE-3-ACETIC*

ACID (*AUX/IAA*) transcription factor family, delayed shedding of floral organs by interfering with auxin signaling at the AZ (Basu et al., 2013). Meir et al. (2006) showed that levels of expression of *Mj-Aux/IAA1* and *Mj-Aux/IAA2* were repressed by removal of IAA sources in the AZ of *Mirabilis jalapa*. In cestrum (*Cestrum elegans*), the application of synthetic auxins on floret AZs induced the expression of *AUX/IAA* genes (Abebie et al., 2008). Microarray analysis of the transcriptome in the AZ of tomato flowers showed that *AUX/IAA* genes were down-regulated early after the depletion of auxin and that early modified expression of these genes might mediate auxin regulation of ethylene sensitivity in the AZ (Meir et al., 2010). Furthermore, *AUX/IAA* transcription factors play a central role regulating cell wall remodeling genes so that lateral roots emerged in response to the *IDA-HAE-HSL2* signaling cascade (Lavenus et al., 2013; Swarup et al., 2008).

Pedicels were collected from flower clusters of the self-abscising apple cultivar 'Saika' at full bloom (FB) and 10 DAFB to examine molecular events in pedicels with a developing AZ, because abscission may be induced during an earlier phase than expected, based on the abscission model. Transcriptome analyses were performed to compare gene expression profiles between surviving central pedicel (CP) and abscised lateral pedicels (LP). This report focused on the genes associated with auxin signaling enriched in DEG sets by comparing abscising LP with persisting CP.

MATERIALS AND METHODS

Plant Material

Ten-year-old 'Saika' apple (*Malus* × *domestica* Borkh.) trees (n = 17) grafted on M.9 rootstocks were grown at the National Institute of Horticultural and Herbal Science, Suwon, Korea. 'Saika' was selected as a fruit self-thinning cultivar at the Aomori Apple Experiment Station, Japan (Kon et al., 2000) and has been widely distributed as 'Aori No. 9'. All flowers were artificially pollinated with mixed pollen collected from various cultivars to avoid the self-incompatibility resulting from the same S-genotypes. Approximately 20-30 flower clusters were collected at random from each of the ten trees. Only CP and LP without fruit and peduncle were collected separately from each cluster, in triplicate, at FB and at 10 DAFB.

Microscopic Observation

The pedicel tissues including AZ were observed under a light microscope as described by Luft (1973). The samples (about 1 mm^3) were fixed with 2.5% glutaraldehyde in 0.1 M sodium phosphate buffer (pH 7.2) at 4°C for 2 h. The specimens were rinsed, post-fixed with 1% (w/v) osmium tetroxide (OsO_4) at 4°C for 2 h, and held overnight in the same buffer. After fixation, the specimens were dehydrated in a graded series of ethanol (40, 60, 80, 90, 95, and 100% in distilled H_2O (v/v)). To ensure complete dehydration, the specimens were processed through three changes of

propylene oxide for 15, 15, and 30 min per change, and gradually infiltrated for 3 h each with 30, 50, and 100% embedding media in propylene oxide, Epon. The specimens were held overnight in 100% Epon before polymerization at 60°C for 72 h. The sectioned specimens (1.5 μm) were observed under a light microscope (Axioskop 2, Carl Zeiss Inc., Oberkochen, Germany).

RNA Isolation

Frozen tissues were pulverized with a mortar and pestle using liquid nitrogen. Total RNA was extracted separately from CP and LP samples according to the method of Chang et al. (1993), with minor modifications. The extracted RNA was precipitated, and the resulting pellet was resuspended in diethylpyrocarbonate-treated water. RNA quality was assessed by electrophoresis on an 1% agarose gel and quantified using a NanoDrop ND-1000 spectrophotometer (ThermoScientific, Waltham, MA, USA).

cDNA Preparation and Pyrosequencing

mRNAs were isolated from 50 μg of total RNA from each of the mixed CP and LP samples collected at FB and at 10 DAFB using the FastTrack MAG Micro mRNA Isolation Kit (Life Technologies, Foster City, CA, USA), following the manufacturer's protocol. The mRNAs were quantified using an Agilent RNA 6000 Nano LabChip (Agilent Technologies, Santa Clara, CA,

USA), and 200 ng mRNA from CP and LP at FB was used to generate cDNA libraries with the cDNA Rapid Library Preparation Kit (Life Technologies). The cDNA libraries were used for emulsion polymerase chain reaction (PCR), as described by the manufacturer. The quality of cDNA was assessed using an Agilent 2100 BioAnalyzer, and pyrosequencing was performed on a Roche 454 GS-FLX sequencer (Basel, Switzerland).

Trimming, Assembly, and Annotation of the Pedicel Transcriptomes

The raw reads were trimmed using Mothur (Version 1.33.3) software (http://www.mothur.org) to remove the primers and adaptors used to prepare the libraries. The trimmed reads were assembled using Newbler Version 2.3 (http://www.454.com) with the default parameters. Mapping was performed on CLC Genomics Workbench Version 6.5 (http://www.clcbio.com) following the manufacturer's instructions. The reads were mapped against *Malus* × *domestica* reference sequences from Phytozome (http://www.phytozome.net). The total number of reference transcripts was 63,541. Expression values were normalized to reads per kilobase of exon model per million (RPKM) mapped read values (Mortazavi et al., 2008), and other parameters were maintained at the default settings.

Enrichment Analysis

The assembled transcripts were loaded on Blast2GO (http://www.blast2go.com) for functional annotation and gene ontology (GO)

classification. GO annotation was performed using the InterPro scan, ANNEX, GOSlim, and KEGG functions in Blast2GO software. The two-tailed Fisher's exact test was performed to identify differences in expression, and double IDs were removed at $P \leq 0.05$.

Detection of DEGs

The expression profiles obtained using CLC Genomics Workbench were imported into the Bioconductor package (http://www.bioconductor.org), in NOISeq software (http://www.bioconductor.org) using the biological replicates option to identify DEGs. NOISeq uses a non-parametric method to infer the noise distribution from the data and assesses whether a change in counts for each gene is likely to be noise or a DEG (Tarazona et al., 2011). Default parameters were used according to the manual. Genes showing significant differences in relative expression were annotated into functional categories using MapMan software (http://mapman.gabipd.org) to identify over-represented functional groups. The MapMan analysis was based on the *Malus* × *domestica* mapping file as a reference map. The analysis focused on genes associated with auxin signaling.

Quantitative Real-Time Reverse-Transcription PCR (qRT-PCR)

Total RNAs were subjected to qRT-PCR, including mRNAs from CP and LP at 10 DAFB. Each total RNA (1.0 μg) was reverse-transcribed using random hexamers and Superscript III (Invitrogen, Carlsbad, CA, USA),

according to the manufacturer's instructions. Each cDNA (2.0 ng) was used as a template for the qRT-PCR.

Gene-specific primers were designed according to the respective contigs assembled from reads obtained from the results of 454 GS-FLX pyrosequencing. Primer Express software (Applied Biosystems, Foster City, CA, USA) was used to design the primers using the default options listed in Supplementary Table 3-1. cDNA was amplified using the SYBR Premix EX Taq Kit (Takara, Tokyo, Japan) on an Applied Biosystems 7500 Fast Real-Time PCR System, according to the manufacturer's protocol. Each 50 μL reaction contained 18 μL double distilled H_2O, 25 μL 2× premix, 1 μL forward primer (10 μM), 1 μL reverse primer (10 μM), 4 μL cDNA template, and 1 μL ROX reference dye II.

The $2^{-\Delta\Delta C_T}$ method (Livak and Schmittgen, 2001) was used to normalize and calibrate the transcript values relative to the *Malus* × *domestica actin* (MDP0000116906), *ubiquitin* (MDP0000499193), and *nad5* genes (MDP0000136998) as internal standard housekeeping genes. Each experiment was run in triplicate using three biological replicates. A heat map was drawn to visualize patterns of expression and relationships between the DEGs using the gplots library in R (http://www.r-project.org).

RESULTS AND DISCUSSION

Characteristics of the Self-Abscising Apple Cultivar

The self-abscising apple cultivar ‘Saika’ had a selective abscission mechanism in which only central fruit persisted in each cluster, and the four lateral fruits were shed within 30 DAFB. Thus, no artificial thinning is needed for cultivars exhibiting this characteristic. ‘Saika’ fruits formed a hierarchy within a cluster, and the hierarchy was the order in which the flowers were pollinated and developed into fruit. This hierarchical fruit abscission pattern was different from that of ‘X3191’, which may be a sister cultivar to ‘X3177’ used by Celton et al. (2014), according to the flowering order and fruit position.

Central flower opened first in the self-abscising apple cultivar ‘Saika’, after which lateral flowers opened according to their position in the corymb (Fig. 3-1A). This flowering order was directly associated with the hierarchy of flower or fruit dominance. After FB, central fruit exhibited the maximum sink strength, whereas lateral fruit showed limited growth (Fig. 3-1B). Lateral fruits whose pedicels had discolored to yellow at 20 DAFB did not continue to grow and began to abscise in a hierarchical manner (Fig. 3-1C). All lateral fruit were eventually shed, leaving only one fruit per cluster over the entire tree within 30 DAFB (Fig. 3-1D).

Fig. 3-1. Fruit development in the self-abscising apple cultivar ‘Saika’. Lateral fruits abscised within 30 DAFB, leaving central fruit in each cluster. Flower cluster at FB (A), 10 DAFB (B), 20 DAFB (C), and 30 DAFB (D).

AZ Formation in LP in Self-Abscising Apple Fruit

The AZ formed in LP at the domain to be separated near the peduncle (Fig. 3-2A). Protective layers were generated between the AZ and peduncle (Fig. 3-2B). The AZ is composed of six- to eight-layers of smaller, cubical cells with a dense cytoplasm, compared to those of surrounding cells (Tabuchi and Arai, 2000). Cell differentiation of the AZ is gradually initiated at the meristematic cells, spreads to the vascular bundle and cortex, and finally to the epidermal region of the pedicel-like lateral root primordium growing from the endodermis to the epidermis via the cortex (Tabuchi, 1999).

Pedicel Transcriptomes

Pyrosequencing was performed in biological triplicates with cDNA samples from the mixed CPs and LPs at FB and 10 DAFB, respectively (Table 3-1). After trimming, 405,611 reads were obtained for CP, and 391,726 reads were obtained for LP. Although some reads comprised short repeats and non-informative sequences, the longer read lengths provided by 454 GS-FLX increased the possibility of assembling a full transcript. These sequences were assembled into 65,876 contigs (33,360 for CP and 32,516 for LP) and 31,045 singletons (15,752 for CP and 15,293 for LP), following the trimming and cleaning processes.

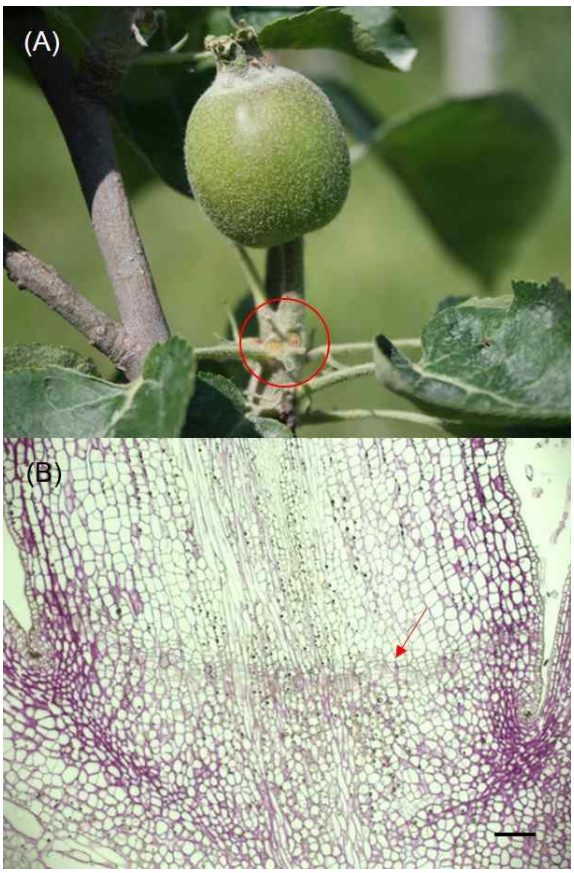

Fig. 3-2. The AZ that developed in LP of self-abscising apple cultivar 'Saika'. (A) AZ located between the pedicel and the peduncle which was manually dissected from longitudinal sections. (B) Micrograph of the peduncle AZ indicated by an arrow. Scale bar = 100 μm.

Table 3-1. Summary of the ‘Saika’ transcriptomes in CP and LP based on the RNA-Seq data.

Read	Central pedicel	Lateral pedicel
Total number of reads	405,611	391,726
Total base pairs (bp)	167,148,300	162,781,108
Number of reads after trimming	405,422	391,584
Assembled reads	286,661	283,508
Total number of contigs	33,360	32,516
Total number of singletons	15,752	15,293
Average read length (bp)	403.5	407.0
Longest read	735	732
Mapped reads	204,316	195,788
Unmapped reads	201,106	195,796

The annotated contigs were assigned to GO terms using Blast2GO to examine the functions of DEGs between CP and LP. The annotations from CP sequences were compared to those from LP sequences using Fisher's exact test at $P \leq 0.05$ to detect significant differences between functional classes (Fig. 3-3). LP showed increased responses for 'catalytic activity (GO:0003824)', 'transferase activity (GO:0016740)', 'lipid metabolic processes (GO:0006629)', 'single-organism metabolic processes (GO:0044710)', and 'generation of precursor metabolites and energy (GO:0006091)'. More genes were related to 'metabolic processes (GO:0008152)' in LP than to those in CP, but not significantly different. GO terms associated with 'binding (GO:0005488)' were assigned to CP, including 'nucleic acid binding (GO:0003676)' and 'DNA binding (GO:0003677)'.

Digital Expression Profiling of Auxin-Related Genes

Aligning the assembled contigs to the apple reference transcripts revealed that 16,647 contigs were common between CP and LP, and 4,708 and 4,546 contigs were specific to CP and LP, respectively. A total of 1,585 DEGs were identified between CP and LP using NOISeq (Fig. 3-4, Supplementary Tables 3-2, 3-3). Genes related to auxin signal transduction were identified by MapMan software (Fig. 3-5, Supplementary Table 3-4). *IAA3/SHORT HYPOCOTYL 2* (*SHY2*) (MDP0000945260) and *IAA14/ SOLITARY-ROOT* (*SLR*) (MDP0000124810) were differentially expressed

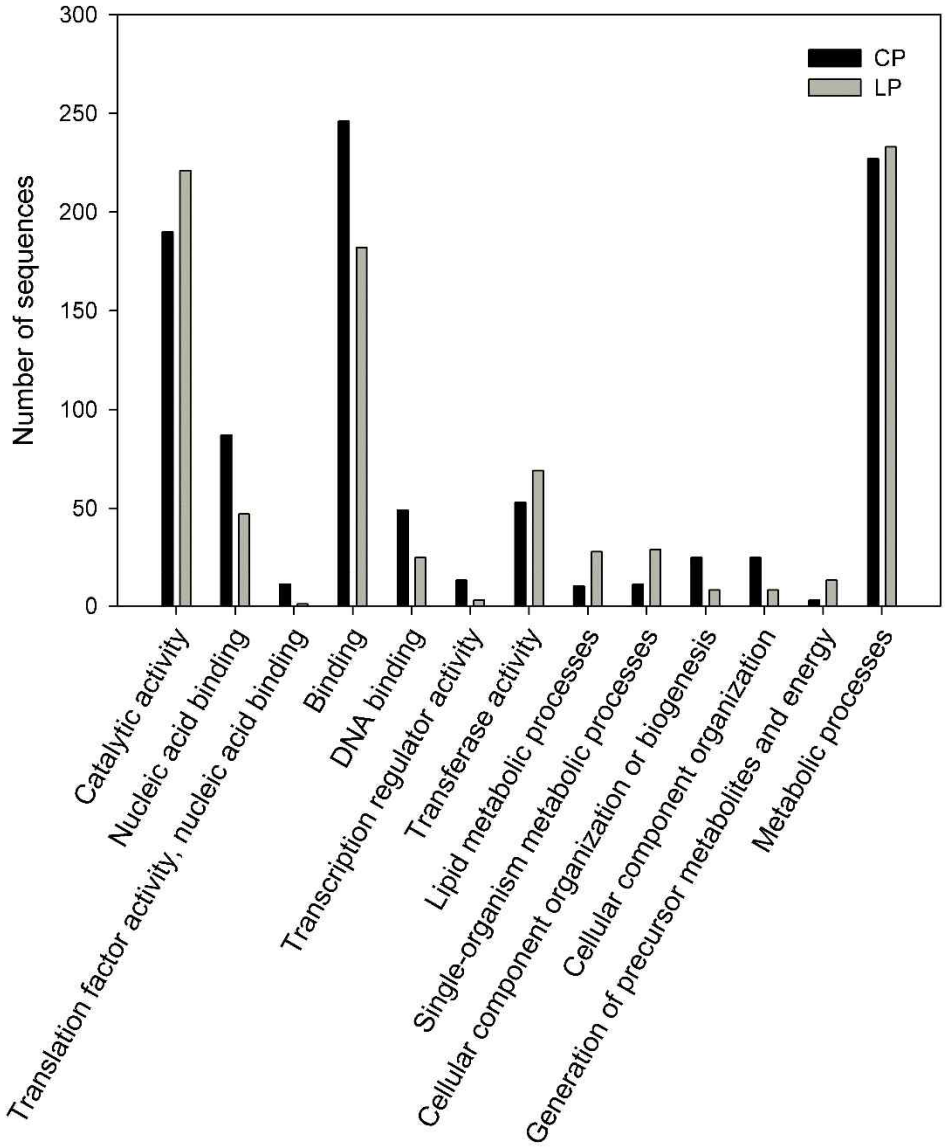

Fig. 3-3. Functional category enrichment analysis of DEGs using Blast2GO. A two-sided Fisher's exact test was used to assess functional differences between CP and LP. Only GO terms with $P \leq 0.05$ are shown.

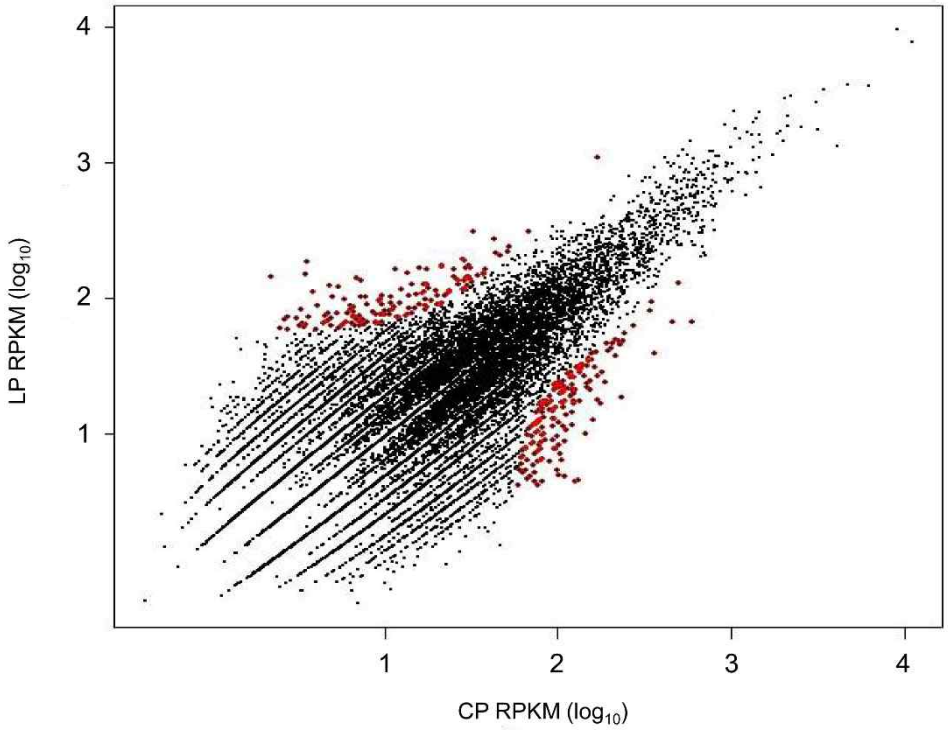

Fig. 3-4. DEGs in CP and LP analyzed using NOISeq software. Distribution of gene expression [$\log_{10}$ transformed RPKM (reads per kilobase per million)] between CP and LP is depicted with differentially expressed transcripts highlighted as red dots.

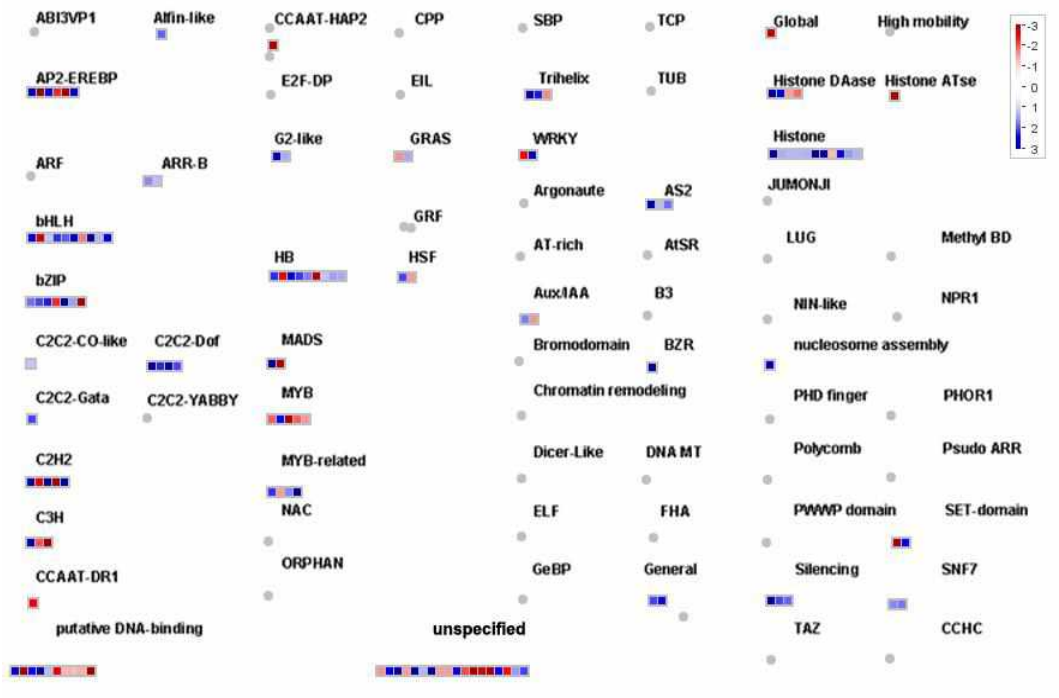

Fig. 3-5. Visualization of differences in gene expression between CP and LP using MapMan software. On the logarithmic color scale ranging from –3 to 3, dark blue represents higher expression in CP than in LP, and red represents higher expression in LP than in CP. The detailed gene lists are shown in Supplementary Table 3-4.

between CP and LP. *AUX/IAA* transcription factors, which are negative regulators of auxin signaling (Overvoorde et al., 2005), are degraded by the proteasome through ubiquitination in the presence of auxin (Dharmasiri and Estelle, 2004). *IAA3/SHY2*, homologous to *Arabidopsis* AT1G04240, was differentially expressed in CP (Fig. 3-5, Supplementary Table 3-4). *IAA3/SHY2* is a key regulatory component of meristem size by auxin and cytokinin (Koren et al., 2013). Furthermore, *SHY2* is involved in regulating lateral root formation (Koren et al., 2013) and negatively regulates the *PIN* gene, which is an auxin efflux carrier (Peng et al., 2013). In contrast, the *IAA14/SLR* transcript was highly expressed in LP (Fig. 3-5, Supplementary Table 3-4). *IAA14/SLR* is a key regulator of auxin-regulated lateral root formation (Fukaki et al., 2002) and emergence (Lavenus et al., 2013). The *IAA3/SHY2-ARF7* module, which is expressed in the root endodermis, regulates the development and emergence of lateral root primordium (Goh et al., 2012).

The auxin influx carrier *AUX2* (MDP0000155074) and the efflux carriers *AHS* (MDP0000225382 and MDP0000298711), *PIN7* (MDP0000497581), and *PIN10* (MDP0000200231) were dominant in CP at FB; however, only *LAX2* (MDP0000749280) was preferentially expressed in LP (Fig. 3-5, Supplementary Table 3-4). According to the auxin signaling model, *AUX/IAA* repressors are dissociated from *ARF* heterodimers and degraded by the proteasome at high auxin concentrations (Hagen and Guilfoyle, 2002). Numerous *ARF* proteins released by *AUX/IAA* transcription factors

were found in CP and LP, but no *ARF* gene was identified as DEGs in CP or LP based on the NOISeq analysis (Supplementary Tables 3-2, 3-3). However, further experiments are required to identify *ARF* genes expressed due to the degradation of *AUX/IAA* proteins during the induction of abscission. Question of whether *ARF* promotes the expression of *IDA*, *HAE*, or *HSL2* gene to trigger abscission process should be answered. In addition, interaction of *AUX/IAA* with *ARF* should be confirmed on protein level by yeast two-hybrid screening or mass spectrometry.

Confirmation of DEGs Using qRT-PCR

Among the DEGs, auxin-related genes were investigated using gene-specific primers and by targeting the RNAs of CP and LP at FB and at 10 DAFB (Supplementary Table 3-1). qRT-PCR was also performed with RNAs from CP and LP at 10 DAFB to investigate the altered expression patterns. Each gene was assigned according to hierarchical clustering, regardless of the priority of the auxin signaling pathway (Fig. 3-6).

The auxin influx carrier, the gene *AUX2*, was dominant in CP at FB, but its expression level was similar in CP and LP at 10 DAFB. *LAX1* and *LAX2* were relatively up-regulated in LP at FB. In addition, these genes were expressed at similar or slightly higher levels in CP at 10 DAFB than in LP. *PIN1* expression at FB or 10 DAFB did not differ between CP and LP. However, *PIN10* was differentially expressed in LP at 10 DAFB. *PIN7* was preferentially expressed in LP at FB. The *AHS* genes MDP0000225382 and

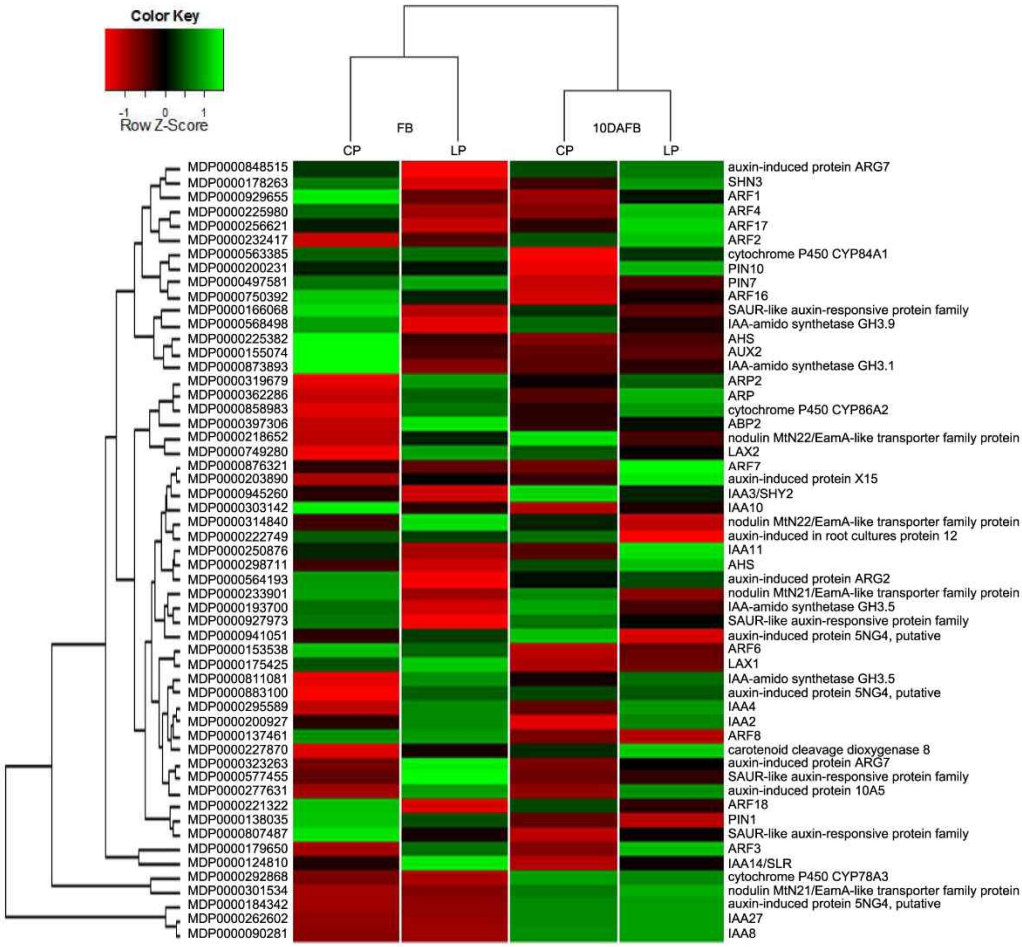

Fig. 3-6. qRT-PCR analysis of DEGs using the NOISeq and MapMan softwares. On the logarithmic color scale, red represents higher expression in CP than in LP, while green represents higher expression in LP than in CP.

MDP0000162143 showed different expression patterns; MDP0000225382 was expressed at a slightly higher level in CP at FB, whereas MDP0000162143 was expressed in LP at 10 DAFB. Another auxin receptor, *auxin binding protein 2* (*ABP2*), was up-regulated in LP and expressed considerably at higher levels at FB than at 10 DAFB.

The *AUX/IAA* transcription factor *IAA3/SHY2* was differentially expressed in CP, and its expression level was higher at 10 DAFB than at FB (Fig. 3-6). In contrast, *IAA14/SLR* was strongly up-regulated in LP; its expression level was three-fold higher in LP than in CP at FB, and two-fold higher in LP than in CP at 10 DAFB. *IAA10* and *IAA11* were up-regulated in CP at FB and in LP at 10 DAFB, respectively. *IAA27* and *IAA8* were expressed at low levels at FB; however, their expression levels increased by 9.9- to 12.4-fold and 8.9- to 11.9-fold, respectively, at 10 DAFB.

The transcription factor genes *ARF3/ETTIN (ETT)* and *IAA14/SLR* were expressed at similar levels at FB, but *ARF3/ETT* was more highly expressed at 10 DAFB than *IAA14/SLR* (Fig. 3-6). The level of expression of *ARF2*, which had a similar expression pattern to that of *ARF3/ETT*, was higher in LPs than in CP. Expression of *ARF1*, *ARF4*, and *ARF16* were up-regulated in CP at FB, and their levels of expression were elevated in LP at 10 DAFB. *ARF17* expression increased in LP at 10 DAFB, but no difference in *ARF18* expression was detected between FB and 10 DAFB. *ARF7* showed slightly increased expression in LP at 10 DAFB.

In addition, *IAA8* and *IAA27* were strongly up-regulated at 10 DAFB in

both CP and LP (Fig. 3-6). *Auxin-repressed protein*, which plays a role in growth arrest (Lee et al., 2013), was exclusively expressed in LP. Several genes involved in suberin and lignin biosynthesis were also expressed in LP (Fig. 3-6), indicating the abundance of the phenylpropanoid biosynthesis gene set. The *SHINE 2* (*SHN2*) transcription factor, which induces suberin biosynthesis, was expressed at a relatively high level in LP at 10 DAFB. *SHN2* is expressed specifically in cell separation regions of *Arabidopsis* anthers and siliques (Shi et al., 2011). Furthermore, CYP86A cytochrome P450, which belongs to the cutin and suberin-associated protein family, was also expressed differentially in LP (Fig. 3-6). These findings demonstrate that formation of the protective layer may be initiated near the peduncle of LP, where the AZ develops.

The major components inducing abscission process are known to be sugar starvation or plant hormones (Bangerth, 2000). Based on microarray experiments using another self-abscising apple hybrid 'X3177', which was released from the Institut National de la Recherche Agronomique (INRA), sugar starvation is the main driving force to induce pedicel abscission (Celton et al., 2014). In central fruit, additional amphivasal vascular bundles transport sugars toward central fruit, and allow central fruit to develop dominance over lateral fruits (Celton et al., 2014).

Focusing on plant hormones, especially auxin, the *AUX*/*IAA* genes are noticeable factors to initiate abscission process (Abebie et al., 2008; Meir et al., 2006; Meir et al., 2010). According to the DEG analysis

(Supplementary Tables 3-2, 3-3) and the results of qRT-PCR (Fig. 3-6), *IAA3*/*SHY2* was up-regulated in persisting pedicels and *IAA14*/*SLR* was differentially expressed in abscising pedicels. *IAA14*/*SLR* may be involved, at least in part, during the early stages of the pedicel abscission process, although the question of how *IAA14*/*SLR* triggers abscission remains to be answered.

The *AUX*/*IAA* genes may be related to the roles of determining the fate of pedicels in early abscission. These transcription factors are linked to meristem differentiation (Koren et al., 2013) or lateral root emergence mechanism (Lavenus et al., 2013), which mediate auxin signal transduction. In CP, *IAA3*/*SHY2* participates in auxin-mediated meristem development. Considering that *IAA14*/*SLR* and *ARF7* were highly expressed in LP, a mechanism similar to that of lateral root emergence may allow the *IAA14*/*SLR-ARF7* signaling cascade to trigger *IDA-HAE-HSL2* signaling cascade in LP (Okushima et al., 2007). Future studies will focus on identifying what genes are regulated directly or indirectly by *IAA14*/*SLR* in abscising pedicel and determining whether these genes trigger the early abscission process in pedicels.

LITERATURE CITED

Abebie, B., A. Lers, S. Philosoph-Hadas, R. Goren, J. Riov, and S. Meir. 2008. Differential effects of NAA and 2,4-D in reducing floret abscission in cestrum (*Cestrum elegans*) cut flowers are associated with their differential activation of *Aux/IAA* homologous genes. Ann. Bot. 101:249-259.

Bangerth, F. 2000. Abscission and thinning of young fruit and their regulation by plant hormones and bioregulators. Plant Growth Regul. 31:43-59.

Basu, M.M., Z.H. González-Carranza, S. Azam-Ali, S. Tang, A.A. Shahid, and J.A. Roberts. 2013. The manipulation of auxin in the abscission zone cells of *Arabidopsis* flowers reveals that indoleacetic acid signaling is a prerequisite for organ shedding. Plant Physiol. 162:96-106.

Botton, A., G. Eccher, C. Forcato, A. Ferrarini, M. Begheldo, M. Zermiani, S. Moscatello, A. Battistelli, R. Velasco, B. Ruperti, and A. Ramina. 2011. Signaling pathways mediating the induction of apple fruitlet abscission. Plant Physiol. 155:185-208.

Butenko, M.A., S.E. Patterson, P.E. Grini, G.E. Stenvik, S.S. Amundsen, A. Mandal, and R.B. Aalen. 2003. *INFLORESCENCE DEFICIENT IN ABSCISSION* controls floral organ abscission in *Arabidopsis* and identifies a novel family of putative ligands in plants. Plant Cell 15:2296-2307.

Celton, J.M., E. Dheilly, M.C. Guillou, F. Simonneau, M. Juchaux, E. Costes, F. Laurens, and J.P. Renou. 2014. Additional amphivasal bundles in pedicel pith exacerbate central fruit dominance and induce self-thinning

of lateral fruitlets in apple. Plant Physiol. 164:1930-1951.

Chang, S., J. Puryear, and J. Cairney. 1993. A simple and efficient method for isolating RNA from pine trees. Plant Mol. Biol. Rep. 11:113-116.

Cho, S.K., C.T. Larue, D. Chevalier, H. Wang, T.L. Jinn, S. Zhang, and J.C. Walker. 2008. Regulation of floral organ abscission in *Arabidopsis thaliana*. Proc. Natl. Acad. Sci. USA 105:15629-15634.

Dal Cin, V., E. Barbaro, M. Danesin, H. Murayama, R. Velasco, and A. Ramina. 2009a. Fruitlet abscission: a cDNA-AFLP approach to study genes differentially expressed during shedding of immature fruits reveals the involvement of a putative auxin hydrogen symporter in apple (*Malus* × *domestica* L. Borkh.). Gene 442:26-36.

Dal Cin, V., R. Velasco, and A. Ramina. 2009b. Dominance induction of fruitlet shedding in *Malus* × *domestica* (L. Borkh.): molecular changes associated with polar auxin transport. BMC Plant Biol. 9:139.

Dharmasiri, N. and M. Estelle. 2004. Auxin signaling and regulated protein degradation. Trends Plant. Sci. 9:302-308.

Fukaki, H., S. Tameda, H. Masuda, and M. Tasaka. 2002. Lateral root formation is blocked by a gain-of-function mutation in the *SOLITARY-ROOT/IAA14* gene of *Arabidopsis*. Plant J. 29:153-168.

Giulia, E., B. Alessandro, D. Mariano, B. Andrea, R. Benedetto, and R. Angelo. 2013. Early induction of apple fruitlet abscission is characterized by an increase of both isoprene emission and abscisic acid content. Plant Physiol. 161:1952-1969.

Goh, T., S. Joi, T. Mimura, and H. Fukaki. 2012. The establishment of asymmetry in *Arabidopsis* lateral root founder cells is regulated by

LBD16/ASL18 and related *LBD/ASL* proteins. Development 139:883-893.

Hagen, G. and T. Guilfoyle. 2002. Auxin-responsive gene expression: genes, promoters, and regulatory factors. Plant Mol. Biol. 49:357-372.

Jinn, T.L., J.M. Stone, and J.C. Walker. 2000. *HAESA*, an *Arabidopsis* leucine-rich repeat receptor kinase, controls floral organ abscission. Genes Dev. 14:108-117.

Kon, T., S. Sato, T. Kudo, K. Fujita, and T. Fukasawa-Akawa. 2000. Apple breeding at Aomori Apple Experiment Station, Japan. Acta Hort. 538:215-218.

Koren, D., N. Resnick, E.M. Gati, E. Belausov, S. Weininger, Y. Kapulnik, and H. Koltai. 2013. Strigolactone signalling in the endodermis is sufficient to restore root responses and involves *SHORT HYPOCOTYL 2* (*SHY2*) activity. New Phytol. 198:866-874.

Lavenus, J., T. Goh, I. Roberts, S. Guyomarc'h, M. Lucas, I. De Smet, H. Fukaki, T. Beeckman, M. Bennett, and L. Laplaze. 2013. Lateral root development in *Arabidopsis*: fifty shades of auxin. Trends Plant Sci. 18:450-458.

Lee, J., C.T. Han, and Y. Hur. 2013. Molecular characterization of the *Brassica rapa* auxin-repressed, superfamily genes, *BrARP1* and *BrDRM1*. Mol. Biol. Rep. 40:197-209.

Liu, D., D. Wang, Z. Qin, D. Zhang, L. Yin, L. Wu, J. Colasanti, A. Li, and L. Mao. 2014. The *SEPALLATA* MADS-box protein *SLMBP21* forms protein complexes with *JOINTLESS* and *MACROCALYX* as a transcription activator for development of the tomato flower abscission zone. Plant J.

77:284-296.

Livak, K.J. and T.D. Schmittgen. 2001. Analysis of relative gene expression data using real-time quantitative PCR and the $2^{-\Delta\Delta C_T}$ method. Methods 25:402-408.

Luft, J.H. 1973. Compounding of Luft's epon embedding medium for use in electron microscopy with reference to anhydride: epoxide ratio adjustment. Mikroskopie 29:337-342.

Mao, L., D. Begum, H.W. Chuang, M.A. Budiman, E.J. Szymkowiak, E.E. Irish, and R.A. Wing. 2000. *JOINTLESS* is a MADS-box gene controling tomato flower abscission zone development. Nature 406:910-913.

McKim, S., G.E. Stenvik, M.A. Butenko, W. Dristiansen, S.K. Cho, S.R. Hepworth, R.B. Aalen, and G.W. Haughn. 2008. The *BLADE-IN-PETIOLE* genes are essential for abscission zone formation in *Arabidopsis*. Development 135:1537-1546.

Meir, S., D.A. Hunter, J.C. Chen, V. Halaly, and M.S. Reid. 2006. Molecular changes occurring during acquisition of abscission competence following auxin depletion in *Mirabilis jalapa*. Plant Physiol. 141:1604-1616.

Meir, S., S. Philosoph-Hadas, S. Sundaresan, K.S. Selvaraj, S. Burd, R. Ophir, B. Kochanek, M.S. Reid, C.Z. Jiang, and A. Lers. 2010. Microarray analysis of the abscission-related transcriptome in the tomato flower abscission zone in response to auxin depletion. Plant Physiol. 154:1929-1956.

Mortazavi, A., B.A. Williams, K. McCue, L. Schaeffer, and B. Wold. 2008. Mapping and quantifying mammalian transcriptomes by RNA-Seq. Nat.

Methods 5:621-628.

Nakano, T., J. Kimbara, M. Fujisawa, M. Kitagawa, N. Ihashi, H. Maeda, T. Kasumi, and Y. Ito. 2012. *MACROCALYX* and *JOINTLESS* interact in the transcriptional regulation of tomato fruit abscission zone development. Plant Physiol. 158:439-450.

Nakano, T., M. Fujisawa, Y. Shima, and Y. Ito. 2013. Expression profiling of tomato pre-abscission pedicels provides insights into abscission zone properties including competence to respond to abscission signals. BMC Plant Biol. 9:13-40.

Okushima, Y., H. Fukaki, M. Onoda, A. Theologis, and M. Tasaka. 2007. *ARF7* and *ARF19* regulate lateral root formation via direct activation of *LBD*/*ASL* genes in *Arabidopsis*. Plant Cell 19:118-130.

Overvoorde, P.J., Y. Okushima, J.M. Alonso, A. Chan, C. Chang, J.R. Ecker, B. Hughes, A. Liu, C. Onodera, H. Quach, A. Smith, G. Yu, and A. Theologis. 2005. Functional genomic analysis of the *AUXIN/INDOLE-3-ACETIC ACID* gene family members in *Arabidopsis thaliana*. Plant Cell 17:3282-3300.

Patterson, S.E. 2001. Cutting loose: abscission and dehiscence in *Arabidopsis*. Plant Physiol. 126:494-500.

Peng, Y., L. Chen, Y. Lu, W. Ma, Y. Tong, and Y. Li. 2013. *DAR2* acts as an important node connecting cytokinin, auxin, *SHY2*, and *PLT1/2* in root meristem size control. Plant Signal. Behav. 8:e24226.

Shi, C.L., G.E. Stenvik, A.K. Vie, A.M. Bones, V. Pautot, M. Proveniers, R.B. Aalen, and M.A. Butenko. 2011. *Arabidopsis* class I *KNOTTED*-like homeobox proteins act downstream in the *IDA-HAE/HSL2* floral

abscission signalling pathway. Plant Cell 23:2553-2567.

Stenvik, G.E., N.M. Tandstad, Y. Guo, C.L. Shi, W. Kristiansen, A. Holmgren, S.E. Clark, R.B. Aalen, and M.A. Butenko. 2008. The EPIP peptide of *INFLORESCENCE DEFICIENT IN ABSCISSION* is sufficient to induce abscission in *Arabidopsis* through the receptor-like kinases *HAESA* and *HAESA-LIKE2*. Plant Cell 20:1805-1817.

Sun, L., M.J. Bukovac, P.L. Forsline, and S. van Nocker. 2009. Natural variation in fruit abscission-related traits in apple (*Malus*). Euphytica 165:55-67.

Swarup, K., E. Benkova, R. Swarup, I. Casimiro, B. Peret, Y. Yang, G. Parry, E. Nielsen, I. De Smet, S. Vanneste, M.P. Levesque, D. Carrier, N. James, V. Calvo, K. Ljung, E. Kramer, R. Roberts, N. Graham, S. Marillonnet, K. Patel, J.D. Jones, C.G. Taylor, D.P. Schachtman, S. May, G. Sandberg, P. Benfey, J. Friml, I. Kerr, T. Beeckman, L. Laplaze, and M.J. Bennett. 2008. The auxin influx carrier *LAX3* promotes lateral root emergence. Nat. Cell Biol. 10:946-954.

Tabuchi, T. 1999. Comparison on the development of abscission zones in the pedicels between two tomato cultivars. J. Jpn. Soc. Hort. Sci. 68:993-999.

Tabuchi, T. and N. Arai. 2000. Formation of the secondary cell division zone in tomato pedicels at different fruit growing stages. J. Jpn. Soc. Hort. Sci. 69:156-160.

Tarazona, S., F. García-Alcalde, J. Dopazo, A. Ferrer, and A. Conesa. 2011. Differential expression in RNA-Seq: a matter of depth. Genome Res. 21:2213-2223.

Van Doorn, W.G., and A.D. Stead. 1997. Abscission of flowers and flower parts. J. Exp. Bot. 48:821-837.

CONCLUSIONS

Forty eight apple genetic resources could be categorized into three groups: 1) a non-abscising group, in which no fruit is abscised; 2) a June drop group, in which the abscission process occurs non-selectively in clusters; and 3) a self-abscising group, in which only central or last fruit in a cluster remains to grow and the others are abscised. The self-abscising group showed a selective abscission pattern. Only central fruit persisted in a cluster and four lateral fruits were shed within 30 DAFB. In the self-abscising group, 'Saika', for example, lateral fruits were dropped, and only one fruit persisted in a cluster when abscission occurred. There was one exception; in *M. coronaria* 'Charlottae', central fruit did not dominate lateral fruits, but was abscised first in a cluster. The fruit nearest to the peduncle survived, although bloomed last. Although the apical flower bloomed earlier, it dropped first from a cluster. Fruits were shed sequentially from the distal fruit toward the peduncle. Finally, only the proximal fruit in a cluster survived.

The homologue which may play a similar role to *JOINTLESS* in tomato was identified at pedicels from self-abscising apple 'Saika' during early abscission. Based on sequence alignment and phylogenetic analysis, this MADS-box, *MdJOINTLESS* was similar to *JOINTLESS*, belonging to *SVP* clade. However, qRT-PCR and transformation results showed that *MdJOINTLESS* might not be responsible for development of the AZ. *MdJOINTLESS* was more highly expressed in persisting CP than in abscised LP. In addition, the introduction of *MdJOINTLESS* construct did not influence the development of AZ in tomato. This might result from the

sequence difference between *MdJOINTLESS* and *JOINTLESS*. To confirm the function of *MdJOINTLESS*, the AZ deformation is needed to be investigated in transgenic apple with *MdJOINTLESS* antisense construct. According to the DNA gel blot analysis, the self-abscising 'Saika' contained one or two *JOINTLESS* homologues in its genome. In addition, three homologues to *SVP* gene existed in apple genome, thus the other homologues, not *MdJOINTLESS*, might be related to the development of the AZ in apple. Based on the phylogenetic analysis with MADS-box genes derived from pedicel cDNA libraries, other MADS-box genes were expressed in pedicels, which did not belong to *SVP* clade. The genes analogous to *SEPALLATA* and *MACROCALYX* might be involved in the formation of the AZ in apple, as *SLMBP21* and *MACROCALYX* genes in tomato.

Transcriptome analysis of pedicels from the self-abscising apple 'Saika' showed the DEGs between persisting CP and abscised LP. From the RNA-Seq, 405,611 and 391,726 reads were obtained from CP and LP libraries, respectively. These sequences were assembled into 65,876 contigs (33,360 for CP and 32,516 for LP) and 31,045 singletones (15,752 for CP and 15,293 for LP). Aligning the contigs to the apple reference transcripts revealed that 16,647 contigs were common between CP and LP, and a total of 1,585 DEGs were identified from NOISeq software. This report focused on the genes associated with auxin signaling which was identified by MapMan software. The *AUX/IAA* transcription factor *IAA3/SHY2* was differentially expressed in CP and *IAA14/SLR* was strongly up-regulated in LP. *IAA3*/*SHY2* may participate in auxin-mediated meristem development in

CP and *IAA14/SLR* gene may at least partly be involved in the early stage of the pedicel abscission. A mechanism similar to that of lateral root emergence may allow the *IAA14/SLR* gene to trigger *IDA-HAE-HSL2* signaling cascade in LP. Future studies will focus on identifying what genes are regulated directly or indirectly by *IAA14/SLR* in LP and determining whether these genes trigger the early abscission process in pedicels. Further experiments are required to identify *ARF* genes expressed due to the degradation of *AUX/IAA* proteins during the induction of abscission. Question of whether *ARF* promotes the expression of *IDA*, *HAE*, or *HSL2* gene to trigger abscission process should be answered. In addition, interaction of *AUX/IAA* with *ARF* should be confirmed on protein level by yeast two-hybrid screening or mass spectrometry.

ABSTRACT IN KOREAN

사과 나무는 스스로 지탱할 수 없을 정도로 과도하게 착과한다. 따라서 상품성 있는 과일을 생산하기 위해서 적과 작업이 필수적인데, 적과의 가장 일반적인 방법인 화학적 적과와 인력 적과는 효율이 일정하지 않거나 노동 집약적인 문제점이 있다. 따라서, 한 과방 내의 과일들이 스스로 탈리되는 자가적과성 품종의 개발이 시간과 노동력을 절감할 수 있는 재배에 유용한 대안이 될 수 있다. 만개기부터 만개 후 30일까지 조기 탈리가 일어나는 양상을 근거로, 48종류의 사과 유전자원을: 1) 과방 내 어떠한 과일도 탈리가 일어나지 않는 비탈리군, 2) 과경 내에서 비선택적으로 탈리가 일어나는 June drop군, 3) 과방 내에 오직 하나의 과일만 남고, 다른 과일은 탈리되는 자가적과성군 등 3개의 군으로 분류하였다. 자가적과성군에 속하는 대부분의 품종은 한 과방 내의 중심과가 나머지 측과의 생육을 지배하여 궁극적으로 탈리에 이르게 하는 방식을 보였다. 그러나 예외적으로 *Malus coronaria* ‘Charlottae’는 중심과가 측과를 지배하지 못하고 오히려 가장 먼저 탈리되었다. 만개기와 과중은 조기 탈리 현상과 크게 연관이 있는 것으로 나타나 만개기가 이를수록 그리고 과중이 작을수록, 조기 탈리는 잘 일어나지 않았다.

과실 탈리는 이층에서 발생하는데, 이 이층의 발달은 토마토의 *JOINTLESS*와 같이 몇 개의 유전자에 의해 조절된다. MADS-box 유전자의 보존 지역을 바탕으로 한 프라이머를 활용해 자가적과성 사과 품종 ‘Saika’의 측과 과경에서 새로운 MADS-box 유전자를 찾아

*MdJOINTLESS*라 명명하였다. 다른 MADS-box 유전자들과 염기 서열을 비교 분석한 결과, *MdJOINTLESS*는 *SVP* (*Arabidopsis thaliana*), *IbMADS3* (*Ipomoea batatas*), *StMADS16* (*Solanum tuberosum*), *PsSVP* (*Pisum sativum*), 및 *JOINTLESS* (*Solanum lycopersicum*)가 포함된 *SVP* 분류군에 속했다. 그러나 *MdJOINTLESS*는 *JOINTLESS*와 염기 서열 간의 상동성이 높았음에도 불구하고, 형질 전환 토마토에서 *JOINTLESS*와 같은 기능을 보이지 않았다. *JOINTLESS* 이외에 *SLMBP21* (*SEPALLATA*)와 *MACROCALYX*와 같은 다른 MADS-box 유전자들이 토마토 과경의 이층 형성에 관여하는 것으로 알려져 있다. 사과 과경의 EST 염기서열 분석을 통해서, 토마토와 유사한 MADS-box 유전자들이 사과의 과경에 이층을 형성하는 데 관여할 가능성이 있다고 판단되었다.

자가적과성 사과 품종 'Saika'의 중심과와 측과의 과경을 대상으로 특이적으로 발현하는 탈리 연관 유전자를 찾기 위해서 전사체 분석을 수행하였다. RNA-Seq을 통해 생성된 데이터 중에서 총 797,647개의 EST가 65,876개의 contig로 합성되었고, 이를 Blast2GO를 활용해 GO 분석을 실시하였다. 프로그램을 활용하여, 중심과와 측과 과경에 특이적으로 발현되는 1,585개의 유전자를 발굴하였다. 이 특이 발현 유전자를 대상으로 qRT-PCR로 확인한 결과, 중심과에서는 *IAA3*/*SHY2* 유전자가, 측과에서는 *IAA14/SLR*이 특이적으로 발현되는 것으로 밝혀졌다. *IAA3*/*SHY2*는 생장점 분화 기작과 관련되어 있어 옥신을 통한 중심과의 생장점 발달에 기여하는 것으로 생각된다. *IAA14/SLR*은 측과의 탈리 기작과 관련이 있으며, 이는 측근 발생 기작과 상당히

유사한 것으로 보인다. 따라서 자가 적과가 발생하는 조기 탈리 시기에 *AUX/IAA* 유전자들이 과경의 생존을 결정하는 역할을 하는 주요 원인인 것으로 여겨진다. 앞으로 *IAA14/SLR*에 의해 어떠한 유전자가 직접적으로 또는 간접적으로 조절되는지 그리고 *IAA14/SLR*에 의해 조절되는 유전자들이 과경의 조기 탈리를 유발시키는지 밝혀내야 할 것이다. 또한 조기 탈리가 일어나는 기간 동안 *AUX/IAA*의 퇴화에 의해 어떠한 *ARF*가 발현되는지 그리고 이러한 *ARF*가 탈리 기작 신호를 핵 내로 전달하는 *IDA*, *HAE*, 또는 *HSL2*와 같은 유전자의 발현을 유도하는지 조사하여야 할 것이며 *AUX/IAA*와 *ARF* 간의 상호작용도 단백질 수준에서 확인되어야 할 것이다.

Supplementary Table 3-1. Primers for genes used in qRT-PCR.

Gene[a]	Forward primer (5' to 3')	Reverse primer (5' to 3')
MDP0000203890	CGGTGGGAAGAAACAAGTGATT	CTGGCCCACCTTGATTGC
MDP0000166068	GAGAAGAACTGCGGATCGAAGA	AGCAGCCTCAGCATCATCAA
MDP0000927973	GCCGCAGCCTCAATTCTGT	CCTGAGATTACGTCCGTGGAGTA
MDP0000323263	CCAGAGCCTGCTTCACCAA	GAGACCCATGTCGTGATCGA
MDP0000577455	TGGCCTCCGACGTCGTA	GACCTGTCGGCCAGTTCCT
MDP0000277631	CGATAAACCGCTTGCAGTTG	GACGTCCCTCAGGACACGTT
MDP0000397306	AATGGGATGACTCCACCAACA	ACGGCCTTGGCATTTCAC
MDP0000749280	CGCTCCTTCCCCGGACTA	GGTGAATGAGCATCAATGTGACA
MDP0000319679	ACAGCGGTCTCGGGAAACT	GAGCTGGACCGGAAACTGAA
MDP0000750392	TCCGGGAAGAATCCTCAGTTT	GGTGGTGCCCCGGAAT
MDP0000137461	GCTCTTCTCGCAGCTCATGA	TTGGCCGCTCAATTGACAT
MDP0000298711	CAGCTGCCGTCCTGTTCTG	TCCAACCGGCCATGGA
MDP0000225382	CGGAGGCAATCTGATCCAA	GGAGGGCAGGCACTTTGAT
MDP0000262602	AAGGGTTCCGAAGCAATCG	AGTTCCGGTTCTTGCATTTCTC
MDP0000250876	TTGCTGCTGGAACCAAGAGA	CACAACCTGACTGGCACCAT
MDP0000221322	TCCATTTTCTGCATTTTGCATT	CCGGCCACCGAAAGTATTG
MDP0000945260	ATGATTCTTCATCCGCCAAAA	TTGGAAGGTGGAGGCTGAGA
MDP0000497581	TCGGCGACGACGGAAA	CGCCTTGATGCGTTGGA
MDP0000200231	CGACGTGGATGGAGACAATG	TCCTCATCTCGGAGCAGTTTC
MDP0000138035	TCATTCAGGTGGCACGTTCA	GACAGTATGGCAATGGACTTTGC
MDP0000848515	CCTGAACCACCCGGTCTTC	CCTTCTGCTCGTAGCCGTACTC
MDP0000564193	GCTACTCCCAGAAGCGTAAACG	TGGAGCCCACCTTTTCTTCA
MDP0000811081	GCCAGAGCGTCTGCGTTT	CGTTAGGTGGTTTGAGGACATG

Supplementary Table 3-1. Continued.

Gene[a]	Forward primer (5' to 3')	Reverse primer (5' to 3')
MDP0000568498	TGGAGCCTGGGTCATTCG	CGAACCCCCTTGGCTGAT
MDP0000124810	ATGAAGATAAGGACGGTGATTGG	AACGAACATCCCCCATGGA
MDP0000873893	GCGTGGTGGAGTACACGAGTT	ACGTAGTGCCCCGGGATT
MDP0000193700	GCTGCAACTGTTTGGACAAATC	TGACCTTGCGCGAACTCA
MDP0000090281	AATCCACGGCAACCAGGTTA	CCCATCCAACCCCAAGATCT
MDP0000362286	TCGGCATCGCCAACTTG	GGCCCTTGAATGCAAAAGAA
MDP0000807487	ATCGCTATTCACTAATCGCACCTA	CCGGAGGCTGACTTGGAA
MDP0000218652	TCTTGGTAGTCTATCGGCATGCT	CGAAGACAACGGCAAAAGGA
MDP0000314840	CCCTCACTCAGCCGCTCAT	TGGAAAATGGCGATCAAACAT
MDP0000301534	AAGAGGCCGGTGAAGAATCTG	GCCTTGTGGGTGGTTGATG
MDP0000883100	GTTGCCTTATCGTCAGCTCTCA	CCCAACAAGGTTCCGGTTCT
MDP0000233901	GCAGAGGCCTTCGTTCTCAA	CCCTAACAACGCTAGCAGGAA
MDP0000941051	AGCAGGAGCCGCATTTACC	TCAAGGACACCGCGAATCA
MDP0000184342	GGGATGCCTTGGTTCTTCCT	CAAGTGCAGGGCCCAAGT
MDP0000222749	GCGGCACCTTCATGATCTTC	GACGGACACCGCGTCTTT
MDP0000155074	TAGTCGGACCAGAGTGCTTCAC	CCTTACCATTGCCTCCTTCCT
MDP0000876321	TTCAATCGAATCCTCGAAGCA	CCGGTGCCAATCCATCAA
MDP0000179650	TTTCCGACCTCGGCTTATGA	CCAGACTCAGCCCGACAGAA
MDP0000225980	GCGGCTATTTGGCATGGA	CAAGATCCGCCATCCTTCAT
MDP0000256621	TGGTTGCACCGAGGACAGT	TGGCTGTGCCCTTCTTCAG
MDP0000153538	TGATACCCCTGGCCAAGTATG	AATCGCATGCCCACAGAAAC
MDP0000175425	CAGACTTTAATGCGCCACCAA	CCTCGCCGTCTTCGTGTT
MDP0000929655	CCACCACCCGGCCACTA	GGAACCGAGGGTTGGTTGA

Supplementary Table 3-1. Continued.

Gene[a]	Forward primer (5' to 3')	Reverse primer (5' to 3')
MDP0000295589	GCCGCCGGTGAGATCA	CCTCCGCCTCGGTTTTCT
MDP0000200927	CGGTAGGCAGTTCAAATGTCTCT	TGTGGCCTTCAAATTCAGACTACT
MDP0000232417	GTGGCAAGCTTGGATGGTTAG	TGCGGCATCAACCAACAA
MDP0000178263	TGCCTCTGCTGTCTCAAACG	TTCGCCACCCATTACTGAAGA
MDP0000563385	GGAAGGTGTTGCGAAGACAAC	GCGGACCACCCGAGAAA
MDP0000858983	ACCTCGGAGGACGCTGTAGTAG	TCATCACGCGCGATTTTTT
MDP0000303142	TCTTTCTGAGGTAAGGTGCTCCAT	GCCTGAAACTGCTACTGGGATT
MDP0000227870	TTGCTCTGTGAAACCACATGTTC	GCACGCCGCTTTTCTTTG
MDP0000270602	GCACACAATCAATGACGACGTT	GAAGAGCCTGCCGGAACA

[a]MDP numbers are the accession ID of the predicted apple (*Malus* × *domestica* protein) genes (Velasco et al., 2010).

Supplementary Table 3-2. DEGs in CP selected by NOISeq software.

ID	Theta[a]	Probability	Annotation
MDP0000363784	1.298452238	0.995869458	Ribosomal protein L39 family protein
MDP0000908305	1.296700148	0.994282058	Nicotianamine synthase 3
MDP0000547461	1.295473432	0.991887540	ACT domain repeat 4
MDP0000125842	1.293282741	0.987891173	Unintegrated
MDP0000360642	1.292024310	0.983832879	Unintegrated
MDP0000129252	1.290175589	0.981939972	RING/U-box superfamily protein
MDP0000602556	1.288534580	0.981417719	Unintegrated
MDP0000178506	1.287634498	0.980232846	RNA binding Plectin/S10 domain-containing protein
MDP0000824440	1.286552489	0.978965403	Bifunctional inhibitor/lipid-transfer protein/seed storage 2S albumin superfamily protein
MDP0000860613	1.286379588	0.975819503	Immunoglobulin E-set superfamily protein
MDP0000512791	1.286249328	0.974424077	CCT motif family protein
MDP0000311294	1.284920649	0.972128643	Unintegrated
MDP0000200882	1.283133068	0.970202708	Ribosomal protein L18e/L15 superfamily protein
MDP0000215486	1.282968071	0.968675171	Major facilitator superfamily protein

ID	Theta[a]	Probability	Annotation
MDP0000362318	1.281616601	0.968258195	Unintegrated
MDP0000336499	1.280143743	0.967814384	Arginine/serine-rich splicing factor 35
MDP0000130979	1.277957831	0.967063001	Unintegrated
MDP0000271553	1.276253477	0.966771943	NAD(P)-binding Rossmann-fold superfamily protein
MDP0000231540	1.275690713	0.965770787	RmlC-like cupins superfamily protein
MDP0000670895	1.274104711	0.965093716	Proteasome alpha subunit F1
MDP0000293049	1.273642809	0.964835687	Bifunctional inhibitor/lipid-transfer protein/seed storage 2S albumin superfamily protein
MDP0000255229	1.272071282	0.963882008	Histone superfamily protein
MDP0000121743	1.269478539	0.963524895	Protein kinase superfamily protein
MDP0000215478	1.269038601	0.962794154	Lactoylglutathione lyase/Glyoxalase I family protein
MDP0000150863	1.268716050	0.962525803	Unintegrated
MDP0000307013	1.268374784	0.962422591	Nucleic acid-binding, OB-fold-like protein
MDP0000329639	1.268318526	0.960690694	Ribosomal protein L7Ae/L30e/S12e/Gadd45 family protein
MDP0000155887	1.267059560	0.959627611	Ribosomal protein S27
MDP0000819132	1.266446633	0.959256048	Zinc finger (C3HC4-type RING finger) family protein

ID	Theta[a]	Probability	Annotation
MDP0000166139	1.265286764	0.959204442	Unintegrated
MDP0000085223	1.264758330	0.958370490	Sulfate transporter 3;1
MDP0000850301	1.263668427	0.958370490	Unintegrated
MDP0000150022	1.263348508	0.958000991	Unintegrated
MDP0000239834	1.258648884	0.957736768	Allene oxide cyclase 4
MDP0000141863	1.258379472	0.957718190	Rotamase FKBP 1
MDP0000314346	1.257876908	0.957584015	Leucine-rich repeat transmembrane protein kinase
MDP0000626096	1.257525408	0.957491124	EF1B/ribosomal protein S6
MDP0000887072	1.256651768	0.955779870	Hydroxyproline-rich glycoprotein family protein
MDP0000126706	1.256535585	0.955625052	Protein of unknown function (DUF567)
MDP0000310247	1.254977816	0.954547519	Bifunctional inhibitor/lipid-transfer protein/seed storage 2S albumin superfamily protein
MDP0000589652	1.254457313	0.954510362	RmlC-like cupins superfamily protein
MDP0000265787	1.253460285	0.953851870	Proteasome maturation factor UMP1
MDP0000813111	1.252446905	0.953676410	Phloem protein 2-A1
MDP0000182066	1.248640767	0.953531913	Diaminopimelate epimerase family protein

ID	Theta[a]	Probability	Annotation
MDP0000281966	1.247982021	0.952922963	Signal recognition particle, SRP9/SRP14 subunit
MDP0000235957	1.247870764	0.952877549	Endoplasmatic reticulum retrieval protein 1B
MDP0000259057	1.246566271	0.952646355	Histone superfamily protein
MDP0000119667	1.245843507	0.952563785	Ribosomal protein L35Ae family protein
MDP0000464691	1.245496022	0.951440839	BON association protein 2
MDP0000336545	1.244329243	0.950388077	Unintegrated
MDP0000414002	1.243698644	0.950138304	NAD(P)-binding Rossmann-fold superfamily protein
MDP0000709748	1.243305603	0.949933944	Pyrophosphorylase 4
MDP0000360837	1.242717154	0.948678887	RNA-binding (RRM/RBD/RNP motifs) family protein
MDP0000128880	1.241993107	0.948532326	Unintegrated
MDP0000772855	1.240885975	0.946666254	Proline-rich family protein
MDP0000160365	1.240515519	0.945720832	Porphyromonas-type peptidyl-arginine deiminase family protein
MDP0000208573	1.239517222	0.945687804	Unintegrated
MDP0000337639	1.239029269	0.945634134	Unintegrated
MDP0000251626	1.237904830	0.945126331	Bifunctional inhibitor/lipid-transfer protein/seed storage 2S albumin superfamily protein

ID	Theta[a]	Probability	Annotation
MDP0000531576	1.236308771	0.945047890	Unintegrated
MDP0000323884	1.232823727	0.945029312	Thioredoxin M-type 4
MDP0000807738	1.228070630	0.944787796	Carbonic anhydrase 2
MDP0000266393	1.226105336	0.943617373	Alpha/beta-hydrolases superfamily protein
MDP0000130716	1.225745925	0.943183882	WRKY DNA-binding protein 7
MDP0000545310	1.225297764	0.942934109	Brassinosteroid-responsive RING-H2
MDP0000364491	1.223441576	0.941842127	Cytochrome b6f complex subunit (petM), putative
MDP0000197775	1.222678696	0.941204277	Uclacyanin 1
MDP0000613004	1.221491445	0.940205185	Ralf-like 24
MDP0000171767	1.220578333	0.940027661	Peptidyl-prolyl cis-trans isomerases
MDP0000235158	1.218969106	0.939759310	Ubiquitin-conjugating enzyme 18
MDP0000175968	1.217464388	0.939024441	Sequence-specific DNA binding transcription factors
MDP0000323095	1.216690409	0.938772603	KNOTTED1-like homeobox gene 3
MDP0000199155	1.215979430	0.938723062	Unintegrated
MDP0000402527	1.215661515	0.938314342	Protein of unknown function, DUF584

ID	Theta[a]	Probability	Annotation
MDP0000430546	1.213684952	0.937505161	Homolog of carrot EP3-3 chitinase
MDP0000806558	1.211789838	0.936954009	Unintegrated
MDP0000792101	1.211788418	0.936943688	Nuclear transport factor 2 (NTF2) family protein
MDP0000335758	1.210138077	0.935257204	Cornichon family protein
MDP0000210084	1.209731598	0.935244819	Unintegrated
MDP0000658289	1.209689910	0.935244819	AT hook motif DNA-binding family protein
MDP0000139736	1.209480750	0.934474858	Protein of unknown function, DUF617
MDP0000203666	1.209227960	0.934293205	WUSCHEL related homeobox 4
MDP0000362097	1.206949152	0.934012468	Acyl-CoA-binding protein 6
MDP0000134766	1.205368204	0.933923706	Cytochrome b-c1 complex, subunit 8 protein
MDP0000887949	1.205109330	0.933640905	Bifunctional inhibitor/lipid-transfer protein/seed storage 2S albumin superfamily protein
MDP0000453329	1.203805281	0.933403517	SNARE-like superfamily protein
MDP0000710378	1.200563485	0.932934935	HSP20-like chaperones superfamily protein
MDP0000364275	1.196109893	0.932705805	Small nuclear ribonucleoprotein F
MDP0000328326	1.195492770	0.932606721	YGGT family protein

ID	Theta[a]	Probability	Annotation
MDP0000265983	1.195459338	0.932233094	Damaged DNA binding;exodeoxyribonuclease IIIs
MDP0000267538	1.194666529	0.931267030	Multiprotein bridging factor 1C
MDP0000565846	1.187533986	0.931267030	Multiprotein bridging factor 1C
MDP0000936776	1.186368415	0.930699364	Octicosapeptide/Phox/Bem1p family protein
MDP0000233668	1.185772582	0.930662208	RING/U-box superfamily protein
MDP0000304878	1.184637619	0.930053257	Unintegrated
MDP0000197200	1.183416130	0.929766328	Yippee family putative zinc-binding protein
MDP0000233092	1.180609655	0.929751878	Chaperone DnaJ-domain superfamily protein
MDP0000257313	1.177601884	0.929696144	BCL-2-associated athanogene 5
MDP0000576346	1.176960954	0.929301874	Cinnamate-4-hydroxylase
MDP0000172234	1.175134624	0.929070680	Protein of unknown function (DUF581)
MDP0000666211	1.173669425	0.929056230	Cox19-like CHCH family protein
MDP0000198500	1.173003727	0.929047973	Peroxin 14
MDP0000345442	1.168733340	0.929045909	Mitochondrial acyl carrier protein 1
MDP0000777771	1.166575618	0.928971596	Transcriptional coactivator p15 (PC4) family protein (KELP)

ID	Theta[a]	Probability	Annotation
MDP0000781178	1.164020961	0.928257369	Bifunctional inhibitor/lipid-transfer protein/seed storage 2S albumin superfamily protein
MDP0000880401	1.163633653	0.927834200	Bifunctional inhibitor/lipid-transfer protein/seed storage 2S albumin superfamily protein
MDP0000723824	1.163446254	0.927157130	Unintegrated
MDP0000152585	1.160124704	0.926170424	Membrane-associated progesterone binding protein 3
MDP0000817278	1.159511929	0.925586244	Protein of unknown function (DUF640)
MDP0000326332	1.154523623	0.925369499	Protein phosphatase 2A-2
MDP0000146639	1.153729990	0.925334407	Reversibly glycosylated polypeptide 3
MDP0000163856	1.153680734	0.925288993	Ribosomal protein L5
MDP0000613462	1.152249026	0.924566510	Dynamin related protein 4C
MDP0000672131	1.150221153	0.924422013	Basic helix-loop-helix (bHLH) DNA-binding superfamily protein
MDP0000232585	1.149792129	0.923055487	Putative lysine decarboxylase family protein
MDP0000627768	1.149437016	0.922411444	Protein kinase superfamily protein
MDP0000251947	1.146308964	0.922008918	TATA binding protein associated factor 21kDa subunit
MDP0000324831	1.144029588	0.921115102	Drought-induced 21
MDP0000464598	1.142994261	0.920388490	Protein of unknown function (DUF1218)

ID	Theta[a]	Probability	Annotation
MDP0000121149	1.142465856	0.918943522	Polyubiquitin 10
MDP0000385309	1.140482276	0.918854760	Prenylated RAB acceptor 1.B1
MDP0000216604	1.140395028	0.918675171	SecE/sec61-gamma protein transport protein
MDP0000370143	1.140147042	0.918429527	Unintegrated
MDP0000596986	1.138822196	0.918429527	EF1B/ribosomal protein S6
MDP0000155073	1.136262638	0.918020808	Pathogenesis-related thaumatin superfamily protein
MDP0000129561	1.136114404	0.917775163	Ribosomal protein L34e superfamily protein
MDP0000241185	1.135346299	0.917636859	Duplicated homeodomain-like superfamily protein
MDP0000359460	1.135317558	0.917254975	Unintegrated
MDP0000253745	1.135306643	0.916784328	Rotamase cyclophilin 2
MDP0000180310	1.135153859	0.916497399	Protein kinase superfamily protein
MDP0000443612	1.134989460	0.916226984	Zinc finger protein 4
MDP0000272747	1.131638935	0.916001982	Unintegrated
MDP0000413387	1.131611947	0.915430187	Ethylene-responsive element binding protein
MDP0000243895	1.130511066	0.914893485	Heat shock transcription factor A2

ID	Theta[a]	Probability	Annotation
MDP0000177183	1.129768655	0.914767567	Calcium-binding EF-hand family protein
MDP0000885802	1.128866972	0.914662290	Unintegrated
MDP0000213543	1.127558950	0.914222608	TCP-1/cpn60 chaperonin family protein
MDP0000532006	1.125861847	0.914185451	SEC14 cytosolic factor family protein/phosphoglyceride transfer family protein
MDP0000240256	1.125786328	0.913332920	TMPIT-like protein
MDP0000006123	1.125468107	0.913103790	Ribosomal protein L7Ae/L30e/S12e/Gadd45 family protein
MDP0000202410	1.123748756	0.913103790	Unintegrated
MDP0000525437	1.123391644	0.912965486	Calcium-binding EF hand family protein
MDP0000523619	1.122647924	0.912915944	UDP-Glycosyltransferase superfamily protein
MDP0000136902	1.122062150	0.912585666	Ankyrin repeat family protein
MDP0000486799	1.121936035	0.912463876	Adenine nucleotide alpha hydrolases-like superfamily protein
MDP0000539579	1.121695777	0.912306994	Unintegrated
MDP0000757585	1.120236121	0.912205846	Unintegrated
MDP0000015854	1.119938778	0.912156304	Serine carboxypeptidase S28 family protein
MDP0000333691	1.119595174	0.911828090	Homeodomain-like superfamily protein

ID	Theta[a]	Probability	Annotation
MDP0000675059	1.119485184	0.909421187	COP1-Interacting protein 8
MDP0000136892	1.117355285	0.908296177	Zinc transporter 1 precursor
MDP0000804526	1.114138600	0.907538601	Unintegrated
MDP0000300540	1.113042199	0.907482867	Unintegrated
MDP0000352118	1.111697246	0.906353728	Unintegrated
MDP0000268941	1.110039043	0.906122533	Unintegrated
MDP0000808967	1.109363013	0.905794319	Unintegrated
MDP0000124047	1.109010085	0.905397985	Branched-chain alpha-keto acid decarboxylase E1 beta subunit
MDP0000138215	1.108580728	0.905069771	Tropomyosin-related
MDP0000508371	1.108465352	0.904797292	Phosphate transporter 1;7
MDP0000244462	1.106393146	0.904361737	Unintegrated
MDP0000647346	1.105268374	0.904285360	Sterile alpha motif (SAM) domain-containing protein
MDP0000141709	1.103633209	0.903907605	Sequence-specific DNA binding transcription factors
MDP0000272880	1.103201653	0.903690860	Unintegrated
MDP0000155233	1.102888298	0.903439022	Unintegrated

ID	Theta[a]	Probability	Annotation
MDP0000245975	1.102117496	0.903102551	Peroxin 7
MDP0000309557	1.101974614	0.903019982	High mobility group B3
MDP0000322710	1.100898832	0.902444059	Thioesterase superfamily protein
MDP0000175733	1.100017520	0.902097267	Senescence-associated gene 101
MDP0000284624	1.098983158	0.901973413	Regulatory component of ABA receptor 1
MDP0000511046	1.098793926	0.901963091	RING/U-box superfamily protein
MDP0000184034	1.097920902	0.901738089	Pollen Ole e 1 allergen and extensin family protein
MDP0000724699	1.097678250	0.901682355	Thioredoxin superfamily protein
MDP0000410683	1.096462774	0.900928908	Pentatricopeptide repeat (PPR) superfamily protein
MDP0000360772	1.094995246	0.900732805	Unintegrated
MDP0000605318	1.094992196	0.900635786	RNA-binding KH domain-containing protein
MDP0000255523	1.094766212	0.900367435	Unintegrated
MDP0000235570	1.092944650	0.899964908	Arabinogalactan protein 26
MDP0000401312	1.092926021	0.899964908	Ribosomal protein L34
MDP0000205983	1.092565484	0.899634630	Histone H2A 12

ID	Theta[a]	Probability	Annotation
MDP0000286353	1.092021675	0.899316737	Got1/Sft2-like vescicle transport protein family
MDP0000257598	1.091180044	0.898858476	Unintegrated
MDP0000413760	1.089984099	0.898784163	Hypoxanthine-guanine phosphoribosyltransferase
MDP0000128979	1.089441643	0.898127735	Ethylene-responsive element binding protein
MDP0000950691	1.088721527	0.898127735	Unintegrated
MDP0000564193	1.088227869	0.898117414	Senescence-associated gene 21
MDP0000194224	1.087069459	0.897578648	Unintegrated
MDP0000322776	1.086049034	0.896651804	Branched-chain amino acid aminotransferase
MDP0000334397	1.080519020	0.896635290	Unintegrated
MDP0000550906	1.076708065	0.896546528	Hypoxanthine-guanine phosphoribosyltransferase
MDP0000770211	1.076253927	0.896445380	SNARE associated Golgi protein family
MDP0000225392	1.075544868	0.895097432	Protein of unknown function, DUF538
MDP0000125070	1.073737791	0.894362563	Proliferating cell nuclear antigen 2
MDP0000232764	1.073286752	0.893683428	Major facilitator superfamily protein
MDP0000747397	1.072879151	0.893666914	Disease resistance-responsive (dirigent-like protein) family protein

ID	Theta[a]	Probability	Annotation
MDP0000216466	1.071346618	0.892985715	Sulfate transporter 3;1
MDP0000146312	1.069648678	0.892285938	TraB family protein
MDP0000346746	1.065891523	0.892180662	DNA-binding storekeeper protein-related
MDP0000771727	1.063604962	0.892015523	DHBP synthase RibB-like alpha/beta domain
MDP0000335450	1.063441432	0.891567583	Regulator of Vps4 activity in the MVB pathway protein
MDP0000296002	1.063325837	0.891262076	Unintegrated
MDP0000137117	1.060719748	0.889806787	Eukaryotic translation initiation factor 3G1
MDP0000251966	1.048847370	0.889660226	Bifunctional inhibitor/lipid-transfer protein/seed storage 2S albumin superfamily protein
MDP0000140907	1.047208079	0.889643712	Lumazine-binding family protein
MDP0000156439	1.047155111	0.889445545	Alpha carbonic anhydrase 1
MDP0000922228	1.046630497	0.889354719	Zinc-binding ribosomal protein family protein
MDP0000158995	1.045362383	0.889026505	Phosphoglycerate mutase, 2,3-bisphosphoglycerate-independent
MDP0000560112	1.042917561	0.887969614	Expansin A1
MDP0000157809	1.041813429	0.887934522	Brassinosteroid signaling positive regulator (BZR1) family protein
MDP0000251956	1.041364768	0.887523739	Pectin lyase-like superfamily protein

ID	Theta[a]	Probability	Annotation
MDP0000755567	1.040019801	0.887439105	Senescence-associated gene 21
MDP0000205823	1.039598721	0.887102634	Basic leucine-zipper 44
MDP0000209261	1.038378497	0.886991165	AMP-dependent synthetase and ligase family protein
MDP0000314765	1.038310523	0.886524647	K-box region and MADS-box transcription factor family protein
MDP0000153265	1.037980481	0.885859962	Unintegrated
MDP0000504439	1.034909053	0.885818677	CYTOCHROME C-1
MDP0000233682	1.034862297	0.885670052	Unintegrated
MDP0000181937	1.033786053	0.885248947	CHY-type/CTCHY-type/RING-type Zinc finger protein
MDP0000127834	1.033616720	0.885215919	Uncoupling protein 5
MDP0000709066	1.031931862	0.884997110	Protein of unknown function (DUF640)
MDP0000232591	1.030843418	0.884408802	Thioredoxin domain-containing protein 9 homolog
MDP0000198702	1.030474502	0.884095038	Amino acid permease 6
MDP0000242500	1.029451551	0.883998018	Protein of unknown function (DUF640)
MDP0000364856	1.027506340	0.883356040	Unintegrated
MDP0000232523	1.026733752	0.883341590	Remorin family protein

ID	Theta[a]	Probability	Annotation
MDP0000153603	1.025102687	0.883225993	Protein phosphatase 2A-3
MDP0000367870	1.024747267	0.883186772	Small nuclear ribonucleoprotein family protein
MDP0000161448	1.024326645	0.883131038	3'-5'-Exoribonuclease family protein
MDP0000198079	1.023860795	0.883131038	Cold shock domain protein 1
MDP0000410728	1.020960222	0.883087689	Basic helix-loop-helix (bHLH) DNA-binding superfamily protein
MDP0000296432	1.016120225	0.882963835	Transthyretin-like protein
MDP0000184208	1.015299647	0.882918421	Quinoprotein amine dehydrogenase
MDP0000680536	1.015045537	0.882740897	Decapping 5
MDP0000491898	1.014728621	0.882581950	Pectate lyase family protein
MDP0000535412	1.014620978	0.882536537	Zinc finger C-x8-C-x5-C-x3-H type family protein
MDP0000329851	1.014604895	0.882439518	Protein kinase superfamily protein
MDP0000622241	1.013168059	0.882439518	Protein of unknown function, DUF538
MDP0000156241	1.012206261	0.882249608	Dof-type zinc finger DNA-binding family protein
MDP0000137305	1.011062118	0.882158781	Plant-specific GATA-type zinc finger transcription factor family protein
MDP0000181887	1.010891248	0.881797539	Unintegrated

ID	Theta[a]	Probability	Annotation
MDP0000272522	1.009508835	0.881180332	Calcium-binding EF-hand family protein
MDP0000188739	1.009305130	0.880998679	Unintegrated
MDP0000142250	1.008420293	0.880911981	Alpha/beta-hydrolases superfamily protein
MDP0000895175	1.008306359	0.880911981	Aspartate/glutamate/uridylate kinase family protein
MDP0000317444	1.007502783	0.880717942	Oxidoreductase, zinc-binding dehydrogenase family protein
MDP0000233503	1.006734571	0.880350508	Protein of unknown function, DUF538
MDP0000210879	1.006581792	0.880309223	Zinc-binding ribosomal protein family protein
MDP0000660304	1.005458628	0.880051193	Protein of unknown function (DUF3411)
MDP0000945260	1.003463502	0.879789035	AUX/IAA transcriptional regulator family protein
MDP0000323291	1.001508761	0.878707373	Basic helix-loop-helix (bHLH) DNA-binding superfamily protein
MDP0000499104	1.000991806	0.878141772	Domain of unknown function (DUF2431)
MDP0000745681	1.000476990	0.878055074	Disease resistance protein (TIR-NBS-LRR class) family
MDP0000758317	0.999808759	0.877702089	Phosphate transporter traffic facilitator1
MDP0000791177	0.995962106	0.877508051	Calcium-binding EF-hand family protein
MDP0000281971	0.995618429	0.877342911	Photosystem II reaction center W

ID	Theta[a]	Probability	Annotation
MDP0000422537	0.995167978	0.877210800	Myb-like HTH transcriptional regulator family protein
MDP0000240478	0.992874321	0.877159194	Eukaryotic elongation factor 5A-1
MDP0000318032	0.992564645	0.877157130	UDP-glucosyl transferase 88A1
MDP0000155770	0.991779261	0.877010569	20S proteasome beta subunit G1
MDP0000417633	0.990219651	0.876911485	Unintegrated
MDP0000786706	0.986899664	0.876702997	Phosphoenolpyruvate carboxykinase 1
MDP0000771149	0.978789997	0.876659648	Dof-type zinc finger DNA-binding family protein
MDP0000322036	0.977643422	0.876257122	F-BOX WITH WD-40 2
MDP0000334150	0.977566177	0.876255057	Unintegrated
MDP0000906542	0.976301016	0.876255057	Bifunctional inhibitor/lipid-transfer protein/seed storage 2S albumin superfamily protein
MDP0000293103	0.974983531	0.876207580	GDSL-like Lipase/Acylhydrolase superfamily protein
MDP0000170826	0.974967819	0.875416976	Protein of unknown function (DUF581)
MDP0000807487	0.974493556	0.875412848	SAUR-like auxin-responsive protein family
MDP0000364214	0.974407950	0.875398398	Unintegrated
MDP0000273575	0.974202931	0.875183717	Ribosomal protein 5B

ID	Theta[a]	Probability	Annotation
MDP0000736365	0.973909522	0.874498390	Unintegrated
MDP0000497756	0.973497230	0.874205268	Mercaptopyruvate sulfurtransferase 1
MDP0000320601	0.973103965	0.873804806	Unintegrated
MDP0000222113	0.972765239	0.873656180	Ubiquitin-conjugating enzyme 28
MDP0000338603	0.972739280	0.873647923	Unintegrated
MDP0000125742	0.972224784	0.873367187	Phospholipase D delta
MDP0000279178	0.970777232	0.873243333	Atypical CYS HIS rich thioredoxin 2
MDP0000289041	0.970646780	0.873189662	Putative lysine decarboxylase family protein
MDP0000155349	0.970365365	0.872789200	Ribosome associated membrane protein RAMP4
MDP0000468488	0.969474763	0.872638510	Acyl carrier protein 4
MDP0000452016	0.968253673	0.872452729	Photosystem I subunit E-2
MDP0000290884	0.967992947	0.872275204	Ornithine carbamoyltransferase
MDP0000261742	0.966866480	0.872083230	Histone deacetylase 9
MDP0000175531	0.966852325	0.872006853	Unintegrated
MDP0000658649	0.965899496	0.871959376	N-terminal nucleophile aminohydrolases (Ntn hydrolases) superfamily protein

ID	Theta[a]	Probability	Annotation
MDP0000163886	0.965793383	0.871476344	Aconitase 2
MDP0000159559	0.964882820	0.871391710	Adenine phosphoribosyltransferase 5
MDP0000204446	0.964849290	0.870861201	SUMO-activating enzyme 1A
MDP0000399594	0.963590249	0.869374948	Oxophytodienoate-reductase 3
MDP0000310632	0.962453690	0.869222195	Acyl-CoA N-acyltransferases (NAT) superfamily protein
MDP0000242945	0.962199206	0.869100405	Unintegrated
MDP0000759922	0.961477292	0.869100405	Early nodulin-like protein 15
MDP0000319171	0.960469672	0.868995128	Alpha/beta-Hydrolases superfamily protein
MDP0000235688	0.957637242	0.868955908	Mitochondrial glycoprotein family protein
MDP0000422411	0.956019772	0.868955908	Unintegrated
MDP0000697468	0.950130135	0.868955908	Aconitase/3-isopropylmalate dehydratase protein
MDP0000455174	0.948419729	0.868763934	Nucleotide-sugar transporter family protein
MDP0000262149	0.946701184	0.868654529	Vacuolar protein sorting 46.1
MDP0000239354	0.945355925	0.868650400	Telomere repeat binding factor 1
MDP0000140553	0.945183350	0.868534803	Glutamine dumper 3

ID	Theta[a]	Probability	Annotation
MDP0000127951	0.942888501	0.868109570	Associated molecule with the SH3 domain of STAM 3
MDP0000586151	0.942600087	0.867851540	Ribosomal protein S5 domain 2-like superfamily protein
MDP0000120830	0.941597273	0.867760713	Allergen-related
MDP0000777832	0.941558236	0.867593510	NADH-ubiquinone oxidoreductase-related
MDP0000730604	0.936940015	0.867451078	Protein of unknown function (DUF1005)
MDP0000942516	0.936714942	0.867195112	MLP-like protein 423
MDP0000295888	0.936593071	0.867141442	Eukaryotic elongation factor 5A-1
MDP0000165749	0.935469943	0.865857485	APR-like 4
MDP0000143951	0.932498199	0.865407481	Proteasome subunit PAB1
MDP0000338330	0.930871037	0.865194864	Unintegrated
MDP0000709727	0.930180449	0.865194864	Ubiquitin system component Cue protein
MDP0000631513	0.928455473	0.864938899	Alpha-1,4-glucan-protein synthase family protein
MDP0000599845	0.927225049	0.864922385	Homeobox 1
MDP0000180043	0.926669941	0.864819173	Xyloglucan endotransglucosylase/hydrolase 32
MDP0000848210	0.924301723	0.864629263	LOB domain-containing protein 25

ID	Theta[a]	Probability	Annotation
MDP0000126986	0.923464016	0.863531087	Plant protein 1589 of unknown function
MDP0000178268	0.923175147	0.863427875	Lipoxygenase 2
MDP0000480293	0.921985687	0.863390719	C2H2-like zinc finger protein
MDP0000337985	0.921725741	0.863050120	Unintegrated
MDP0000663593	0.920136343	0.862961357	Unintegrated
MDP0000881546	0.919784910	0.862961357	Mitochondrial import inner membrane translocase subunit
MDP0000294068	0.919481831	0.862375114	Protein of unknown function (DUF640)
MDP0000268523	0.917114627	0.862259516	BURP domain-containing protein
MDP0000661416	0.916123898	0.862063413	A20/AN1-like zinc finger family protein
MDP0000271360	0.910212380	0.862003550	Adenine nucleotide alpha hydrolases-like superfamily protein
MDP0000120543	0.909881047	0.861790934	Nucleotide-diphospho-sugar transferases superfamily protein
MDP0000219780	0.908425106	0.861790934	Calmodulin 5
MDP0000841489	0.907865023	0.861786805	Urease accessory protein D
MDP0000151410	0.907340791	0.861460656	Glycosyl hydrolase 9B13
MDP0000656428	0.906588858	0.861388407	Acyl-CoA N-acyltransferases (NAT) superfamily protein

ID	Theta[a]	Probability	Annotation
MDP0000637620	0.904442194	0.861051936	Heat shock protein 101
MDP0000336563	0.900215343	0.860926018	GRF1-interacting factor 3

[a] The theta value is differential expression statistics, as (M* + D*)/2. M values are the $\log_2$-ratio of the two conditions and D statistics is the value of the difference between conditions.

$$M**=\frac{M_S}{a_0+\sigma_M} \qquad D*=\frac{D_S}{a_0+\sigma_D}$$

σ^2_M and σ^2_D are the standard errors of M_s and D_s statistics, respectively, and a_0 is computed as 90th percentile of all the values in σ_M and σ_D.

Supplementary Table 3-3. DEGs in LP selected by NOISeq software.

ID	Theta[a]	Probability	Annotation
MDP0000148686	1.200424217	0.993425398	Unintegrated
MDP0000320408	1.199286501	0.988853109	Sterol-4alpha-methyl oxidase 1-1
MDP0000323987	1.197018522	0.985521427	Xyloglucan endotransglucosylase/hydrolase 5
MDP0000238718	1.192858746	0.983044340	Unintegrated
MDP0000028677	1.189732293	0.982629428	RING/U-box superfamily protein
MDP0000218935	1.187174918	0.981958550	CCR-like
MDP0000376256	1.184901773	0.981056478	OPC-8:0 CoA ligase1
MDP0000143351	1.182794422	0.980658079	Unintegrated
MDP0000538645	1.181908888	0.979708529	Ubiquitin-like superfamily protein
MDP0000299424	1.178743969	0.979083065	Heavy metal transport/detoxification superfamily protein
MDP0000186794	1.178697373	0.978467922	Plastid ribosomal protein l11
MDP0000262888	1.173774960	0.978441087	Ubiquitin-like superfamily protein
MDP0000122086	1.173603121	0.977761952	NAD(P)-binding Rossmann-fold superfamily protein
MDP0000243419	1.172794520	0.977390389	Unintegrated

ID	Theta[a]	Probability	Annotation
MDP0000189454	1.172271957	0.977140616	PapD-like superfamily protein
MDP0000234947	1.170644554	0.974717199	Glutamyl-tRNA reductase family protein
MDP0000148123	1.170303447	0.972766493	Leucine-rich repeat transmembrane protein kinase
MDP0000800032	1.168448800	0.972434151	Vacuolar proton ATPase A1
MDP0000384344	1.167965891	0.971288498	Late embryogenesis abundant protein (LEA) family protein
MDP0000464704	1.167186942	0.967927917	Cytokinin response factor 4
MDP0000240206	1.166307058	0.967376765	Telomerase activating protein Est1
MDP0000352267	1.164565809	0.963946000	Unintegrated
MDP0000170418	1.163389696	0.963291636	Lactate/malate dehydrogenase family protein
MDP0000904458	1.162837447	0.962315251	Fasciclin-like arabinogalactan 2
MDP0000231646	1.162237315	0.960279911	Vesicle-associated membrane protein 726
MDP0000205579	1.161201555	0.959931054	Polyketide cyclase/dehydrase and lipid transport superfamily protein
MDP0000601491	1.158226504	0.959280819	Light-harvesting chlorophyll-protein complex II subunit B1
MDP0000557670	1.158215835	0.958998018	Family of unknown function (DUF572)
MDP0000271403	1.156741109	0.958702832	Low temperature and salt responsive protein family

ID	Theta[a]	Probability	Annotation
MDP0000175827	1.156632351	0.957953513	Peptidase S24/S26A/S26B/S26C family protein
MDP0000269371	1.154211294	0.957792503	Oxidoreductase, zinc-binding dehydrogenase family protein
MDP0000285682	1.153685821	0.956446619	Heavy metal transport/detoxification superfamily protein
MDP0000569928	1.151466753	0.956052349	RNA-binding (RRM/RBD/RNP motifs) family protein
MDP0000325346	1.150903657	0.955887210	Photosystem I P subunit
MDP0000408705	1.149266247	0.955672529	NAD(P)-linked oxidoreductase superfamily protein
MDP0000171994	1.148739711	0.955119313	O-Glycosyl hydrolases family 17 protein
MDP0000274850	1.147733176	0.952960119	Unintegrated
MDP0000258930	1.146798564	0.952885806	Unintegrated
MDP0000349965	1.146076157	0.952636033	Prefoldin 1
MDP0000610678	1.145213246	0.952448188	Pectin lyase-like superfamily protein
MDP0000275150	1.145093150	0.951506895	Cell wall invertase 4
MDP0000657531	1.143714782	0.951451160	ATP-dependent caseinolytic (Clp) protease/crotonase family protein
MDP0000481097	1.143055624	0.951296342	Photosystem I subunit G
MDP0000686466	1.142678150	0.950900008	Fasciclin-like arabinogalactan-protein 11

ID	Theta[a]	Probability	Annotation
MDP0000162816	1.141737639	0.950881430	Voltage dependent anion channel 1
MDP0000182782	1.141566649	0.950002064	Basic helix-loop-helix (bHLH) DNA-binding superfamily protein
MDP0000854530	1.141113344	0.946150194	Trichome birefringence-like 14
MDP0000284023	1.140458066	0.945855008	Pentapeptide repeat-containing protein
MDP0000124128	1.139694104	0.945227479	RING-box 1
MDP0000123549	1.137697881	0.944560730	Nuclear transport factor 2 (NTF2) family protein with RNA binding domain
MDP0000221498	1.137389712	0.944544216	Unintegrated
MDP0000139577	1.136211368	0.944486417	Unintegrated
MDP0000607436	1.135878397	0.943815540	Zinc-binding dehydrogenase family protein
MDP0000119960	1.134460025	0.943621501	Protein of unknown function, DUF642
MDP0000361781	1.133398327	0.943483197	Unintegrated
MDP0000141538	1.133324317	0.942837090	Cation exchanger 1
MDP0000203768	1.132669123	0.942083643	Cellulose synthase like E1
MDP0000347520	1.132465830	0.941817356	Unintegrated
MDP0000141009	1.131736958	0.941057716	Zinc-binding ribosomal protein family protein

ID	Theta[a]	Probability	Annotation
MDP0000261585	1.131674825	0.940706795	Low-molecular-weight cysteine-rich 69
MDP0000309425	1.130349470	0.940620097	Light-harvesting chlorophyll-protein complex II subunit B1
MDP0000283022	1.130139761	0.940483858	Ribosomal protein L13 family protein
MDP0000269988	1.128260678	0.940002890	Ribosomal protein L12/ATP-dependent Clp protease adaptor protein ClpS family protein
MDP0000337690	1.128029169	0.937110891	Unintegrated
MDP0000207157	1.126184511	0.936080836	HSP20-like chaperones superfamily protein
MDP0000364447	1.124954666	0.935560647	Ribosomal protein L13 family protein
MDP0000135890	1.124656209	0.934842292	Isochorismatase family protein
MDP0000126575	1.124571246	0.934538849	P-Loop containing nucleoside triphosphate hydrolases superfamily protein
MDP0000549646	1.123662307	0.934338618	Thiazole biosynthetic enzyme, chloroplast (ARA6) (THI1) (THI4)
MDP0000541168	1.122720642	0.934322104	Unintegrated
MDP0000178270	1.119935974	0.933481959	Unintegrated
MDP0000781460	1.118344566	0.932957642	Ketol-acid reductoisomerase
MDP0000769716	1.117084306	0.932003963	Cystathionine beta-lyase
MDP0000843137	1.116750494	0.931853274	Membrane-associated mannitol-induced

ID	Theta[a]	Probability	Annotation
MDP0000226874	1.115573059	0.931545702	Exostosin family protein
MDP0000139910	1.115489172	0.930761291	Glucose-6-phosphate/phosphate translocator 2
MDP0000619099	1.114356690	0.930412435	Mitochondrial ribosomal protein S14
MDP0000759015	1.114141773	0.930234910	Nucleotide binding; protein binding
MDP0000803797	1.112534461	0.930216332	Ribosomal protein S28
MDP0000492021	1.112505064	0.930160598	Smg-4/UPF3 family protein
MDP0000320539	1.111277674	0.930106928	Monodehydroascorbate reductase 4
MDP0000122902	1.110382561	0.929762200	Trigger factor type chaperone family protein
MDP0000136440	1.110163262	0.928934440	Vacuolar protein sorting 45
MDP0000306850	1.109893944	0.928773429	Calmodulin-domain protein kinase 5
MDP0000282119	1.109220988	0.928375031	GDSL-like Lipase/acylhydrolase superfamily protein
MDP0000164974	1.108056228	0.928019982	Ribosomal protein S9
MDP0000313905	1.107002243	0.927124102	Mitochondrial substrate carrier family protein
MDP0000091523	1.106894283	0.926927999	2-Oxoglutarate (2OG) and Fe(II)-dependent oxygenase superfamily protein
MDP0000223258	1.106877995	0.926430518	Zinc finger, C3HC4 type (RING finger) family protein

ID	Theta[a]	Probability	Annotation
MDP0000325409	1.106738061	0.926399554	Phosphoglycerate kinase 1
MDP0000183277	1.106217877	0.925641978	Unintegrated
MDP0000308771	1.106131653	0.925641978	F-BOX with WD-40 2
MDP0000236441	1.104534094	0.925070184	Heavy metal transport/detoxification superfamily protein
MDP0000866082	1.103328513	0.924636694	Alpha/beta-hydrolases superfamily protein
MDP0000268873	1.102868891	0.924473619	FGGY family of carbohydrate kinase
MDP0000137809	1.101004712	0.923883247	Plastid-lipid associated protein PAP/fibrillin family protein
MDP0000130060	1.100690060	0.923501362	RNA-binding (RRM/RBD/RNP motifs) family protein
MDP0000159598	1.099726438	0.923437371	Tubulin/FtsZ family protein
MDP0000325482	1.099559239	0.922027496	Sulfoquinovosyldiacylglycerol 2
MDP0000324386	1.097585573	0.921827264	Phosphofructokinase family protein
MDP0000838088	1.096947380	0.921827264	Calcium-binding EF-hand family protein
MDP0000133861	1.095018408	0.921307076	Cyclin B2; 3
MDP0000590110	1.093192996	0.920706383	Homocysteine methyltransferase 2
MDP0000231744	1.093020835	0.919152011	AT hook motif DNA-binding family protein

ID	Theta[a]	Probability	Annotation
MDP0000134655	1.092352985	0.918790769	*Arabidopsis thaliana* protein of unknown function (DUF794)
MDP0000279433	1.092014390	0.918464619	Solanesyl diphosphate synthase 2
MDP0000182259	1.090376268	0.918066221	Heavy metal transport/detoxification superfamily protein
MDP0000926111	1.089784519	0.917467591	RING/U-box superfamily protein
MDP0000182420	1.084436048	0.917395343	Unintegrated
MDP0000807587	1.082111007	0.917157956	Unintegrated
MDP0000212614	1.081498478	0.916588226	Unintegrated
MDP0000142484	1.081257148	0.915923541	Unintegrated
MDP0000135784	1.080159777	0.915300140	2-Oxoglutarate (2OG) and Fe(II)-dependent oxygenase superfamily protein
MDP0000257355	1.077613762	0.914976055	Unintegrated
MDP0000378275	1.077049436	0.914976055	Acyl-CoA N-acyltransferases (NAT) superfamily protein
MDP0000868659	1.075851103	0.913537280	Plant protein of unknown function (DUF868)
MDP0000277802	1.072682503	0.913524895	Polyketide cyclase/dehydrase and lipid transport superfamily protein
MDP0000896804	1.070151870	0.913436132	Pseudouridine synthase family protein
MDP0000268677	1.070019091	0.911999422	Ferritin/ribonucleotide reductase-like family protein

ID	Theta[a]	Probability	Annotation
MDP0000787168	1.069201295	0.911929238	PHE ammonia lyase 1
MDP0000570588	1.066094653	0.911504005	Hydroxypyruvate reductase
MDP0000143861	1.064178177	0.911468913	Mo25 family protein
MDP0000010907	1.064061285	0.911109735	Ribosomal protein L5
MDP0000574554	1.063493541	0.911025101	Expansin A15
MDP0000339542	1.063105474	0.910762943	Purple acid phosphatase 3
MDP0000259191	1.061949080	0.910195277	Mannosyltransferase family protein
MDP0000265859	1.060753202	0.910038395	Ribosomal protein L14
MDP0000280980	1.060628143	0.909970275	Serine carboxypeptidase-like 20
MDP0000190498	1.059451474	0.909968211	3-Phosphoserine phosphatase
MDP0000276122	1.058821202	0.909770044	Cofactor assembly of complex C
MDP0000280299	1.058771576	0.908256956	NAD(P)-binding Rossmann-fold superfamily protein
MDP0000941863	1.056618203	0.908225993	Unintegrated
MDP0000717863	1.054650873	0.907720254	Unintegrated
MDP0000897919	1.054063650	0.907437454	Unintegrated

ID	Theta[a]	Probability	Annotation
MDP0000370175	1.052501634	0.907377591	Unintegrated
MDP0000167963	1.049306783	0.906269094	Protein phosphatase 2C family protein
MDP0000240829	1.048013513	0.906207167	SBP (S-ribonuclease binding protein) family protein
MDP0000479020	1.044091882	0.905934687	Alpha/beta-hydrolases superfamily protein
MDP0000337079	1.043411677	0.905509454	Transducin family protein/WD-40 repeat family protein
MDP0000858175	1.042396981	0.905490876	Gamma-subunit 1
MDP0000917194	1.042366597	0.905270002	Protein phosphatase 2C family protein
MDP0000246192	1.041994544	0.904776649	FKBP-like peptidyl-prolyl cis-trans isomerase family protein
MDP0000302512	1.040190208	0.904545455	Pentatricopeptide (PPR) repeat-containing protein
MDP0000149467	1.038830720	0.904537198	Glutamate-1-semialdehyde-2,1-aminomutase
MDP0000268364	1.036899299	0.903907605	WRKY family transcription factor family protein
MDP0000211280	1.036494613	0.901781438	26S proteasome, regulatory subunit Rpn7; Proteasome component (PCI) domain
MDP0000207799	1.036494432	0.901201387	Unintegrated
MDP0000555633	1.035773915	0.900662621	Yellow stripe like 6
MDP0000265036	1.034920963	0.900061927	Translin family protein

ID	Theta[a]	Probability	Annotation
MDP0000831483	1.032516917	0.899725456	Bromodomain and extraterminal domain protein 9
MDP0000193721	1.030596381	0.898841962	2-Oxoglutarate (2OG) and Fe(II)-dependent oxygenase superfamily protein
MDP0000674735	1.030117123	0.898585996	Heptahelical protein 4
MDP0000791959	1.029703955	0.898555033	Protein of unknown function (DUF1218)
MDP0000916486	1.029182774	0.898084386	Calcium-binding EF-hand family protein
MDP0000732600	1.028893505	0.898043101	Ribosomal protein L13 family protein
MDP0000294813	1.028756541	0.897981174	Spermidine synthase 3
MDP0000351222	1.025745995	0.896860292	Ergosterol biosynthesis ERG4/ERG24 family
MDP0000186168	1.024547283	0.896814879	GTP-binding protein-related
MDP0000841946	1.021698162	0.896752952	Unintegrated
MDP0000088302	1.021014456	0.896311205	Vesicle associated protein
MDP0000341558	1.017121375	0.896263727	Unintegrated
MDP0000482160	1.015302427	0.895933449	Unintegrated
MDP0000321949	1.013130302	0.895702254	Unintegrated
MDP0000153100	1.010801027	0.895644455	Calcium dependent protein kinase 1

ID	Theta[a]	Probability	Annotation
MDP0000250721	1.009287148	0.895456610	Phospholipid/glycerol acyltransferase family protein
MDP0000637194	1.008326116	0.895456610	KNOTTED-like from Arabidopsis thaliana
MDP0000194322	1.006522875	0.894855916	LUC7 related protein
MDP0000488898	1.005997265	0.893377921	Nuclear transport factor 2 (NTF2) family protein with RNA binding domain
MDP0000873667	1.005667315	0.893305673	Xyloglucan endotransglucosylase/hydrolase 16
MDP0000952041	1.005602774	0.892081579	NFU domain protein 3
MDP0000170822	1.004949551	0.892054744	Tetraspanin8
MDP0000241994	1.004849547	0.891586161	Cyclin B1;4
MDP0000610238	1.004018934	0.891429279	HSP20-like chaperones superfamily protein
MDP0000243676	1.003450826	0.891070102	NAD(P)-binding Rossmann-fold superfamily protein
MDP0000216719	1.002316686	0.891037074	BTB/POZ domain-containing protein
MDP0000131645	1.001907414	0.890704731	Unintegrated
MDP0000235104	1.001812349	0.890403352	Tubulin beta 8
MDP0000153205	1.000865706	0.890106102	Protein of unknown function (DUF579)
MDP0000149050	1.000216715	0.890079267	Unintegrated

ID	Theta[a]	Probability	Annotation
MDP0000649496	0.999747106	0.889852200	Calcium-dependent protein kinase 13
MDP0000183375	0.999564213	0.889530179	Embryonic cell protein 63
MDP0000950619	0.998012032	0.889111139	Cinnamyl alcohol dehydrogenase 9
MDP0000270446	0.996679123	0.889007927	Unintegrated
MDP0000855100	0.996449317	0.889007927	Ribosomal protein L34
MDP0000378491	0.996152706	0.888731319	AICARFT/IMPCHase bienzyme family protein
MDP0000151697	0.995419991	0.888671456	RING/FYVE/PHD zinc finger superfamily protein
MDP0000311726	0.994442848	0.888599207	Solanesyl diphosphate synthase 2
MDP0000599427	0.991951625	0.888229709	Fatty acid desaturase A
MDP0000477453	0.991605775	0.887897366	2-Oxoglutarate (2OG) and Fe(II)-dependent oxygenase superfamily protein
MDP0000593964	0.986117912	0.887457683	Ribosomal L38e protein family
MDP0000738458	0.985423186	0.887294608	Sequence-specific DNA binding transcription factors
MDP0000311291	0.983530317	0.887088184	Glutathione peroxidase 7
MDP0000141206	0.981746820	0.887081992	Delta tonoplast integral protein
MDP0000821298	0.980308027	0.886811576	Photosystem II reaction center PsbP family protein

ID	Theta[a]	Probability	Annotation
MDP0000233588	0.979284968	0.886382215	DNA glycosylase superfamily protein
MDP0000575967	0.978649487	0.886340930	Regulator of chromosome condensation (RCC1) family protein
MDP0000310196	0.978242695	0.886285195	Unintegrated
MDP0000800352	0.978114820	0.885137478	Photosystem II subunit R
MDP0000189373	0.977676221	0.885092065	NAP1-related protein 2
MDP0000349570	0.977099001	0.884986789	Unintegrated
MDP0000482479	0.976174202	0.884926926	Unintegrated
MDP0000240886	0.975190297	0.884497564	CAX interacting protein 1
MDP0000304843	0.974990322	0.884346875	ATP citrate lyase (ACL) family protein
MDP0000327325	0.973875354	0.884243663	Ribosomal protein S12/S23 family protein
MDP0000740655	0.973274950	0.884035175	Chloroplastic drought-induced stress protein of 32 kD
MDP0000202810	0.972816495	0.883756502	Unintegrated
MDP0000222943	0.972444570	0.883560400	Copper transport protein family
MDP0000361550	0.972094914	0.883560400	Unintegrated
MDP0000269765	0.970021350	0.883312691	Tetratricopeptide repeat (TPR)-like superfamily protein

ID	Theta[a]	Probability	Annotation
MDP0000168900	0.969327874	0.883192965	Unintegrated
MDP0000768772	0.967158604	0.882903972	TOXICOS EN LEVADURA 2
MDP0000189331	0.965409931	0.882887458	Unintegrated
MDP0000126417	0.963283823	0.882218644	Phloem protein 2-B10
MDP0000157034	0.962933064	0.881890430	AT hook motif DNA-binding family protein
MDP0000165459	0.962760910	0.881805796	MALE GAMETOPHYTE DEFECTIVE 2
MDP0000266699	0.962223825	0.881789282	Nudix hydrolase homolog 19
MDP0000222437	0.960931884	0.881031707	P-Loop containing nucleoside triphosphate hydrolases superfamily protein
MDP0000812195	0.960787512	0.881031707	P-Loop containing nucleoside triphosphate hydrolases superfamily protein
MDP0000862430	0.959845248	0.880909917	Protein of unknown function (DUF1279)
MDP0000163548	0.958589697	0.880336058	Thioredoxin superfamily protein
MDP0000208635	0.956883012	0.880265874	S-Adenosyl-L-methionine-dependent methyltransferases superfamily protein
MDP0000692464	0.955815637	0.880024358	Cox19-like CHCH family protein
MDP0000120595	0.954323958	0.879390637	HXXXD-type acyl-transferase family protein
MDP0000193898	0.953913439	0.879019074	Sugar transporter 1

ID	Theta[a]	Probability	Annotation
MDP0000941476	0.951358796	0.878936504	Chalcone-flavanone isomerase family protein
MDP0000135022	0.948387670	0.878692924	Trypsin family protein with PDZ domain
MDP0000147635	0.948198985	0.878511271	Glycosyl hydrolase 9B7
MDP0000138500	0.947707569	0.878441087	Expansin A8
MDP0000186518	0.944195852	0.878418380	Histidine-containing phosphotransmitter 3
MDP0000218990	0.943718569	0.877968376	Ankyrin repeat family protein
MDP0000198183	0.943609967	0.877539014	RAB GTPase homolog A1F
MDP0000256347	0.942395039	0.877539014	Serine/threonine protein kinase 1
MDP0000179749	0.941592852	0.877470894	Unintegrated
MDP0000722255	0.941119726	0.877452316	Fatty acid desaturase 2
MDP0000135301	0.940664080	0.877415160	Thylakoid lumenal P17.1 protein
MDP0000228494	0.940171963	0.876409875	Expansin a8
MDP0000925883	0.940004463	0.875906201	UDP-XYL synthase 5
MDP0000288293	0.938478083	0.875767897	MLP-like protein 423
MDP0000394944	0.931438103	0.875641978	Pectin lyase-like superfamily protein

ID	Theta[a]	Probability	Annotation
MDP0000294379	0.929791133	0.875637850	MLP-like protein 423
MDP0000321244	0.926519447	0.875262158	Rubisco activase
MDP0000873376	0.925336991	0.875002064	Cupredoxin superfamily protein
MDP0000759336	0.925047714	0.874618116	Chalcone-flavanone isomerase family protein
MDP0000453114	0.921436428	0.874514904	Ethylene-forming enzyme
MDP0000730595	0.919271819	0.874510775	Tetratricopeptide repeat (TPR)-like superfamily protein
MDP0000177217	0.916379469	0.874211461	tRNA synthetase class II (D, K, and N) family protein
MDP0000199150	0.915185057	0.873938981	60S acidic ribosomal protein family
MDP0000232522	0.915012819	0.873868797	Alpha/beta-hydrolases superfamily protein
MDP0000770759	0.912908195	0.873433243	Ferrochelatase 2
MDP0000364293	0.912621705	0.873053423	Uroporphyrinogen decarboxylase
MDP0000147384	0.911418947	0.871513500	Copper ion binding; cobalt ion binding; zinc ion binding
MDP0000284154	0.911196048	0.871117166	Unintegrated
MDP0000329265	0.909801682	0.870588721	Unintegrated
MDP0000123747	0.906966101	0.870541243	2-Isopropylmalate synthase 1

ID	Theta[a]	Probability	Annotation
MDP0000534564	0.906049656	0.870204773	Nucleotide-diphospho-sugar transferases superfamily protein
MDP0000771587	0.904902723	0.869542152	Ribophorin II (RPN2) family protein
MDP0000804620	0.903662993	0.869542152	Zinc finger C-x8-C-x5-C-x3-H type family protein
MDP0000897180	0.903267546	0.869542152	Unintegrated
MDP0000150042	0.900998521	0.869230452	DDB1-CUL4 associated factor 1
MDP0000913740	0.900855032	0.869164396	Unintegrated

[a] The theta value is differential expression statistics, as (M* + D*)/2. M values are the $\log_2$-ratio of the two conditions and D statistics is the value of the difference between conditions.

$$M*^{*} = \frac{M_S}{a_0 + \sigma_M} \qquad D* = \frac{D_S}{a_0 + \sigma_D}$$

σ^2_M and σ^2_D are the standard errors of M_s and D_s statistics, respectively, and a_0 is computed as 90th percentile of all the values in σ_M and σ_D.

Supplementary Table 3-4. Genes visualized in Fig. 3-5 using MapMan software.

Gene	Description	Fold change
MDP0000945260	IAA3, SHY2 (SHORT HYPOCOTYL 2)	1.7241417
MDP0000124810	SLR, IAA14 (INDOLE-3-ACETIC ACID INDUCIBLE 14)	-1.5909001
MDP0000314765	SOC1, AGL20 (AGAMOUS-LIKE 20)	3.6570275
MDP0000574222	AGL3, SEP4 (SEPALLATA 4)	-2.9279351
MDP0000317257	MYB113, AtMYB113	-1.9279350
MDP0000422537	ATPHAN, ATMYB91, MYB91, AS1 (ASYMMETRIC LEAVES 1)	2.3939931
MDP0000894463	MYB73, ATMYB73	-3.2498631
MDP0000249611	ATMYB4, MYB4	-1.9279350
MDP0000950559	ATMYB4, MYB4	-1.5128975
MDP0000241185	Myb family transcription factor	2.1875422
MDP0000335890	ATRL5 (ARABIDOPSIS RAD-LIKE 5)	-1.5128975
MDP0000277813	Myb family transcription factor	1.6570275
MDP0000239354	TRB1, ATTRB1	4.0720650
MDP0000203666	WOX4 (WUSCHEL RELATED HOMEOBOX 4)	2.1875422

Gene	Description	Fold change
MDP0000608923	HAT4, ATHB2 | ATHB-2 (ARABIDOPSIS THALIANA HOMEOBOX PROTEIN 2)	-2.5128975
MDP0000172744	HAT22	2.6570275
MDP0000323095	KNAT3 (KNOTTED1-LIKE HOMEOBOX GENE 3)	2.1309586
MDP0000599845	ATHB-1 (ARABIDOPSIS THALIANA HOMEOBOX 1)	1.7350299
MDP0000637194	BP, BP1, KNAT1 (KNOTTED-LIKE FROM ARABIDOPSIS THALIANA)	-2.9279351
MDP0000163095	HAT22	1.1595278
MDP0000859459	ATHB6	1.4871025
MDP0000233235	GL2 (GLABRA 2)	1.3939930
MDP0000205983	HTA12	2.3939931
MDP0000255229	H2B, HTB2	3.0720649
MDP0000259057	HTA3, H2AXB, G-H2AX, GAMMA-H2AX (GAMMA HISTONE VARIANT H2AX)	3.6570275
MDP0000320059	No original description	-1.2498631
MDP0000334368	HTA2 (histone H2A)	1.2944574
MDP0000336462	Histone H4	1.3939930
MDP0000361591	H2B, HTB2	1.2944574

Gene	Description	Fold change
MDP0000364547	Histone H3.2	1.3350993
MDP0000364547	Histone H3.2	1.3350993
MDP0000477621	HIS1-3 (HISTONE H1-3)	1.5314965
MDP0000931380	HMGA (HIGH MOBILITY GROUP A)	3.0720649
MDP0000277688	MRG family protein | chr4	-3.9279351
MDP0000261742	HDA9 (HISTONE DEACETYLASE 9)	3.3939931
MDP0000348722	HDA15, ATHDA15	2.6570275
MDP0000780720	HDA8, ATHDA8	-1.5128975
MDP0000256797	HDA2	-1.8348256
MDP0000237694	SET domain-containing protein	-3.5128975
MDP0000155873	ATXR3, SDG2 (SET DOMAIN-CONTAINING PROTEIN 2)	2.3939931
MDP0000219093	SGA1, SGA01, ASF1B (ANTI- SILENCING FUNCTION 1B)	3.0720649
MDP0000244598	GCN5-related N-acetyltransferase (GNAT) family protein	2.0720649
MDP0000656428	GCN5-related N-acetyltransferase (GNAT) family protein	1.8794199
MDP0000487015	LBD38 (LOB DOMAIN-CONTAINING PROTEIN 38)	3.3939931

Gene	Description	Fold change
MDP0000220708	LBD21 (LOB DOMAIN-CONTAINING PROTEIN 21)	1.2419900
MDP0000848210	LBD25 (LOB DOMAIN-CONTAINING PROTEIN 25)	1.8090305
MDP0000128979	RAP2.3, ERF72, ATEBP (ETHYLENE-RESPONSIVE ELEMENT BINDING PROTEIN)	2.8794198
MDP0000464704	CRF4 (CYTOKININ RESPONSE FACTOR 4)	-4.9279350
MDP0000413387	RAP2.3, ERF72, ATEBP (ETHYLENE-RESPONSIVE ELEMENT BINDING PROTEIN)	2.5314965
MDP0000400129	AP2 domain-containing protein	-2.2498631
MDP0000235028	No original description	-3.7352900
MDP0000848905	RAP2.3, ERF72, ATEBP (ETHYLENE-RESPONSIVE ELEMENT BINDING PROTEIN)	2.6570275
MDP0000737899	AL6 (ALFIN-LIKE 6)	1.8794199
MDP0000595519	NF-YB11 (NUCLEAR FACTOR Y, SUBUNIT B11)	-2.9279351
MDP0000831483	GTE8	-2.8024042
MDP0000255104	Transcription factor	2.8794198
MDP0000141709	Transcription factor	2.2944574
MDP0000727700	Transcription factor	-1.6649007
MDP0000585643	ATRR4, ARR9 (RESPONSE REGULATOR 9)	1.6570275

Gene	Description	Fold change
MDP0000509768	ATRR4, ARR9 (RESPONSE REGULATOR 9)	1.2419900
MDP0000333691	KAN2 (KANADI 2)	2.6570275
MDP0000182154	Myb family transcription factor	1.3939930
MDP0000669451	RGA2, GAI (GIBBERELLIC ACID INSENSITIVE)	-1.6060070
MDP0000662303	RGA2, GAI (GIBBERELLIC ACID INSENSITIVE)	1.4199883
MDP0000268364	ATWRKY44, WRKY44, TTG2 (TRANSPARENT TESTA GLABRA 2)	-2.4304354
MDP0000130716	WRKY11, ATWRKY11	2.8794198
MDP0000225159	Basic helix-loop-helix (bHLH) family protein	2.6570275
MDP0000319746	SAC51 (SUPPRESSOR OF ACAULIS 51)	-2.7352900
MDP0000124019	Basic helix-loop-helix (bhlh) family protein	1.1651744
MDP0000175968	Transcription Factor	2.1875422
MDP0000267178	Basic helix-loop-helix (bhlh) family protein (bhlh096)	1.9465340
MDP0000323291	ILR3 (iaa-leucine resistant3)	2.6570275
MDP0000401086	Basic helix-loop-helix (bHLH) family protein	-1.7352899
MDP0000410728	Basic helix-loop-helix (bHLH) family protein	3.3939931

Gene	Description	Fold change
MDP0000869137	Transcription factor	1.2944574
MDP0000672131	Basic helix-loop-helix (bHLH) family protein (bHLH096)	2.6570275
MDP0000251332	GBF1	1.8090305
MDP0000239026	AtbZIP44 (*Arabidopsis thaliana* basic leucine-zipper 44)	2.0720649
MDP0000146312	TraB family protein	2.2944574
MDP0000219041	HYH (HY5-HOMOLOG)	-2.2498631
MDP0000205823	AtbZIP44 (*Arabidopsis thaliana* basic leucine-zipper 44)	3.0720649
MDP0000586302	TED 5, HY5 (ELONGATED HYPOCOTYL 5)	1.4871025
MDP0000319187	DNA binding/transcription factor	-3.5128975
MDP0000243895	ATHSFA2, HSFA2	2.0720649
MDP0000471588	LIL3	-1.5128975
MDP0000202669	ATCOL4, COL4, zinc finger (B-box type) family protein	1.1545271
MDP0000156241	Dof-type zinc finger domain-containing protein	3.2419899
MDP0000771149	Dof-type zinc finger domain-containing protein	2.2419899
MDP0000201509	OBP4	3.2419899

Gene	Description	Fold change
MDP0000273251	ADOF1	2.0720649
MDP0000157809	BZR1 (BRASSINAZOLE-RESISTANT 1)	3.8794198
MDP0000309557	NFD3, NFD03, HMGB3 (HIGH MOBILITY GROUP B 3)	2.7725046
MDP0000137305	BME3-ZF, BME3, zinc finger (GATA type) family protein	2.0720649
MDP0000443612	ZFP4 (ZINC FINGER PROTEIN 4)	3.0720649
MDP0000804620	Zinc finger (CCCH-type) family protein	-2.5128975
MDP0000757090	ATZFP1 | ZFP1 (ZINC-FINGER PROTEIN 1)	3.3939931
MDP0000260192	Zinc finger (c2h2 type) family protein	-3.5128975
MDP0000480293	Zinc finger (c2h2 type) family protein	3.3939931
MDP0000181641	Zinc finger (ccch-type) family protein	3.6570275
MDP0000147872	TZP	-1.9868287
MDP0000176924	KH domain-containing protein, zinc finger (CCCH type) family protein	-3.2498631
MDP0000324584	NF-YB13 (NUCLEAR FACTOR Y, SUBUNIT B13)	-2.5128975
MDP0000777771	KELP	2.0720649
MDP0000336563	GIF2, SSXT protein-related/transcription co-activator-related	2.3939931

Gene	Description	Fold change
MDP0000269136	VPS20.2 (VACUOLAR PROTEIN SORTING-ASSOCIATED PROTEIN 20.2)	1.6570275
MDP0000262149	VPS46.2	1.7725047
MDP0000598703	DNA-binding family protein	2.8794198
MDP0000231744	DNA-binding family protein	-3.3873668
MDP0000252977	Zinc knuckle (CCHC-type) family protein	2.3939931
MDP0000125070	ATPCNA2, PCNA2 (PROLIFERATING CELL NUCLEAR ANTIGEN 2)	3.0720649
MDP0000233569	Transcription elongation factor-related	1.2647101
MDP0000157034	DNA-binding family protein	-2.5128975
MDP0000477220	DNA-binding family protein, AT-hook protein 1 (AHP1)	-1.2905052
MDP0000417845	SAP domain-containing protein	-1.2689719
MDP0000373085	ATSIZ1, SIZ1	-1.3264844
MDP0000261067	Developmentally regulated GTP-binding protein, putative	-3.3202524
MDP0000152648	Zinc finger (FYVE type) family protein	-1.5909001
MDP0000811595	ATP12 protein-related	2.6570275
MDP0000661416	Zinc finger (AN1-like) family protein	3.0720649

Gene	Description	Fold change
MDP0000134418	Zinc finger (FYVE type) family protein	-1.5128975
MDP0000535412	Nucleic acid binding/zinc ion binding	3.5314965
MDP0000254568	TRAF-type zinc finger-related	1.2944574
MDP0000232523	Remorin family protein	3.7725046
MDP0000804605	LOL1 (LSD ONE LIKE 1)	-1.5128975
MDP0000471588	LIL3	-1.5128975
MDP0000752954	Leucine zipper factor-related	2.6570275
MDP0000201190	ZIGA4 (ARF GAP-like zinc finger-containing protein ZiGA4)	-2.0434122
MDP0000251794	CwfJ-like family protein, zinc finger (CCCH-type) family protein	-3.3873668
MDP0000133008	Zinc-binding family protein	-2.7352900
MDP0000259773	Zinc finger (CCCH-type) family protein, RNA recognition motif (RRM)-containing protein	-3.7352900
MDP0000336563	GIF2, SSXT protein-related/transcription co-activator-related	2.3939931
MDP0000142045	No original description	-2.3873668
MDP0000263150	Zinc finger (AN1-like) family protein	1.5314965